



Pontificia Universidad Católica de Chile
Facultad de Ciencias Biológicas
Programa de Doctorado en Ciencias Biológicas
Mención en Ciencias Fisiológicas

TESIS DOCTORAL

**PALMITIC ACID INHIBITS THE AUTOPHAGIC FLUX
IN HYPOTHALAMIC NEURONS**

Por

MARÍA PAZ HERNÁNDEZ CÁCERES

Mayo 2020



Pontificia Universidad Católica de Chile
Facultad de Ciencias Biológicas
Programa de Doctorado en Ciencias Biológicas
Mención en Ciencias Fisiológicas

TESIS DOCTORAL

**PALMITIC ACID INHIBITS THE AUTOPHAGIC FLUX
IN HYPOTHALAMIC NEURONS**

Tesis entregada a la Pontificia Universidad Católica de Chile en cumplimiento parcial
de los requisitos para optar al grado de Doctor en Ciencias Biológicas
Mención en Ciencias Fisiológicas

Por

MARÍA PAZ HERNÁNDEZ CÁCERES

Directora de tesis:

Dra. Eugenia Morselli

Comisión de tesis:

Dra. Francisca Bronfman

Dra. María de los Ángeles García

Dr. Juan Carlos Sáez

Dr. Claudio Pérez-Leighton

Mayo 2020

AGRADECIMIENTOS

En primer lugar, quisiera agradecer a la Dra. Eugenia Morselli, quien sin conocerme me acepto en su laboratorio como su primera alumna de doctorado, y que, con su simpatía, buena disposición, apoyo y paciencia me ayudo a formarme como profesional, fomentando el desarrollo del pensamiento crítico y científico, siempre en un ambiente de confianza.

Además, quisiera agradecer a mi comisión evaluadora conformada por la Dra. Francisca Bronfman, la Dra. María de los Ángeles García, el Dr. Juan Carlos Sáez y el Dr. Claudio Pérez-Leigthon, cuya participación en la discusión y estructuración de mi tesis fue fundamental.

También quisiera agradecer a mis compañeras y compañeros de laboratorio: a la Dra. Yennifer Ávalos, a Lilian Toledo, a Paulina Burgos, a Flavia Cifuentes, a Pablo Lagos, a Carla Narro, a Patricia Rivera, y a mi compañera adoptiva de lab Charlotte Hill, quienes aparte de apoyarme a nivel científico y experimental, fueron un gran apoyo emocional, sin los cuales no podría haber sobrellevado estos años de constante presión y muchas veces frustración. Muchas gracias por sus risas y apoyo moral, son un grupo de profesionales que siempre recordaré con cariño.

Por su parte, quisiera agradecer a Karina Cereceda y Sergio Hernández, quienes además de ayudarme experimentalmente, fueron un gran apoyo moral y emocional.

También quisiera agradecer al 5to piso del Departamento de Fisiología en general, ya que gracias a la buena voluntad y disposición de todos quienes trabajan allí fue posible llevar a cabo muchos de los experimentos que se presentan en este manuscrito, particularmente al

Laboratorio del Dr. Gareth Owen y al Laboratorio del Dr. Alejandro Godoy, especialmente a Daniela Carreño, Patricia Fuenzalida, y Verónica Torres, quienes siempre me facilitaron sus equipos y dependencias con la mejor de las disposiciones.

Además, quisiera agradecer las colaboraciones que surgieron durante el desarrollo de esta tesis, a la Dra. Patricia Burgos, al Dr. Mauricio Budini, al Dr. Alfredo Criollo y al Dr. Rodrigo Troncoso, cuyo apoyo experimental fue fundamental para el desarrollo de este proyecto. Además, al Dr. Li Yu y a la Dra. Ying Li, de la Tsinghua University, en donde realicé mi pasantía doctoral, quienes me ayudaron y apoyaron con la mejor de las disposiciones tanto a nivel experimental en el laboratorio, como durante toda mi estadía en China.

De manera muy importante, quisiera agradecer el gran apoyo incondicional que recibí todo este tiempo de mis padres, Marianela y Emiliano, mis hermanos, Pablo y Sebastián y al gran amor de mi vida Francisco. Sin su apoyo, risas y ayuda en la cotidianidad de la vida, no habría sido fácil sobrellevar este proceso exitosamente. De manera especial, quisiera agradecer a mi abuelita Carmen y mi tía Violeta, quienes siempre me entregaron apoyo espiritual y cariño incondicional. Por todo esto, les dedico con mucho cariño y amor esta tesis.

También, quisiera agradecer a la Comisión Nacional de Investigación Científica y Tecnológica (CONICYT), al Fondo Nacional de Desarrollo Científico y Tecnológico, (FONDECYT), y a la Pontificia Universidad Católica de Chile, por el soporte financiero que permitieron la realización de esta tesis. Finalmente, este proyecto se logró con apoyo de la Unidad de Microscopía Avanzada UC (UMA UC).

INDEX

INDEX	III
FIGURES INDEX	VII
TABLES INDEX	IX
ABBREVIATIONS	X
RESUMEN	XIII
ABSTRACT	XVI
1. INTRODUCTION	1
1.1. The obesity epidemics	1
1.2. Fatty acids uptake and transport into the brain	2
1.3. High fat diet-induced obesity increases brain levels of saturated fatty acid	6
1.4. Role of the hypothalamus in the regulation of energy balance and body metabolism...	7
1.5. Insulin signaling in the hypothalamus	9
1.6. Overview of the autophagic process	12
1.7. Hypothalamic autophagy regulates metabolic homeostasis	22

1.8. Regulation of autophagy by high fat diet	24
2. HYPOTHESIS	28
3. GENERAL AIM	28
4. SPECIFIC AIMS	28
5. MATERIALS AND METHODS	30
5.1. Hypothalamic cell line N43/5 and treatments	30
5.2. Primary hypothalamic neurons and treatments	30
5.3. Preparation of palmitic acid-BSA complex	31
5.4. Methods to evaluate autophagy and the autophagic flux	31
5.5. siRNA transfections	32
5.6. Real Time PCR (RT-PCR)	33
5.7. Western blot analysis	34
5.8. Immunofluorescence and fluorescence microscopy	34
5.9. Methods to evaluate lysosomal activity	35
5.10. Electron microscopy	37

5.11. Rab7-GTP pull down assay	37
5.12. Isolation and characterization of the lysosomal fraction and realization of SILAC in N43/5 hypothalamic neuronal cells	38
5.13. 2-NBDG uptake	39
5.14. Results and statistical analysis	39
6. RESULTS	40
6.1. Palmitic acid inhibits autophagic flux in hypothalamic neuronal cells	40
6.2. Palmitic acid does not affect autophagy related genes involved in autophagosome formation in N43/5 cells	42
6.3. Palmitic acid induces lysosomal swelling and reduces autophagosome-lysosome fusion in N43/5 cells exposed to Bafilomycin A1	43
6.4. Palmitic acid does not abolish lysosomal acidity or lysosomal activity in N43/5 cells.....	44
6.5. Palmitic acid reduces the dynamics of endolysosomal structures in N43/5 cells	45
6.6. Palmitic acid induces the formation of large autophagic vesicles in N43/5 hypothalamic neuronal cells	45

6.7. Palmitic acid induces the accumulation of large cellular degradative compartments in N43/5 hypothalamic neuronal cells	46
6.8. Palmitic acid increases Rab7 activation in N43/5 cells	48
6.9. Palmitic acid affects the levels of proteins linked to the endolysosomal and to the autophagic pathways	49
6.10. Palmitic acid reduces insulin sensitivity in N43/5 cells	51
6.11. Inhibition of autophagy reduces insulin sensitivity in N43/5 cells	52
7. DISCUSSION	71
8. CONCLUSIONS	84
9. REFERENCES	85

FIGURE INDEX

Figure 1: General scheme of autophagy	13
Figure 2: Overview of the autophagic process	17
Figure 3: Role of autophagy in POMC and AgRP neurons in the control of energetic metabolism	26
Figure 4: Palmitic acid inhibits the autophagic flux in hypothalamic cells	55
Figure 5: Effect of palmitic acid on autophagy related proteins and <i>Atg</i> genes in N43/5 cells.....	57
Figure 6: Palmitic acid exposure increases the size of LAMP1 positives vesicles and, in presence of BafA1, decreases LAMP1 and LC3 co-localization in N43/5 cells	59
Figure 7: Palmitic acid does not reduce lysosomes acidity or lysosomal cathepsin B activity in N43/5 cells	60
Figure 8: Palmitic acid reduces endolysosomal motility in N43/5 cells.....	62
Figure 9: Palmitic acid induces the accumulation of big autophagic vesicles in N43/5 cells.....	63
Figure 10: Palmitic acid induces the accumulation of large cellular degradative compartments (DGCs) in N43/5 cells	65

Figure 11: Palmitic acid increases Rab7 activation in N43/5 cells	66
Figure 12: Palmitic acid reduces insulin sensitivity in N43/5 cells	68
Figure 13: Inhibition of autophagy reduces insulin sensitivity in N43/5 cells	69

TABLES INDEX

Table 1. SILAC based proteomic analysis from isolated lysosomes of N43/5 hypothalamic cells treated with palmitic acid (PA) associated with the endolysosomal and the autophagic trafficking pathways	67
--	----

ABBREVIATIONS

AgRP/NPY: Agouti-related peptide/neuropeptide Y

AKT: Protein kinase B

AMP: Adenosine monophosphate

AMPK: AMP-activated protein kinase

ARC: Arcuate nucleus

ATG: Autophagy related genes/proteins

ATP: Adenosine triphosphate

BafA1: Bafilomycin A1

BBB: Blood-brain barrier

BLOC1: Biogenesis of lysosome-related organelles complex 1

BMI: Body-mass index

BORC: BLOC-1 related complex

CMA: Chaperone-mediated autophagy

CNS: Central nervous system

CVO: Circumventricular organs

DGCs: Cellular degradative compartments

EM: Electron microscopy

ER: Endoplasmic reticulum

ESCRT: Endosomal sorting complex required for transport

FA: Fatty acid

FABP: Fatty acid-binding protein

FATP: Fatty acid transport protein

FFA: Free fatty acid

FIP200: Focal adhesion kinase family interacting protein of 200 kDa

GLUT: Glucose transporter

HFD: High fat diet

HOPS complex: Homotypic fusion and protein sorting complex

IF: Immunofluorescence

IR: Insulin receptors

IRS: IR substrate

LAMP1: Lysosomal-associated membrane protein 1

LC3: Microtubule-associated protein 1A/1B-light chain 3

MBH: Medio-basal hypothalamus

MSFD2A: Major facilitator superfamily domain-containing protein 2A

mTORC1: Mechanistic target of rapamycin complex 1

MUFA: Monounsaturated fatty acid

PA: Palmitic acid

PAS: Phagophore assembly site

PE: Phosphatidylethanolamine

PI(3,5)P₂: Phosphatidylinositol-3,5-bisphosphate

PI3K: Phosphoinositide 3-kinase

PI3P: Phosphatidylinositol 3-phosphate

PIKFYVE: Phosphoinositide kinase, FYVE-type zinc finger containing

PLEKHM1: Pleckstrin homology and RUN domain containing M1

POMC: Proopiomelanocortin

PTEN: Phosphatase and tensin homolog

PUFA: Polyunsaturated fatty acid

PVN: Paraventricular nucleus

RILP: Rab-interacting lysosomal protein

SatFA: Saturated fatty acids

SILAC: Stable isotope labeling with amino acid in cell culture

SNAP29: Synaptosomal-associated protein 29

SNAREs: Soluble N-ethylmaleimide-sensitive factor attachment protein receptors

SQSTM1: p62/Sequestosome-1

STX17: Syntaxin 17

TBC1D15: TBC1 domain family member 15

TG: Triglycerides

TGN: Trans-Golgi network

ULK1: Unc-51-like kinase 1

VAMP8: Vesicle-associated membrane protein 8

VPS: Vacuolar sorting protein

WB: Western blot

α -MSH: α -melanocyte-stimulating hormone

RESUMEN

La obesidad es considerada una epidemia mundial, tanto en países desarrollados como en vías de desarrollo. Uno de los factores más importantes que promueven el desarrollo de obesidad es el consumo de dietas altas en grasas (HFD) ricas en ácidos grasos saturados, como el ácido palmítico (PA). La ingesta crónica de una HFD se ha asociado con el incremento de enfermedades metabólicas, como la resistencia a la insulina. Se ha observado en ratones, que luego del consumo crónico de una HFD el PA se acumula en el hipotálamo, el área del cerebro encargada de mantener la homeostasis energética y de regular el metabolismo corporal. Uno de los mecanismos homeostáticos celulares clave que es afectado después del consumo de una HFD es la autofagia, el cual es un proceso catabólico mediado por los lisosomas, destinado a la degradación y reciclaje de componentes citoplasmáticos y orgánulos dañados. Durante el proceso de autofagia, el cargo celular es secuestrado dentro de una vesícula de doble membrana, llamada autofagosoma, la cual se fusiona con un lisosoma, formando un autolisosoma, donde, gracias a la actividad de las enzimas lisosómicas, el cargo autofágico es degradado. Todo el proceso desde la síntesis del autofagosoma hasta su degradación lisosomal se denomina flujo autofágico. Es importante destacar que la desregulación del proceso de autofagia en neuronas del hipotálamo promueve el desarrollo de trastornos metabólicos, lo que sugiere que la autofagia hipotalámica tendría un papel clave en el control del metabolismo corporal. Además, niveles elevados de PA se han asociado con una disminución de la autofagia y con resistencia a la insulina en el hipotálamo. Sin embargo, actualmente se desconoce el mecanismo específico por el cual el PA disminuye la autofagia en las neuronas hipotalámicas.

En este proyecto, proponemos que la inhibición de la autofagia inducida por el PA en neuronas hipotalámicas posee un papel fundamental en el desarrollo de trastornos metabólicos asociados a la obesidad, como la resistencia a la insulina. La hipótesis de esta tesis es que *el ácido palmítico inhibe el flujo autofágico y disminuye la sensibilidad a la insulina en las células neuronales hipotalámicas*. Los resultados arrojaron que, en la línea celular hipotalámica N43/5 y en cultivo primario de neuronas hipotalámicas de rata, el PA aumentó el número de estructuras autofágicas y los niveles de SQSTM1/p62, una proteína degradada durante el proceso de autofagia, sugiriendo que el PA inhibe el flujo autofágico en células neuronales hipotalámicas. Además, los niveles de expresión de distintos genes relacionados con la autofagia y que son esenciales para la formación del autofagosoma no variaron por la exposición al PA, lo que sugiere que el PA promueve la acumulación de estructuras autofágicas como consecuencia de la disminución del flujo autofágico en las células N43/5. Adicionalmente, mediante microscopía electrónica, observamos que el PA indujo la acumulación de grandes compartimentos celulares degradativos en las células neuronales hipotalámicas N43/5. Sin embargo, el PA no disminuyó la acidez lisosomal ni su actividad enzimática en la línea de células hipotalámicas. No obstante, la exposición de PA si afectó la dinámica de vesículas endolisomales, disminuyendo la velocidad y la distancia recorrida por éstas, en las células N43/5. Luego, evaluamos por inmunofluorescencia la fusión de los autofagosomas con los lisosomas utilizando células N43/5 transfectadas con el constructo mcherry-GFP-LC3, y también mediante el análisis de co-localización entre marcadores de autofagosomas y lisosomas. Observamos que el PA es capaz de disminuir la fusión entre ambos organelos, así como de incrementar la acumulación de estructuras autofágicas de gran tamaño. Además, mediante un ensayo de pull-down cuantificamos el estado de activación de Rab7, una proteína involucrada tanto en la fusión del

autofagosoma con el lisosoma como también en el tráfico endolisosomal, y observamos que en células N43/5 expuestas a PA los niveles Rab7 unida a GTP incrementaron, sugiriendo que el PA podría perjudicar la formación de autolisosomas a través de regulación de la actividad de Rab7. Además, mediante la técnica de etiquetado de isótopos estables con aminoácidos en cultivo celular (SILAC), encontramos en lisosomas aislados de células N43/5 tratadas con PA, un aumento en los niveles de diversas proteínas involucradas con el control del tráfico endolisosomal y con la maduración autofágica, lo que podría explicar el mecanismo por el cual el PA afecta la autofagia en las neuronas hipotalámicas. Finalmente, se evaluó si la exposición al PA contribuye al desarrollo de desórdenes metabólicos, confirmando que el PA disminuye la sensibilidad a la insulina en las células hipotalámicas N43/5. Además, tanto la inhibición de la autofagia como del flujo autofágico redujeron la sensibilidad a la insulina en estas células.

En resumen, este estudio sugiere que, en células neuronales hipotalámicas, la inhibición del flujo autofágico inducida por PA desregula el tráfico endolisosomal y reduce la sensibilidad a la insulina. Este estudio puede ayudar a dilucidar los mecanismos celulares que subyacen a los efectos del PA en la promoción de trastornos metabólicos asociados con la obesidad.

ABSTRACT

Obesity is considered as a global epidemic both in developed and developing countries. One of the most important factors promoting obesity epidemic is the consumption of high fat diets (HFD) rich in saturated fatty acids such as palmitic acid (PA). Chronic intake of HFD is associated with the onset of metabolic diseases, including insulin resistance. Importantly, following chronic HFD exposure, PA accumulates in mice hypothalamus, the brain area responsible for the maintenance of energy homeostasis and for the regulation of body metabolism. One of the key cellular homeostatic processes impaired after HFD consumption is autophagy, a catabolic pathway aimed at recycling cytoplasmic components and damaged organelles by a lysosome-mediated process. During autophagy, the cellular cargo is sequestered within a double membrane vesicle called autophagosome, which fuses with a lysosome, to form the autolysosome, where, thanks to the activity of lysosomal enzymes, the autophagic cargo is degraded. The entire process from the autophagosome synthesis, up to their lysosomal degradation is termed autophagic flux. Importantly, autophagy dysregulation in hypothalamic neurons leads to metabolic disorders suggesting a key role for hypothalamic autophagy in the control of body metabolism. In addition, increased PA levels have been associated with autophagy impairment and with insulin resistance in the hypothalamus. However, the specific mechanism by which PA decreases autophagy in hypothalamic neurons is currently unknown. We propose PA-mediated inhibition of autophagy in hypothalamic neurons as a key mediator of obesity-associated metabolic disorders as insulin resistance.

The hypothesis of this thesis is that *palmitic acid inhibits the autophagic flux and decreases insulin sensitivity in hypothalamic neuronal cells*. We observed, in the N43/5 hypothalamic cell line and in primary hypothalamic neurons, that PA increases the number of autophagic structures and the amount of SQSTM1/p62, a protein degraded by the autophagic pathway, suggesting that PA inhibits the autophagic flux in hypothalamic neuronal cells. Importantly, the levels of several autophagy related genes essential for autophagosome formation were not increased by PA exposure, suggesting that PA induces the accumulation of autophagic structures as consequence of decreased autophagic flux in N43/5 cells. Moreover, by electron microscopy, we observed that PA induces the accumulation of large cellular degradative compartments in N43/5 hypothalamic neuronal cells. However, PA does not affect lysosomal acidity or their activity in our model. Then, we evaluated autophagosome-lysosome fusion by immunofluorescence, using N43/5 cells transfected with mCherry-GFP-LC3 and by assessing the co-localization between autophagosome and lysosome markers. We observed that PA decreased autophagosome-lysosome fusion, and that PA induced the accumulation of big autophagic structures. Furthermore, using a pull down assay, we quantified the activation state of Rab7, a protein involved in autophagosome-lysosome fusion, and we determined that PA increases the amount of Rab7 in the GTP-bound form, suggesting that PA impairs autolysosomes formation through the regulation of Rab7 activity. Additionally, through stable isotope labeling with amino acid in cell culture (SILAC), we found in isolated lysosomes from N43/5 cells treated with PA, increased levels of additional proteins involved with the control of endolysosomal trafficking and with autophagic maturation, which can further explain the mechanism by which PA impairs autophagy in hypothalamic neurons. Finally, we evaluated whether PA exposure contributes to metabolic disorders in our cellular model, and we confirmed

that PA decreases insulin sensitivity in hypothalamic N43/5 cells. Furthermore, inhibition of autophagy or autophagic flux also affects insulin sensitivity in these cells.

In summary, this study suggests that, in hypothalamic neuronal cells, autophagic flux inhibition induced by PA causes endolysosomal trafficking dysregulation and reduces insulin sensitivity. These data may help to elucidate the cellular mechanisms that underlie the effects of PA on the promotion of obesity-associated metabolic disorders.

1. INTRODUCTION

1.1. The obesity epidemics

Nowadays, obesity is considered as a global epidemic both in developed and developing countries. Obesity causes approximately 3.4 million annual deaths, and ranks as the 5th cause of death worldwide (Smith and Smith, 2016). Moreover, this chronic disease has been associated with several comorbidities such as type 2 diabetes, cardiovascular disease, hypertension, osteoarthritis, and even some types of cancer (Kopelman, 2000; Smith and Smith, 2016).

The body-mass index (BMI), a formula that combines weight and height, is used to determine if a subject has a normal body weight, if he is overweight or obese (Kopelman, 2000). The World Health Organization reports that worldwide, in 2016, 39% of adults were overweight (BMI 25.0–29.9 kg/m²), while 13% were obese (BMI > 30.0 kg/m²); these rates are expected to rise in the near future (2018). Importantly, the obesity epidemic directly affects Chile, which is now the most obese country in Latin America, reaching a 74,2% prevalence of adults with overweight or obesity (ENS, 2018).

Obesity is a multifactorial disorder and different genetic and environmental factors predispose to its development (Kopelman, 2000). Changes in lifestyle, resulting in increased consumption of dietary fats and reduced physical activity, have contributed to the rise of this metabolic disease (Flier, 2004). Consumption of the so-called “western style high fat diet”, hereafter indicated as “high fat diet” (HFD), which contains elevated levels of saturated fatty acids (SatFAs), increases body weight and is associated with the onset of metabolic diseases,

such as insulin resistance (Milanski et al., 2009; Posey et al., 2009; Zhang et al., 2009a). Physiological variations of plasma fatty acids (FAs) concentrations can be detected and integrated by FA sensing neurons in critical brain areas involved in the regulation of feeding behavior and lipid metabolism (Blouet and Schwartz, 2010; Migrenne et al., 2011). Importantly, the rate of FAs entry into the brain is relative to their plasma concentration (Miller et al., 1987), which is affected by the diet (Morselli et al., 2016). Moreover, an unbalance between different FA families, or excess of some of them, generates deleterious effects, including neurodegenerative and metabolic diseases (Hussain et al., 2013; Morselli et al., 2014b). Thus, it is critical to understand how FAs, particularly SatFAs, dysregulate cellular and molecular mechanisms involved in the onset of obesity associated diseases.

1.2. Fatty acids uptake and transport into the brain

FAs are classified by their carbon (C) chain length as short-chain (<12 C), medium-length (between 12 and 18 C) and long-chain (>18 C). Additionally, they are further classified based on the number of double bonds as SatFAs (no double bonds), monounsaturated (MUFAs) (one double bond) and polyunsaturated (PUFAs) (>one double bond) (Le Foll, 2019). The proportion of each FA absorbed and metabolized by the tissues depends on the food sources and dietary intake. On one hand, SatFAs have generally been associated with several deleterious effects on metabolism (Vessby, 2003), while MUFAs and PUFAs have shown beneficial properties (Bellenger et al., 2019).

Dietary fat is mainly composed of triglycerides (TG), cholesterol ester and phospholipids (Thomson et al., 1989). Briefly, once digested by enzymes in the mouth, stomach

and small intestine, TG are broken down into smaller particles such as monoglycerides, free fatty acids (FFAs) and cholesterol. These macromolecules are uptaken by intestinal cells where they are reorganized in structures called chylomicrons that are then released in the bloodstream to reach muscle, adipose tissues and the liver (Mu and Hoy, 2004; Ramirez et al., 2001). Lipoprotein lipases, produced by heart, liver, adipose tissue and other tissues, release the FAs from the lipoproteins and the majority of them bind to albumin. FA–albumin complexes are then transported to the bloodstream. Finally, FAs dissociate from albumin and are taken up by tissues in the body (Mitchell and Hatch, 2011; Pohl et al., 2004).

FAs are transported from the circulation to the brain where they can be converted into long-chain fatty acid-Coenzyme A and metabolized by mitochondrial β -oxidation to provide energy for the cell (Bazinet and Laye, 2014; Chen and Bazinet, 2015; Obici and Rossetti, 2003). As previously mentioned, brain FAs uptake is proportional to their plasma concentration (Miller et al., 1987), which is directly affected by the diet (Morselli et al., 2016). The central nervous system (CNS) possesses a very high concentration of FAs, secondary only to the adipose tissue (Chen and Bazinet, 2015). FAs are key components of cellular membranes and precursors for biosynthesis of phospholipids and sphingolipids (Bazinet and Laye, 2014), in addition, they play critical roles in signaling and they influence neuronal function, from early development up to natural aging (Bazinet and Laye, 2014). The mechanism of transportation of FAs from the periphery to the CNS, by crossing the blood-brain barrier (BBB) has been only partially elucidated (Dragano et al., 2019; Le Foll, 2019). The BBB (Spector, 1988) is a complex structure composed of endothelial cells that line the vessel wall, pericytes, astrocytes foot processes and a basal lamina (Daneman and Prat, 2015; Engelhardt et al., 2014). Together with neurons and microglia, the BBB forms the neurovascular unit, which is key to neurovascular coupling and

to the delivery of nutrients and oxygen from the circulatory system into the brain (Abbott et al., 2010; Banks, 2019). Endothelial cells of the BBB protect the brain against potentially dangerous substances through tight junctions. Furthermore, most brain areas lack fenestrations, limiting paracellular passage (Brightman and Reese, 1969; Fenstermacher et al., 1988; Hawkins and Davis, 2005; Le Foll, 2019). FAs cross the BBB (Spector, 1988), either by passive diffusion through the lipid bilayer by a process called FA flip-flop (Hamilton, 1999) or by facilitated transport of FAs, which requires saturable FA transporters (Mitchell and Hatch, 2011; Oomura et al., 1975; Wang et al., 2006). Once FAs dissociate from albumin (Bazinet and Laye, 2014) they can diffuse passively through the lipid bilayers, dependent on the lipophilic properties of the FA (Hamilton, 1999). Short-chain FA display the highest permeability while FA with a carbon chain over 12 C cannot directly pass through the BBB because of their ionic charge (Levin, 1980). Thus, to rapidly diffuse across the plasma membrane, long-chain FAs such as palmitic acid (PA), arachidonic acid and docosahexaenoic acid (DHA), which form a large proportion of the brain FAs, are transformed into a non-ionized form. This allows the flip-flop mechanism to occur independently of transport proteins (Hamilton et al., 2002; Hamilton et al., 2007; Kamp et al., 2003). Additionally, FAs can cross the BBB using different transporter proteins, which are located on the surface of brain endothelial cells (Mitchell and Hatch, 2011; Mitchell et al., 2011; Pelerin et al., 2014). FA transport proteins are: FA transport protein (FATP) 1 and 4 (Fitscher et al., 1998; Ochiai et al., 2017), FAT/CD36 (Abumrad et al., 2005), and intracellular FA binding proteins 1-7 (FABP) (Le Foll, 2019; Zimmerman et al., 2001). Recent data indicate that FATP1 and FATP4 are the most important FA transport proteins expressed on the BBB while CD36 has an important role in the transport of FAs across human brain microvessel endothelial cells (Bruce et al., 2017; Duca and Lam, 2014). In addition,

neurons from the ventromedial hypothalamus express FATP-1 and CD36 suggesting they are also able to uptake FAs (Le Foll et al., 2009). Also, the orphan receptor MSFD2A (major facilitator superfamily domain-containing protein 2A) has been shown to act as a transporter for DHA at the BBB (Ben-Zvi et al., 2014).

Transport mechanisms are key to brain areas with a BBB, however, circumventricular organs (CVO) located at the interface between the brain and the periphery present a highly fenestrated BBB. These sensory CVOs are: subfornical organ; organum vasculosum of the lamina terminalis; area postrema and the median eminence. In the medio-basal hypothalamus (MBH), a crucial area in the control of food intake and energy homeostasis, the arcuate nucleus (ARC), lying just above the median eminence at both sides of the third ventricle (Williams, 2012), also exhibits a “leaky” BBB due to the presence of tanycytes and fenestrated capillaries (Banks, 2019; Dehouck et al., 2014). In this region, the lesser number of tight junctions between endothelial cells allows the penetration of molecules from the circulation (Bennett et al., 2009). Thus, the fenestrated nature of the BBB surrounding the MBH facilitates FAs sensing affecting food intake and energetic metabolism (Valdearcos et al., 2015). Contrary to physiological conditions, during increased and sustained availability of nutrients, the hypothalamic nutrient-sensing system could be dysregulated and the pool of long chain FAs increased (Morgan et al., 2004; Obici et al., 2002a), alters energy intake and energy expenditure regulation (Dragano et al., 2019). Moreover, under pathological conditions, such as obesity and type 2 diabetes, there is an increase in circulating long chain FAs and increased uptake by the brain, which leads to an increase in hypothalamic levels of long chain fatty acyl-CoA impacting on the regulation of caloric intake and energy expenditure (Dietrich and Horvath, 2013; Dragano et al., 2019; Karmi et al., 2010).

1.3. High fat diet-induced obesity increases brain levels of saturated fatty acids

As previously mentioned, the fenestrated nature of the BBB near the MBH may facilitate FAs sensing process in order to regulate food intake and energetic metabolism. However, this privileged position also makes the MBH vulnerable to the stress-promoting and potentially toxic effects of circulating factors from the environment, including those associated with chronic over-nutrition. Research has shown that hypothalamic neurons are particularly susceptible to nutrient-induced oxidative stress and mitochondrial dysfunction (Singh et al., 2012). Moreover, studies indicate that obesity and chronic HFD consumption, especially diets rich in SatFAs correlate with reduced BBB integrity (Gustafson et al., 2007; Kanoski et al., 2010; Ouyang et al., 2014; Rhea et al., 2017). Particularly, an increased BBB permeability has been observed in HFD-induced obesity, and it has been associated to a decreased expression in several tight junction proteins (Kanoski et al., 2010) and with downregulation of cytoskeletal proteins including vimentin and tubulin (Ouyang et al., 2014), which could alter membrane fluidity preventing tight junction alignment or transport of tight junctions in diet-induced mice (Rhea et al., 2017). In these conditions, not only the transport of FAs is affected, but also those of other hormones/macromolecules. As an example, the transport rate of insulin across the BBB is about half in obese mice when compared to lean mice (Rhea and Banks, 2019; Urayama and Banks, 2008), suggesting alterations in the BBB might be tightly related to the development of metabolic dysfunctions development such as insulin resistance (Rhea and Banks, 2019).

Importantly, chronic HFD increases the levels of SatFAs in the CNS (Rodriguez-Navas et al., 2016), specifically, the long-chain SatFA palmitic acid (PA) (16:0) augmented in mice hypothalamus after chronic HFD feeding (Vagena et al., 2019).

1.4. Role of the hypothalamus in the regulation of energy balance and body metabolism

The hypothalamus is the brain area responsible for the maintenance of energy homeostasis and for the regulation of body metabolism (Blouet and Schwartz, 2010; Carmo-Silva and Cavadas, 2017). The regulation of these processes arises from the ability of the hypothalamic neurons to regulate energy balance and food intake, by directly sensing FAs or glucose (Blouet and Schwartz, 2010; Lam et al., 2005) and by integrating hormonal and neuronal signals indicative of the nutritional status (Lopez et al., 2007). These neurons alter their membrane potential and activity in response to these stimuli, resulting in the activation of ion channels and enzymes or release of a variety of substrate transporters, thus regulating food intake and energetic homeostasis (Le Foll, 2019; Le Foll et al., 2009; Levin, 2006; Migrenne et al., 2011; Oomura et al., 1975; Wang et al., 2006). The principal area containing these neuronal circuits is the ARC, but within the hypothalamus the paraventricular nucleus (PVN) and the dorsomedial hypothalamus also have a role in the regulation of energy balance (Gali Ramamoorthy et al., 2015).

In the ARC, the hypothalamus coordinates a neuronal network that regulates caloric intake, spontaneous physical activity, feeding behavior, thermogenesis, and distinct aspects of whole body metabolism (Sohn, 2015). Importantly, as already mentioned, this region is close to the median eminence, which is susceptible to leakage from the BBB; ARC neurons are, therefore, consistently exposed to nutrients and hunger and satiety hormones (Sohn, 2015). In addition, projections from this hypothalamic nucleus will reach the PVN to regulate energy balance (Cone, 2005).

In the ARC, there are, among others, two critical first-order neuronal populations for the detection of nutritional and hormonal signals such as leptin or insulin, as well as for the sensing of intracellular metabolites (Andrews et al., 2008; Benoit et al., 2004): the anorexigenic proopiomelanocortin (POMC) neurons and the orexigenic agouti-related peptide/neuropeptide Y (AgRP/NPY) neurons. These neurons have opposite effects in the regulation of appetite and satiety and play a key role in the control of body weight (Mandelblat-Cerf et al., 2015).

POMC neurons produce signals that decrease food intake, induce satiety, and promote energy expenditure, thereby reducing body weight (Mountjoy, 2010). Lack of these neurons in POMC-knockout mice promotes hyperphagia and obesity (Yaswen et al., 1999), and direct and specific activation of POMC neurons through chemogenetic and optogenetic stimulation methods suppresses food intake (Zhan et al., 2013). It has been widely shown that, after a meal, nutrients promote the secretion of two hormones: leptin (mainly from the adipose tissue) and insulin (from the pancreas) (Williams et al., 2010), which activate POMC neurons in the ARC, thus inhibiting food intake. After being activated, POMC neurons express the POMC pro-peptide, which is processed to produce the α -melanocyte-stimulating hormone (α -MSH). α -MSH is an agonist of the melanocortin receptors localized on melanocortin neurons, which are located in the PVN; their activation promotes the anorexigenic response (Yang et al., 2011). Consistently, mutations in the gene coding for the melanocortin-4 receptor result in hyperphagia and obesity in mice and humans (Farooqi et al., 2003). Altogether, this evidence demonstrates the existence of a specialized anorexigenic neuronal circuit (Avalos et al., 2017).

The other first-order neuronal population consists of the orexigenic AgRP/NPY neurons: they promote food intake and reduce energy expenditure, thereby increasing body weight

(Sainsbury and Zhang, 2010). Stimulation of AgRP/NPY neurons leads to hyperphagia in mice (Farooqi et al., 2003; Krashes et al., 2011); conversely, ablation of AgRP/NPY neurons leads to suppression of food intake in adult mice (Luquet et al., 2005). Additionally, recent evidence suggests that acute activation of AgRP/NPY neurons causes insulin resistance and impairs insulin-stimulated glucose uptake in brown adipose tissue in mice (Luquet et al., 2005). These results provide new evidence about the role of AgRP/NPY neurons in glucose homeostasis in addition to their orexigenic role.

Thus, POMC and AgRP/NPY neurons are functionally antagonistic and through the release of specific neuropeptides modulate neural networks regulating food intake, energy expenditure and body weight (Avalos et al., 2017; Mandelblat-Cerf et al., 2015; Sohn, 2015; Yaswen et al., 1999; Zhan et al., 2013).

1.5. Insulin signaling in the hypothalamus

Accumulating evidence indicates that HFD consumption boosts the development of obesity and metabolic diseases such as insulin resistance (Benoit et al., 2009; De Souza et al., 2005; Oh et al., 2013). Importantly, CNS exposure to PA via direct infusion or by oral gavage impairs hypothalamic insulin signaling (Benoit et al., 2009), indicating that an increase in this FA affects insulin response. Insulin, produced by β -pancreatic cells, is released in the circulation, it crosses the BBB in a receptor-dependent manner and reaches the hypothalamus (Banks, 2004), where it binds POMC and AgRP/NPY neurons which express insulin receptors (IR) (Cone et al., 2001; Lenard and Berthoud, 2008), IR has 2 heterogeneous binding sites for insulin, where the first insulin molecule binds at high affinity and the second insulin binds at a

lower affinity (De Meyts, 1976). Upon IR activation by insulin, the intrinsic tyrosine kinases undergo autophosphorylation, leading to the recruitment and phosphorylation of the IR substrate (IRS) protein-1, 2, and 3 (Czech et al., 1988; Kahn and White, 1988). The phosphorylation of IRS proteins on serine residues might enhance or inhibit insulin actions. On one side, protein kinase B (AKT) activation in response to IR stimulation triggers the phosphorylation of IRS proteins on serine residues inducing a positive-feedback loop for insulin action. On the other side, insulin also activates the downstream phosphoinositide 3-kinase (PI3K) signaling cascade leading to AKT activation and other downstream transmitters such as I κ B kinase, extracellular-signal-regulated kinase (ERK), Jun N-Terminal Kinase (JNK), protein kinase C (PKC), and mammalian Target of Rapamycin (mTOR), which negatively phosphorylate IRS proteins on specific sites and inhibit the receptor activity (negative-feedback loop) (Gual et al., 2005; Lawrence et al., 1997). Finally, these intracellular signaling events promote Glucose Transporter 4 (GLUT4) translocation from an intracellular storage compartment to the cell surface (Slot et al., 1991), allowing glucose uptake into insulin-responsive cells.

Importantly, despite others GLUTs have been described in the hypothalamus, including GLUT1 and GLUT3 (Jurcovicova, 2014; Yu et al., 1995), GLUT4 is, up to date, the only insulin-dependent GLUT required for the transportation of glucose into the cell that has been described in hypothalamic neurons (Jurcovicova, 2014; Leloup et al., 1996; Thierry Alquier et al., 2006). Thus, the translocation of GLUT4, induced by insulin, is necessary for glucose uptake in hypothalamic neurons (Changou et al., 2017; Jurcovicova, 2014; Ren et al., 2015; Thierry Alquier et al., 2006).

Central delivery of insulin increases hypothalamic expression of α -MSH and inhibits NPY and AgRP gene expression (Benoit et al., 2002; Schwartz et al., 1992), reducing food intake and body weight (Niswender et al., 2003). In addition, it has been reported that insulin, through its action on hypothalamic ARC neurons, regulates hepatic glucose production (Konner et al., 2007; Obici et al., 2002b), glycogen synthesis (Perrin et al., 2004), and fat metabolism (Koch et al., 2008; Shin et al., 2017), via autonomous nervous system connections (Chen et al., 2017). Thus, insulin signaling pathway in the hypothalamus modulate the central regulation of feeding and whole body energy homeostasis (Chen et al., 2017).

As mentioned above, HFD consumption predisposes to obesity-induced insulin resistance. In addition, PA direct infusion into the CNS alters hypothalamic insulin responsiveness deregulating energy homeostasis control (Benoit et al., 2009; De Souza et al., 2005; Oh et al., 2013). Several mechanisms have been proposed to explain the loss of hypothalamic insulin action induced by HFD or due to increased brain FAs content, including a reduced hypothalamic insulin uptake as consequence of impaired transport across the BBB (Banks et al., 1997; Urayama and Banks, 2008). However, it has been shown that direct delivery of insulin in the brain did not reverse obesity-induced metabolic dysregulation (Heni et al., 2014; Ikeda et al., 1986), suggesting that the defect in insulin uptake into the brain is not the only mechanism (Benomar and Taouis, 2019).

It has been shown that long-term HFD consumption, as well as PA injection in the hypothalamus, inhibits hypothalamic autophagy (Meng and Cai, 2011; Portovedo et al., 2015), a catabolic pathway aimed at recycling cytoplasmic components and damaged organelles by a lysosome-mediated process (Yang and Klionsky, 2010). Importantly, defective autophagy is

associated with impaired insulin sensitivity in the hypothalamus (Meng and Cai, 2011), suggesting that a crosstalk between autophagy and insulin signaling could be involved in the onset of insulin resistance (Codogno and Meijer, 2010; de Mello et al., 2019).

1.6. Overview of the autophagic process

Autophagy is a mechanism in which intracellular components and dysfunctional organelles are delivered to lysosomes for degradation and recycling (Yang and Klionsky, 2020). The term “autophagy” literally means “self-eating,” and the autophagic process constitutes a major intracellular degradation system capable of ridding cells of proteins with long half-lives, as well as protein aggregates, and organelles (Kaur and Debnath, 2015). Thus, this catabolic process helps maintaining the balance among synthesis, degradation, and recycling of cellular components and it is involved in the preservation of cellular homeostasis and function (Yang and Klionsky, 2010).

Depending on the mechanism of how cargos are delivered to lysosomes for degradation, there are three general types of autophagy, including macroautophagy, microautophagy and chaperone-mediated autophagy (CMA) (Parzych and Klionsky, 2014; Yang and Klionsky, 2020; Yang and Klionsky, 2010). Microautophagy involves the transport of cytosolic material into lysosomes through direct invagination or protrusion of the lysosomal membrane (Mijaljica et al., 2011). During CMA, unfolded soluble proteins selectively translocate across the lysosomal membrane, based on the recognition of a CMA-specific consensus motif, the pentapeptide KFERQ (Wu et al., 2015). Macroautophagy is the best-characterized and most highly conserved mechanism from yeast to mammals, among the three types of autophagy

(Eskelinen, 2008b; Eskelinen and Saftig, 2009; Feng et al., 2014). Macroautophagy, hereafter referred to as “autophagy”, requires the sequestration of degradation targets in special double membrane organelles known as autophagosomes. Once the material destined for degradation is enclosed, the outer membrane of the autophagosomes fuses to lysosomes, forming a new vesicle called autolysosome. This ultimately leads to the degradation of the sequestered material along with the inner membrane of the autophagosomes (Fig. 1) (Eskelinen and Saftig, 2009). The essential metabolites derived from degradation return then back to the cytoplasm for the synthesis of new macromolecules (i.e., proteins) or energy production (Kaur and Debnath, 2015).

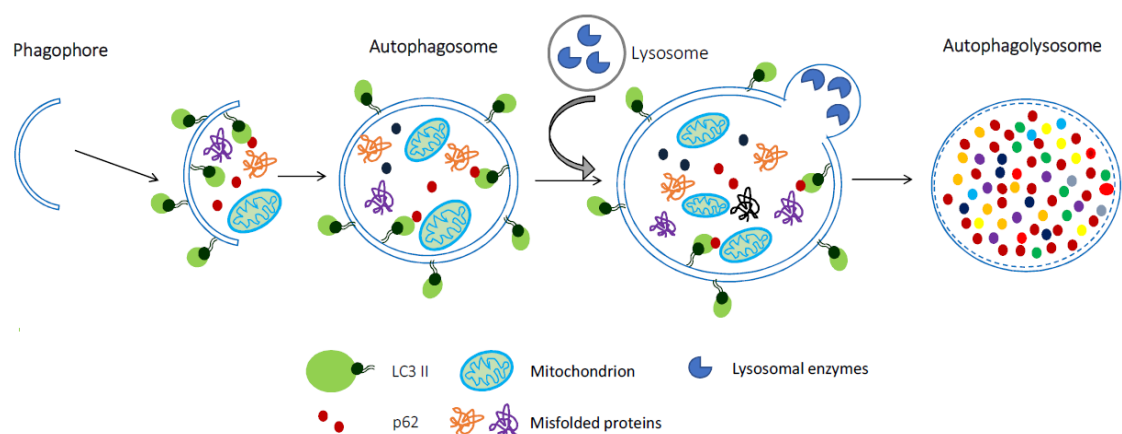


Figure 1: General scheme of autophagy. This process begins with the formation of the isolation membrane (phagophore). The autophagosome, a double membrane vesicle that integrates the protein LC3-II, surrounds the cargo, mostly damaged organelles like mitochondria, misfolded proteins and autophagy-receptor proteins such as p62. The fusion of lysosomes with autophagosomes causes the formation of autolysosomes, where autophagic substrates are exposed to hydrolytic enzymes resulting in their degradation and recycling. The details of the process are discussed in the main text. Figure from Ávalos et al., 2018. *Cell and molecular mechanisms behind diet-induced hypothalamic inflammation and obesity*.

Based on the physiological status of the cell, the autophagic process can occur in basal conditions to maintain cellular homeostasis, or can be induced in response to stress conditions such as nutrient deprivation or an increase in misfolded proteins (Eskelinen and Saftig, 2009). Hence, autophagy is an adaptive mechanism that increases cell's ability to survive under mild stress conditions. Considering the key role of autophagy in the clearance of damaged proteins and organelles, dysregulation of this mechanism leads to several diseases such as neurodegeneration and metabolic disorders (Mizushima and Komatsu, 2011). Importantly, autophagy impairment has been widely associated with obesity and with the onset of insulin resistance (Avalos et al., 2017; Carmo-Silva and Cavadas, 2017; Codogno and Meijer, 2010; de Mello et al., 2019).

Different “autophagy-related proteins” (ATGs) (Klionsky et al., 2003) are involved in the autophagic process, which can be divided into five stages (initiation, nucleation, elongation, fusion with the lysosome, and cargo degradation) followed by the release of breakdown products into the cytosol (Fig. 2).

The “initiation stage” involves the activation of the unc-51-like kinase 1 (ULK1)/focal adhesion kinase family interacting protein of 200 kDa (FIP200)/ATG13 complex (ULK1 complex), which is achieved by modulation of metabolic sensors (Ravikumar et al., 2010). The most important is the Serine/Threonine (Ser/Thr) kinase activity of the mammalian target of rapamycin complex 1 (mTORC1), which inhibits the ULK1 complex under basal conditions. Conversely, in metabolic stress conditions such as nutrient deprivation, cells deplete adenosine triphosphate (ATP), increasing adenosine monophosphate (AMP) levels and enhancing the activity of the AMP-activated protein kinase (AMPK), which also has a Ser/Thr kinase activity.

AMPK can phosphorylate ULK1 at different sites that, unlike mTORC1, will activate ULK1 complex and thereby, initiate autophagy (Kim et al., 2011). Once activated, the ULK1 complex translocates to membranous sites where the autophagosome forms, also known as “phagophore assembly site” (PAS), which are located at the plasma membrane, the primary cilia or interaction sites between the endoplasmic reticulum (ER) and the mitochondria (Mizushima and Komatsu, 2011; Reggiori and Ungermann, 2017). In mammals, these sites are referred to as omegasomes (Reggiori and Ungermann, 2017).

Then, the isolation membrane of the new autophagosome is generated during the “nucleation stage”. A kinase complex formed by Vacuolar Sorting Protein (VPS) 34 (VPS34), Beclin-1, and VPS15 and Autophagy related 14-like protein (ATGL14) generates phosphatidylinositol 3-phosphate (PI3P) where the isolation membrane is formed, which will generate the new autophagosome (Itakura and Mizushima, 2010; Ravikumar et al., 2010). ATG9-containing vesicles cycle between the PAS/omegasome and the Golgi/endosomes, and they contribute to the recruitment of membranes for the nucleation of the phagophore (Reggiori et al., 2004; Reggiori and Ungermann, 2017; Yamamoto et al., 2012).

Then, the phagophore extends during the “elongation stage”, a process that is tightly regulated by two ubiquitin-like systems: the microtubule-associated protein 1A/1B-light chain 3 (MAP1LC3A, also known as LC3-I) system and the ATG5–ATG12 system (Ohsumi and Mizushima, 2004). In basal conditions, the LC3-I protein is uniformly distributed across the cytoplasm; however, when autophagy is induced, LC3-I is cleaved by ATG4. Then, ATG3 modifies the lipid phosphatidylethanolamine (PE) on LC3-I, generating LC3-II and redistributing LC3 to phagophore/ autophagosomal membranes (Tanida et al., 2004). The

second conjugation system is represented by the ATG5–ATG12 complex, facilitated by ATG7, an E1-like protein, and ATG10, an E2-like protein. The ATG5–ATG12 complex then interacts with ATG16L, forming a new complex that works like an E3 enzyme, assisting the incorporation of LC3-II into the membrane of the phagophore (Hanada et al., 2007).

The selection of the autophagic cargo occurs in parallel to the processes of sensing, initiation and elongation. Proteins are targeted for autophagy by ubiquitination and labeled primarily with the receptor p62/Sequestosome-1 (SQSTM1), which, through an LC3 interacting region (LIR) (Johansen and Lamark, 2011; Pankiv et al., 2007), recruits LC3-II to the isolation membrane (Pankiv et al., 2007). Once the target cargo is bound by LC3-II, the initiation machinery is recruited. The final closure of the phagophore leads to the formation of the autophagosome. This step is completed by a membrane abscission process mediated by the endosomal sorting complex required for transport (ESCRT) (Takahashi et al., 2018; Yu and Melia, 2017). This new autophagosome is a double membraned vesicle, which contains the targeted cargo (Ravikumar et al., 2010). Upon closure, the nascent autophagosome dissociates from the assembly site and undergoes maturation (Zhao and Zhang, 2019).

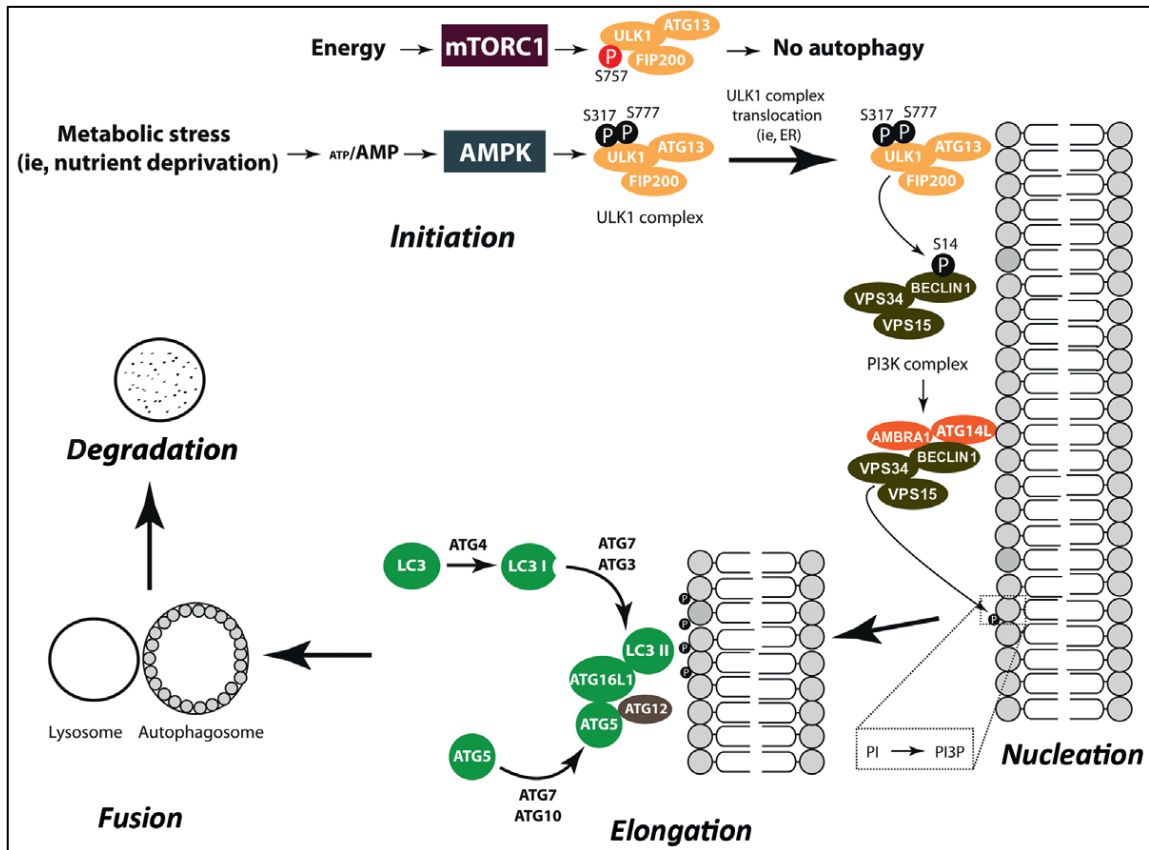


Figure 2: Overview of the autophagic process. Autophagy initiation involves the activation of multiple molecular components, which are regulated by energy/nutritional status. Activation of the ULK1–FIP200–ATG13 complex initiates phagophore nucleation, which is the first step in the process of autophagosome formation. Thanks to the activity of different ATG proteins, the phagophore elongates forming the autophagosome, which encloses the cytosolic material that will be degraded. Once the autophagosome is completed, it fuses with the lysosome to allow the degradation of the enclosed materials to proceed. See the text for additional information. AMBRA, Activating molecule in BECLIN1-regulated autophagy; AMPK, AMP-activated protein kinase; ATG, autophagy-related; FIP200, focal adhesion kinase family interacting protein of 200 kDa; LC3, microtubule-associated protein 1A/1B-light chain 3; mTORC1, mammalian target of rapamycin complex 1; P, inorganic phosphate; PI3K, phosphatidylinositol 3-kinase; PI3P, phosphatidylinositol (3,4,5)-trisphosphate; TSC1/TSC2, tuberous sclerosis protein 1/2; Ub, ubiquitin; ULK1, unc-51-like kinase; VPS, vacuolar protein sorting. Figure

from Hernandez-Caceres et al., 2016. *Mutant P53 Located In The Cytoplasm Inhibits Autophagy* (Hernandez-Caceres et al., 2016).

Autophagosome maturation refers to the process involving the progression of nascent autophagosomes to degradative autolysosomes (Eskelinen, 2005). In multicellular organisms, autophagosomes are formed simultaneously at different sites, and nascent autophagosomes fuse with either early/late endosomes to form amphisomes (which its final fate is the lysosome), and with lysosomes to form autolysosomes, where the cargo will be degraded (Eskelinen, 2005; Zhao and Zhang, 2019). During the maturation process, all ATG proteins are removed from the surface of the autophagosome. This process requires the removal of PI3P and LC3 by phosphoinositide phosphatases and possibly other factors and by members of the ATG4 protease family, respectively. (Cebollero et al., 2012; Galluzzi et al., 2017; Wu et al., 2014). It must be noted that the conversion of PI3P into phosphatidylinositol-3,5,-biphosphate PI(3,5)P₂ by mammalian PIKfyve kinases is an important mechanism to dissipate PI3P during endosome maturation (McCartney et al., 2014; Odorizzi et al., 1998).

Subsequently, autophagosomes are transported toward the perinuclear region of the cell, where acidic lysosomes are mainly concentrated. Here, autophagosomes fuse with endolysosomes vesicles to generate autolysosomes (Korolchuk and Rubinsztein, 2011). Microtubules and actin filaments are the two main components of the cell's cytoskeleton and both have been implicated in the trafficking of autophagosomes (Monastyrska et al., 2009). By using a dynein-dependent transport on microtubules autophagosomes are mobilized toward lysosomes. In neurons, autophagosomes acquire retrograde mobility by fusing with dynein-

loaded late endosomes to form amphisomes, which are then trafficked to the soma, the main location of mature acidic lysosomes (Cheng et al., 2015).

The vesicle trafficking process requires, among other proteins, Rab GTPases, which cycle between inactive (GDP) and active (GTP) conformation states. Rab GTPases are activated by GEFs (guanine nucleotide exchange factors), driving GTP binding, and then inactivated by GAPs (GTPase activating proteins), that hydrolyze the bound GTP to GDP, causing loss of effector binding and extraction from membranes (Lamber et al., 2019). The small GTPase Rab7 is located on late endosomes, lysosomes, and recruited to autophagosomes (Gutierrez et al., 2004). This GTPase is able to recruit various effectors including motor proteins and tethering factors to target membranes, thus it is important both for the movement and for the fusion of autophagosomes with endolysosomal vesicles (Cabrera et al., 2014; Hegedus et al., 2016; Pankiv et al., 2010). Rab7 links autophagosomes to microtubule motors through FYCO1 (FYVE and coiled-coil domain-containing 1), thereby mediating kinesin-driven movement towards the cell periphery (Pankiv et al., 2010). In addition, Rab7 interacts with Rab-interacting lysosomal protein (RILP) and with dynein protein in order to facilitate the transport of autophagosomes, autolysosomes and lysosomes to the perinuclear region (Jordens et al., 2001; Kawai et al., 2007; Wijdeven et al., 2016).

Once the autophagosome and the lysosome encounter the outer membrane of the autophagosome fuses with the lysosome forming an autolysosome. The fusion of endolysosomal vesicles with autophagosomes broadly require three set of protein families: Rab GTPases, membrane-tethering complexes and soluble N-ethylmaleimide-sensitive factor attachment protein receptors (SNAREs) (Nakamura and Yoshimori, 2017). Rab proteins

localize to specific membranes and recruit tethering complexes that act as bridges to bring the compartments intended for fusion together (Stenmark, 2009; Zhen and Stenmark, 2015). These tethering complexes, in turn, help SNARE proteins to physically drive the fusion of opposing lipid bilayers (Nakamura and Yoshimori, 2017).

On one hand, syntaxin 17 (STX17), a SNARE protein, on the autophagosomes forms the “trans-SNARE complex” with vesicle-associated membrane protein 8 (VAMP8), another SNARE protein, on the lysosomes and with synaptosomal-associated protein 29 (SNAP29) in the cytoplasm (Itakura et al., 2012), which mediate autophagosome-lysosome fusion. As mentioned, ATG14L, which is essential for inducing autophagy, also participates in autophagosome-lysosome fusion by binding with STX17 and SNAP29 (Diao et al., 2015).

On the other hand, Rab7 not only regulates autophagosome movement but also plays a key role in autophagosome-lysosome fusion and in cargo degradation (Gutierrez et al., 2004), through the recruitment of several tethering factors to promote the assembly of trans-SNARE complexes for fusion (Guerra and Bucci, 2016). In addition, it has recently been described a lysosome-associated multiprotein complex named BLOC-1 related complex (BORC), which interacts with the small GTPase ARL8 on lysosomes, to promote ARL8-dependent association to kinesins, resulting in lysosome movement toward the cell periphery (Jia et al., 2017). BORC coordinates peripheral deployment of lysosomes with autophagosome-lysosome fusion. The movement of autophagosomes and lysosomes affects the frequency of autophagosome-lysosome fusion and the recruitment of fusion factors (Zhao and Zhang, 2019). Once lysosomes and autophagosomes fuse, the inner membrane of the autophagosome breaks down and the process of autophagosomal cargo degradation begins (Yu et al., 2018). The degradation

products, including amino acids and sugars, are recycled and turn back to the cytosol thanks to the activity of lysosome efflux transporters (Rong et al., 2011; Yu et al., 2010). The last step of the autophagic process is known as autophagic lysosome reformation and is fundamental for lysosome homeostasis (Yu et al., 2010). During this process, lysosomes are reformed by recycling of lysosomal components from autolysosomes, which allows the maintenance of the number of catabolically active lysosomes (Yu et al., 2010).

The whole process of autophagy, from the synthesis of the autophagosomes up to their lysosomal degradation is defined as autophagic flux (Yang and Klionsky, 2010). Proper function and integrity of the lysosome is essential for the whole autophagic process to occur. Degradation of the inner membrane and autophagosome cargo including LC3-II is dependent on lysosomal hydrolases such as cathepsin B, D, and L. Finally, the degraded autolysosome content is released into the cytosol for protein synthesis and to maintain cellular homeostasis (Geronimo-Olvera and Massieu, 2019).

Autophagy impairment results in the accumulation of misfolded proteins and superfluous or damaged organelles. Defective autophagy could lead to cell death and causes different type of diseases, depending on the cell type involved (Sridhar et al., 2012). As an example, genetic inactivation of autophagy in the CNS causes spontaneous neurodegeneration (Hara et al., 2006; Komatsu et al., 2006). Importantly, defective autophagy in the MBH leads to over-eating, impaired energy expenditure, increased weight gain, and obesity-associated metabolic complications, such as insulin resistance (Coupe et al., 2012; Meng and Cai, 2011; Quan et al., 2012). These studies indicate hypothalamic neuronal autophagy is necessary to

maintain metabolic homeostasis and to prevent metabolic diseases, which will be discussed in details in the next section.

1.7. Hypothalamic autophagy regulates metabolic homeostasis

The role of autophagy in the development of metabolic diseases has been studied in several tissues critical for the regulation of body metabolism, including pancreas (specifically in β cells) (Ebato et al., 2008; Jung et al., 2008), adipose tissue (Singh et al., 2009; Zhang et al., 2009b), liver (Yang et al., 2010), muscle (Masiero et al., 2009), and hypothalamus (Coupe et al., 2012; Meng and Cai, 2011; Quan et al., 2012).

As already mentioned, the hypothalamus is a fundamental brain region for the regulation of energy homeostasis and body metabolism. Different studies have identified a possible connection between the inhibition of hypothalamic autophagy with the impairment of energy balance and with the onset of metabolic dysfunctions (Coupe et al., 2012; Kaushik et al., 2011; Oh et al., 2016; Portovedo et al., 2015; Quan et al., 2012; Rubinsztein, 2012).

Specifically, hypothalamic inhibition of autophagy by shRNA-mediated *Atg7* knockdown leads to increased body weight due to hyperphagia and decreased energy expenditure, as well as insulin resistance upon HFD consumption, suggesting that hypothalamic autophagy plays a key role in the maintenance of energy homeostasis (Meng and Cai, 2011; Morselli et al., 2014a). Moreover, the specific deletion of *Atg7* in hypothalamic POMC expressing neurons increases body weight, promotes food intake and reduces energy expenditure in mice fed a normal diet. Importantly, these mice show increased blood glucose

levels, reduced glucose tolerance and insulin resistance (Coupe et al., 2012; Kaushik et al., 2012; Quan et al., 2012). Interestingly, insulin resistance occurs in *Atg7* POMC-knockout mice with a body weight similar to age-matched controls (Kaushik et al., 2012), suggesting that the loss of autophagy in POMC neurons is sufficient to dysregulate glucose homeostasis before the onset of obesity.

In addition, inhibition of autophagy in POMC neurons promotes adipose accumulation and impairs fasting-induced lipolysis. POMC-specific *Atg7* knockout mice show increased liver weights and triglycerides content. Additionally, these mice are resistant to fasting-induced loss of body fat and display reduced circulating levels of free FAs and glycerol (Kaushik et al., 2012), suggesting decreased fasting-induced lipolysis when compared with control mice. Additionally, it has been demonstrated that POMC-specific deletion of *Atg12* promotes adiposity, increases food intake, and drives glucose intolerance in mice fed with HFD for 12 weeks (Malhotra et al., 2015). In contrast to mice where autophagy is inhibited in POMC neurons, knockout of *Atg7* in orexigenic AgRP neurons generates mice with reduced fat mass and decreased hyperphagic response to fasting (Kaushik et al., 2011). In conclusion, the inhibition of autophagy in orexigenic neurons generates a lean phenotype while the inhibition of autophagy in anorexigenic neurons leads to an obese phenotype.

Altogether, these studies indicate neuronal hypothalamic autophagy is critical for the control of cellular energy balance, and for the maintenance of whole-body metabolism. Autophagy impairment, mainly in POMC neurons, has been shown to contribute to the onset of obesity and obesity-associated metabolic disorders, particularly insulin resistance (Avalos et al., 2017; Carmo-Silva and Cavadas, 2017; Kim and Lee, 2014).

1.8. Regulation of autophagy by high fat diet

As mentioned above, increased amounts of long-chain SatFAs specifically acting in the hypothalamus cause metabolic disorders (Posey et al., 2009). Chronic consumption of a HFD rich in SatFAs increases the amount of SatFAs in the brain, specifically in the hypothalamus, and inhibits hypothalamic autophagy in mice, impairing the hypothalamic regulation of energy balance (Fig. 3) (Meng and Cai, 2011; Morselli et al., 2014a; Portovedo et al., 2015; Thaler et al., 2012; Vagena et al., 2019). However, up to date, the molecular mechanisms that cause inhibition of hypothalamic autophagy following HFD consumption have not been elucidated.

Specifically, chronic HFD feeding for 4 months decreases the expression of autophagic markers in mice ARC, as evidenced by a reduction of ATG5 and ATG7 protein levels, both involved in autophagosome formation. Moreover, the protein levels of LC3-II in the hypothalamus of HFD-fed mice are significantly lower than those of chow-fed mice, indicating a decrease in autophagy (Meng and Cai, 2011). In accordance with this study, the protein levels of LC3-II and Beclin-1 decreased, while the levels of SQSTM1 increased in the hypothalamus of HFD-induced obese mice (Portovedo et al., 2015). These data demonstrate that chronic feeding with an HFD impairs hypothalamic autophagy, inducing the accumulation of protein aggregates and loss of cellular homeostasis (Portovedo et al., 2015).

Conversely, after 20 weeks of 60% HFD feeding, the percentage of POMC neurons with detectable autophagosomes increases more than 10-folds, which could be due to an increase in autophagosome formation or a decrease in autophagosome degradation in POMC neurons (Thaler et al., 2012). Accordingly, studies performed in the CLU-189 adult mouse hypothalamic

cell line treated for 12 h with preconditioned medium collected from a microglial cell line previously exposed to palmitate show a reduction in Beclin-1 protein and an increase in the levels of LC3-II and SQSTM1 (Portovedo et al., 2015). These data suggest a dysregulation of the autophagic process when neuronal cells are exposed to SatFAs.

As previously indicated, PA is the most common SatFA found in animals, and it is significantly increased in the plasma of obese people (Opie and Walfish, 1963) and in the brain of mice following HFD consumption (Morselli et al., 2014b; Rodriguez-Navas et al., 2016). As mentioned above, the long-chain SatFA PA (16:0) accumulates in the hypothalamus of mice after 4 and 8 weeks of HFD feeding (Vagena et al., 2019). Whether the increase in PA, caused by long-term consumption of HFD specifically affects autophagy is unknown.

Nowadays, different signaling pathways involved in autophagy regulation have been identified (Mehrpour et al., 2010), however if and how PA modulates autophagy in hypothalamic neurons is still unknown. Considering these data, we hypothesized that PA is a key mediator of HFD-associated metabolic disorders, such as insulin resistance, because it inhibits autophagic flux in hypothalamic neurons.

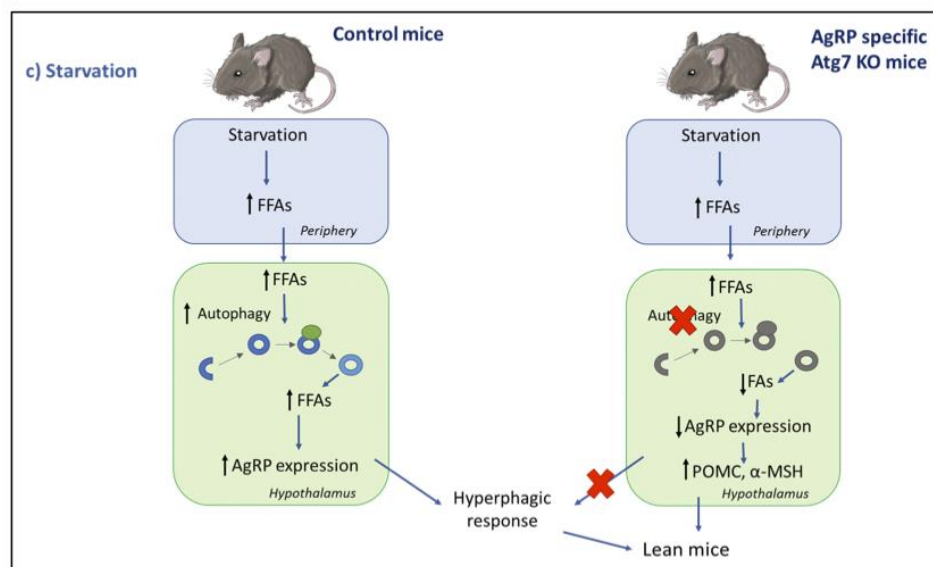
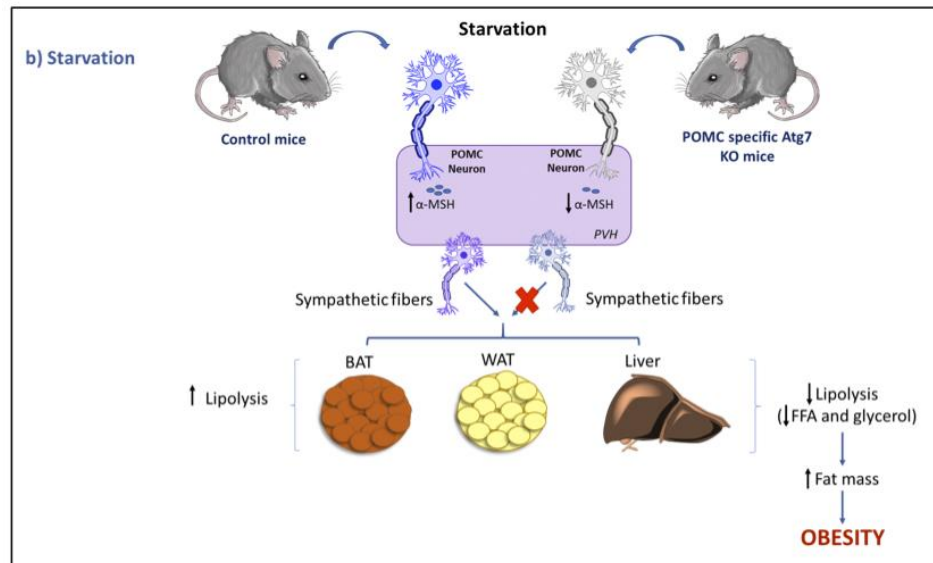
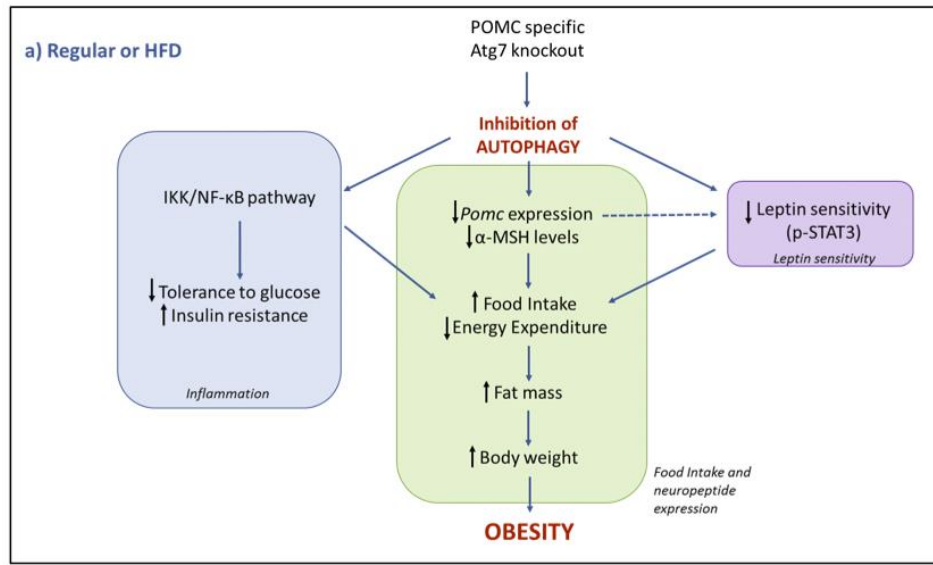


Figure 3: Role of autophagy in POMC and AgRP neurons in the control of energetic metabolism. Effect of the POMC-specific autophagy-related gene 7 (*Atg7*) knockout (KO) in mice fed with regular or high-fat diet (HFD) (A) and starvation (B). Briefly, inhibition of autophagy specifically in POMC neurons promotes obesity in mice, due to an increase in food intake and a decrease in energy expenditure caused by diminished *Pomc* expression and α -MSH levels. Depletion of autophagy in POMC neurons also impairs glucose tolerance and drives insulin resistance. Importantly, both dysregulation of glucose homeostasis and obesity are caused by activation of the IKK/NF- κ B proinflammatory signaling pathway. In addition, mice depleted of *Atg7* in POMC neurons are leptin resistant and hyperphagic. (A) POMC-specific *Atg7* KO mice subjected to starvation show a decrease in the release of α -MSH into the PVH which, in turn, inhibits sympathetic outflow to peripheral tissues such as liver, WAT, and BAT, decreasing starvation-induced lipolysis and augmenting fat mass (B). (C) Effect of the AgRP-specific autophagy-related gene 7 (*Atg7*) KO in mice subjected to starvation. Starvation-induced lipolysis increases FFA levels at periphery. These FAs cannot activate autophagy in AgRP neurons. This decreases the level of intracellular FAs, which reduces *AgRP* expression and, consequently, increases POMC and α -MSH levels, inhibiting hyperphagic response to starvation and generating a lean phenotype in mice. α -MSH, α -melanocyte stimulating hormone; BAT, brown adipose tissue; FA, fatty acids; FFA, free fatty acids; IKK/NF- κ B, I κ B kinase/nuclear factor- κ B; KO, knockout; PVH, paraventricular nucleus of the hypothalamus; STAT3, signal transducer and activator of transcription 3; WAT, white adipose tissue. Figure from Ávalos et al., 2018. *Cell and molecular mechanisms behind diet-induced hypothalamic inflammation and obesity*.

2. HYPOTHESIS

Palmitic acid inhibits the autophagic flux and decreases insulin sensitivity in hypothalamic neuronal cells.

3. GENERAL AIM

To evaluate whether and how palmitic acid inhibits the autophagic flux and its impact on insulin sensitivity in hypothalamic neuronal cells.

4. SPECIFICS AIMS

(1) To assess if palmitic acid inhibits the autophagic flux in hypothalamic neurons.

1.1. To analyze, *in vitro*, in the hypothalamic neuronal cell line N43/5, if palmitic acid inhibits the autophagic flux through the evaluation of the proteins LC3 and SQSTM1 in presence or absence of BafA1.

1.2. To characterize, *in vitro*, the cytosolic structures of the hypothalamic neuronal cell line N43/5 exposed to palmitic acid using electron microscopy assays.

1.3. To determine, *in vitro*, in the hypothalamic neuronal cell line N43/5, if palmitic acid inhibits the autophagic process, by evaluating the expression of Autophagy Related Genes (ATG) involved in autophagosome formation.

1.4. To evaluate, *in vitro*, in the hypothalamic neuronal cell line N43/5, if palmitic acid regulates the autophagosome-lysosome fusion process.

1.5. To corroborate, *in vitro*, in cultures of primary hypothalamic neurons, if palmitic acid inhibits the autophagic flux through the evaluation of the proteins LC3 and SQSTM1 in presence or absence of BafA1.

(2) To evaluate if palmitic acid affects lysosomal activity in hypothalamic neurons.

2.1. To determine, *in vitro*, in the hypothalamic neuronal cell line N43/5 if palmitic acid exposure changes lysosomal morphology.

2.2. To assess *in vitro*, in the hypothalamic neuronal cell line N43/5, if palmitic acid exposure regulates lysosomal acidification and/or lysosomal hydrolases activity.

2.3. To analyze, *in vitro*, if palmitic acid modulates lysosomal transport, in the hypothalamic neuronal cell line N43/5.

(3) To characterize proteins in isolated lysosomes from N43/5 cells treated with palmitic acid through stable isotope labeling with amino acid in cell culture (SILAC).

(4) To determine if palmitic acid decreases insulin sensitivity, in hypothalamic N43/5 cells.

5. MATERIALS AND METHODS

5.1. Hypothalamic cell line N43/5 and treatments: N43/5 cells (Cellutions Biosystems) were cultured in Dulbecco's modified eagle medium (DMEM) high glucose (11995-040, Gibco, USA) supplemented with 10% of fetal bovine serum (FBS) (10437028, Gibco), 100 U/ml penicillin streptomycin (15140122, Gibco) and maintained at 37 °C with 5% CO₂, as described in previous studies (Belsham et al., 2004; Morselli et al., 2014b). To evaluate the changes in the autophagic flux in response to PA exposure, cells were incubated with DMEM high glucose supplemented with 2% of FBS 24 h before treatments and then exposed to 100 µM PA (P0500, Sigma-Aldrich, St. Louis, MO, USA) conjugated to fatty acid-free bovine serum albumin (BSA) (152401, MP Biomedicals, Santa Ana, CA, USA). BSA treatment was used as control. To determine the effect of 6 h treatments on insulin signaling, cells were serum starved in medium DMEM/F-12 (11330-32, Gibco) overnight prior to treatments. Then, cells were co-treated with insulin (1 nM) (I0516, Sigma-Aldrich) of phosphate buffered saline (PBS).

5.2. Primary hypothalamic neurons and treatments: Briefly, embryonic day 18 pregnant Sprague Dawley rats were euthanized by CO₂. Embryos brains were carefully isolated, meninges removed and hypothalami separated. Hypothalami were collected and digested with trypsin – EDTA (Gibco) in HBSS for 10 minutes at 37°C. Then, the solution of trypsin – EDTA was removed and hypothalami gently dissociated by repeatedly pipetting them up and down using a fire-polished glass Pasteur, in DMEM medium (Gibco) supplemented with horse serum. Next, homogenized cell suspension was passed through a 70 µM and 40 µM cell strainer. After counting, cells were seeded on poly-L-lysine treated culture plates. Hypothalamic neurons were

maintained in medium Neurobasal supplemented with B-27, L-glutamine, penicillin streptomycin and maintained at 37 °C with 5% CO₂ for 10 days (DIV10). From DIV2 3 μM AraC was added to cultured hypothalamic cells, for inhibition of uncontrolled proliferation of non-neuronal cells (Schwieger et al., 2016). At DIV10 cell cultures were incubated with PA 100 μM or BSA for 16 h.

5.3. Preparation of palmitic acid-BSA complex: Palmitic acid (PA; P0500, Sigma-Aldrich) was conjugated to fatty acid-free (FFA) bovine serum albumin (BSA; MP Biomedicals) as previously described (Gremmels et al., 2015). A stock solution of 5 mM of PA-BSA was prepared. BSA (0.45 g) was dissolved in 0.9% NaCl (7.5 ml), adjusted to pH 7.4. PA (22.43 mg) was dissolved in 100% EtOH, then titrated with 1 M NaOH to pH 10. Next, EtOH was evaporated in Speed-e-Vac, and the precipitated was dissolved in 0.9% NaCl (4.5 ml) in a thermoblock at 95°C during 15 minutes. Then, the BSA solution was added to PA solution, and the final volume was adjusted to 15 ml with 0.9% NaCl. Finally, PA-BSA solution was passed through a 0.45 μm syringe filter and stored at -20°C. PA-BSA complex was used at a final concentration of 100 μM, as mentioned above.

5.4. Methods to evaluate autophagy and the autophagic flux: Autophagic flux was evaluated by immunofluorescence (IF), by staining against the protein LC3, which identifies autophagic puncta, and by western blot (WB), to evaluate LC3I →LC3II conversion, as indicative of autophagosome formation. Autophagic flux was measured by WB through quantification of p62/SQSTM1, an autophagy receptor specifically degraded by autophagy (Klionsky et al., 2016) and using the mCherry-GFP-LC3-N43/5 cell line (cell line which expresses the tandem

fluorescent-tagged LC3 (mCherry-GFP-LC3)), which allows monitoring autophagosomes and autolysosomes formation based on the different pH stability of GFP and mCherry fluorescent proteins (Castillo et al., 2017; Kimura et al., 2007; Klionsky et al., 2016; Pankiv et al., 2007). This tool has been generated in the laboratory of our collaborator Dr. Patricia Burgos (Universidad San Sebastián). In addition, fusion between autophagosomes and lysosomes was measured by co-immunolocalization of LC3 and the lysosomal marker lysosomal-associated membrane protein 1 (LAMP1) by fluorescence microscopy (Klionsky et al., 2016). In addition, cells were incubated at the time points indicated in each experiment with the autophagic flux inhibitor Bafilomycin A1 (BafA1, 100 nM) (B1793, Sigma-Aldrich) or with its vehicle DMSO (BM-0660, Winkler). Finally, as positive control for autophagy induction, we exposed cells to 1 μ M rapamycin, a mTORC1 inhibitor (Rubinsztein et al., 2012), as indicated in the results section.

5.5. siRNA transfections: Cells were cultured in six-well plates and transfected at 50% confluence with siRNAs targeting murine Beclin 1 (BECN1) (SASI_Mm01_00048143, Sigma-Aldrich) or murine autophagy related gene 7 (ATG7) (SASI_Mm01_00044616, Sigma-Aldrich). Transfection was performed using Lipofectamine RNAiMAX® Transfection Reagent (Invitrogen, *Carlsbad, CA, USA*) according to the manufacturer's instructions. As negative control, cells were incubated with Lipofectamine RNAiMAX® Transfection Reagent only (mock). 48 h after siRNA transfection, cells were treated as indicated or directly lysed for protein or RNA extraction.

5.6. Real Time PCR (RT-PCR): RNA was extracted using the RNeasy Kit (Qiagen Sciences, Inc., Germantown, MD, USA) according to the manufacturer's instructions. Total RNA (1 µg) was reverse transcribed using the SuperScript III First-Strand Synthesis System (Invitrogen) according to the manufacturer's instructions. For analysis of the expression of *Autophagy related genes (Atg)* in N43/5 cells, RNA was extracted using the E.Z.N.A.® Total RNA Kit (OMEGA Bio-Tek, Norcross, GA, USA) according to the manufacture's indications. cDNA was synthesized using iScript™ cDNA kit (Bio-Rad) from 1 µg of total RNA. Quantitative PCR reactions were carried out on a Step One System Real Time PCR (Applied Biosystems) using Fast SYBR Green Master Mix (4385370, Life Technologies). Specific forward and reverse primers sequences used to evaluate gene expression were:

Atg7 Fw: CTGTTACCCAAAGTTCTTG, Rv: TCTAAGAAGGAATGTGAGGAG;
Sqstm1/p62 Fw: AATGTGATCTGTGATGGTTG, Rv: GAGAGAAGCTATCAGAGAGG;
Lc3 Fw: GCTCATCAAGATAATCAGACG, Rv: GCATAAACCATGTACAGGAAG; *Atg5*
Fw: TCAACCGGAAACTCATGGAA, Rv: CGGAACAGCTTCTGGATGAA; *Atg16* Fw:
AGGCGTTCGAGGAGATCATT, Rv: TTCTGCTTGTAGTTTCTGGGTCA; *Beclin*
Fw: TTGGGTGATGTGGGGAAAGG, Rv: AGACAGCACAGGAGGCATTC; *Fip200* Fw:
ACCACGCTGACATTTGACACT, Rv: CTCCATTGACCACCAGAACC; *Gabarap* Fw:
GCCTACAGTGATGAAAGCGTCTA, Rv: GAGCCTGAAGGAGGAACTGG. *Hprt1*: Fw:
AAGCCTAAGATGAGCGCAAG, Rv: TTACTAGGCAGATGGCCACA. *Hprt1* was used as
housekeeping gene. The $\Delta\Delta C_T$ method was used for relative quantification analysis.

5.7. Western blot analysis: Cells were lysed in RIPA buffer and 30-40 µg of denatured proteins from each sample were resolved in 8 or 12% SDS-PAGE. Gels were transferred to nitrocellulose membranes and incubated with 5% BSA (BM-0150, Winkler, RM, Chile) - tris-buffered saline-0.1% Tween-20 (TBS-T) to block nonspecific binding. Membranes were incubated with the primary antibodies anti LC3A/B (4108, Cell Signaling Technology, Danvers, MA, USA), SQSTM1/p62 (H00008878-M01, Abnova, Jhouzih St., Taipei, Taiwan), p-Insulin Receptor β (Tyr1150/1151) (3024, Cell Signaling Technology), IR (ab131238, Abcam), p-AKT (Ser473) (9271, Cell Signaling Technology), AKT (9272, Cell Signaling Technology), BECN1 (H-300; sc-11427, Santa Cruz Biotechnology, Inc., Dallas, Texas, USA), Rab7 (1:1000; sc-376362, Santa Cruz Biotechnology, Inc.), at dilution of 1:1000 in 5% BSA-TBS-T overnight on a rocking platform at 4°C. Then, membranes were washed 3 times for 10 min in TBS-T and revealed with the appropriate horseradish peroxidase-labeled secondary antibodies (Goat Anti-Mouse IgG (H + L)-HRP Conjugate, 1706516; Goat Anti-Rabbit IgG (H + L)-HRP Conjugate, 1706515; Bio-Rad, CA, USA) and the chemiluminescent substrate. GAPDH (1:1000; sc-365062, Santa Cruz Biotechnology, Inc.) and β -actin (1:10000; A1978, Sigma-Aldrich) were used as loading control. To evaluate insulin signaling the same samples were run on parallel gels, one for p-AKT and the other for AKT. Analysis of data was performed by comparing p-AKT versus β -actin and AKT versus β -actin. The obtained ratios were analyzed.

5.8. Immunofluorescence and fluorescence microscopy: For fluorescence microscopy determinations in N43/5 cells, cells, cultured on coverslips, were fixed with cold methanol (-20 °C) for 10 min or with 4% (w:v) paraformaldehyde (PFA) for 20 minutes at room temperature. After PFA fixation, cells were permeabilized with triton 0,1% for 20 minutes at room

temperature. Then, cells were blocked in 3% BSA in PBS for 1 h and then incubated with the following primary antibodies overnight at 4 °C. The primary antibodies used are LC3A/B (1:250; Cell Signaling Technology), SQSTM1/p62 (1:300; Abnova), LAMP1 (1:500; 553792, BD Pharmingen, USA), Rab7 (1:100; sc-376362, Santa Cruz Biotechnology, Inc.) Primary antibodies staining was followed by conjugation with its respective secondary antibody (1:300; Alexa Fluor®, Life Technologies) for 1 h at room temperature. Nuclei were counterstained with DAPI. Confocal images were taken in an inverted fluorescence microscopy Leica DMI600 (Dr. Patricia Burgos Laboratory, Universidad San Sebastián) or in an inverted confocal microscope LSM 880 Zeiss with Airyscan detection (Unidad de Microscopía Avanzada UC (UMA UC)). Images were quantified using ImageJ software (NIH, Bethesda, MD), and by using the Spot Detector plugin within the open source software, ICY (Institut Pasteur and France BioImaging). Co-localization, fluorescence intensity analysis, and size measurement of LAMP1 and LC3 dots were made accordingly to Bustamante et al. (2020).

5.9. Methods to evaluate lysosomal activity: To determine lysosomal function the following experiments were performed:

(A) *Lysosomal pH measurement.* We evaluated, by confocal microscopy, the pH of lysosomes of cells treated with PA, using 100 nM LysoTracker Red DND-99 probes (L7528, Invitrogen), which accumulates and emits fluorescence in acidic compartments. Cells were incubated with this probe for the last 45 minutes of treatments, and then washed twice with PBS. Following, cells were fixed with 4% (w:v) PFA for 20 minutes at room temperature and nuclei were counterstained with DAPI. Subsequently, images were taken in an inverted fluorescence

microscopy Leica DMI600 (Dr. Patricia Burgos Laboratory, Universidad San Sebastián), and quantified using ImageJ software.

(B) Lysosomal enzyme activity: We measured using the Magic Red kit (Immunochemistry Technologies, LLC) the activity of cathepsin B, a lysosomal member of the papain-like family of cysteine proteases, as indicated by the manufacturer's instructions. This kit uses a permeable cathepsin B substrate that, once hydrolyzed, liberates membrane-impermeable fluorescent cresyl violet within the organelles that contain a catalytically active cathepsin B (Bright et al., 2016; Creasy et al., 2007; Pryor, 2012). Briefly, for N43/5 cell line, cells were plated on glass bottom dishes, treated with PA for 6 h or BafA1 for 2 h and then loaded with Magic Red probe for 20 min in DMEM medium in humidified 5% CO₂ atmosphere at 37°C. They were washed 3 times with PBS and then loaded with Hoechst, to stain the nuclei, for 10 min and finally washed 3 additional times with PBS. Cells were maintained in DMEM medium with HEPES. Experiments have been performed following manufacturer's instructions. Images were taken in an inverted fluorescence microscope Leica DMI600 (Dr. Patricia Burgos Laboratory, Universidad San Sebastián), and cells analyzed using the open source software, ICY.

(C) Lysosomal movement: To label and track lysosomes, N43/5 cells were incubated with 100 nM LysoTracker Red DND-99, during the latest 45 min of PA (6 h, 100 μM) or BSA treatment, and then washed twice with PBS. Then, live cells were maintained in DMEM (supplemented with 2% FBS) at 37°C and 5% CO₂ and visualized in an inverted confocal microscope LSM 880 Zeiss with Airyscan detection (UMA UC). Time-lapse images were collected every 3.39 s for 90 frames. Analysis of the live cell imaging studies including tracking, velocity and

displacement were performed with the ICY software (<http://icy.bioimageanalysis.org/>). The pseudobinary threshold was determined with the plugin for batch analysis. Then, we configured size, detector type and dimensional parameters using the spot detector plugin. Further, we established the movement of the signals detected configuring the tracking parameters with the spot tracking plugin. Finally, we obtained the speed and displacement of each channel with the track manager using the Track Processor Instant Speed plugin.

5.10. Electron microscopy: Cells were fixed in 2.5% glutaraldehyde (16210, EMS, PA, USA) in 0.2 M phosphate buffer (PB) pH 7.4 at room temperature for 16 hours. Then, cells were washed 3 times with PB and post-fixed in 1% osmium tetroxide/1% ferrocyanide for 1 hour at 4°C. Subsequently, cells were double-stained with 2% uranyl acetate and lead citrate overnight at 4°C. After dehydration in graded series of ethanol, cells were embedded in epoxy resin 812 and sectioned using a Leica ultramicrotome (Leica Microsystems, Vienna, Austria). Images were taken in a transmission electron microscopy Hitachi H-7650 (Tokyo, Japan). These experiments were performed in collaboration with Dr. Li Yu (Tsinghua University, Beijing, China).

5.11. Rab7-GTP pull down assay: Rab7-GTP pulldown assays were performed in collaboration with the laboratory of Dr. Vicente Torres (Universidad de Chile), as previously described (Diaz et al., 2014; Torres et al., 2008). Briefly, cells were lysed in a buffer containing 25 mM HEPES (pH 7.4), 100 mM NaCl, 5 mM MgCl₂, 1% NP 40, 10% glycerol, 1 mM dithiothreitol and protease inhibitors. Extracts were incubated for 5 min on ice and clarified by centrifugation (10,000xg, 1 min, 4°C). Postnuclear supernatants were used for pulldown assays

with 30 µg of GSH beads precoated with GST-RILP (Rab7-GTP pulldown) per condition. Beads were incubated with supernatant for 15 min at 4°C in a rotating shaker. Thereafter, beads were collected, washed with lysis buffer containing 0.01% NP 40 and samples were analyzed by WB.

5.12. Isolation and characterization of the lysosomal fraction and realization of SILAC in

N43/5 hypothalamic neuronal cells: Stable labeling with amino acids in cell culture (SILAC) analysis were performed in collaboration with the laboratories of Dr. Budini, Dr. Criollo (Universidad de Chile) and Dr. Burgos (Universidad San Sebastián), as part of the collaborative Anillo Project “Mechanisms of Autophagy in Obesity” (172066). In brief, N43/5 cells were exposed to 100 µM of PA for 6 h in presence of heavy L-Lysine:2 HCL (13C6, 99%) and L-Arg (13C6, 99%, 15N4, 99%). BSA was used as a control. For lysosomal isolation we used an adapted protocol from Storrie, B. et al. (Storrie and Madden, 1990) and Dr. Ana Maria Cuervo’s laboratory. Cells were lysed using a nitrogen cavitation chamber with a subsequently two rounds of Nycodenz gradient ultracentrifugation to separate lysosomal fractions. Different fractions were analyzed by western blot to evaluate the grade of purity (LAMP1, LAMP2A and Cathepsin D). Following lysosomes isolation, samples were sent to mass spectrometry analysis at the Plateforme Protéomique Structurale et Fonctionnelle, Institut Jacques Monod - CNRS et Université Paris-Diderot (France). SILAC proteomic analysis was performed by Mascot 2.5.1 coupled to Proteome Discoverer 2.2 and the Swissport database of Proteome Discoverer. To determine the rate of significant abundance, a p value of <0.05 and a False Discovery Rate < 0.01 were established. The abundance ratio above 1.5 and below 0.5 were considered up-regulated and down-regulated, respectively.

5.13. 2-NBDG uptake: To assess the insulin-dependent glucose uptake, N43/5 cells were stimulated with insulin 1 nM for 30 min and incubated with the fluorescent analog of glucose (2-NBDG, 300 nM) for 15 min at 37 °C, as previously described (Bernal-Sore et al., 2018). Cells were transferred to an inverted Nikon Ti Eclipse microscope equipped with 40X oil objective [numerical aperture, N.A. 1.3]. A Xenon lamp was coupled to the monochromator device (Cairn Research Ltd, Faversham, UK). Digital images were acquired by means of a cooled CCD camera (Hamamatsu ORCA 03, Japan). Images were quantified by ImageJ software (NIH, Bethesda, MD). These experiments were performed in collaboration with Dr. Rodrigo Troncoso (Universidad de Chile).

5.14. Results and statistical analysis: Results are shown as mean \pm SEM from at least 3 independent experiments. Two groups were compared using two-tailed Student's t tests. For more than two groups, one- or two-way ANOVA was used, as appropriate, followed by post hoc adjustment. All analyses were performed with GraphPad software (San Diego, CA, USA). P value of <0.05 was considered statistically significant.

6. RESULTS

6.1. Palmitic acid inhibits autophagic flux in hypothalamic neuronal cells

It has been previously shown that autophagy is dysregulated *in vivo* in the hypothalamus of male mice chronically fed with HFDs (Meng and Cai, 2011; Morselli et al., 2014a; Portovedo et al., 2015). Considering that in the brain of mice fed with the same diet for 16 weeks palmitic acid (PA) is significantly increased (Morselli et al., 2016; Morselli et al., 2014b; Rodriguez-Navas et al., 2016), we determined the effect of this SatFA on the autophagic flux in the N43/5 hypothalamic neuronal cell line, a model of POMC neurons (Oh et al., 2016). Accordingly, cells were treated with 100 μ M PA, a concentration of PA similar to the one identified in the brain of obese mice chronically exposed to HFDs (Rodriguez-Navas et al., 2016).

Autophagy can be monitored by two different approaches: (1) direct observation of autophagy related structures; and (2) quantification of autophagy/lysosome-dependent degradation of proteins. Importantly, to accurately estimate the autophagic activity, it is fundamental to determine the autophagic flux, which is defined as the amount of autophagic degradation (Yoshii and Mizushima, 2017). LC3 is currently the most widely used autophagosome marker because the amount of LC3-II reflects the number of autophagosomes and autophagy-related structures. It must be noted, however, that the LC3-II amount at a given time point does not necessarily estimate the autophagic activity, because not only autophagy activation but also inhibition of autophagosome degradation increases the levels of LC3-II (Klionsky et al., 2016; Yoshii and Mizushima, 2017). Thus, to measure the autophagic flux, it is essential to use an autophagy substrate such as the protein SQSTM1/p62, which directly binds

to LC3 and is selectively degraded through the autophagic process (Pankiv et al., 2007). In addition, in order to corroborate whether PA is affecting the autophagic flux in our cellular models, we also used BafA1 a potent V-ATPase inhibitor, which impairs lysosomal acidification and autophagic cargo degradation (Mauvezin and Neufeld, 2015). Therefore, the difference in the amount of LC3-II between samples with and without this lysosomal inhibitor represents the level of the autophagic flux (Yoshii and Mizushima, 2017).

Figure 4 shows that PA treatment affects the lipidation of LC3 as observed by the increase in the protein levels of LC3-II (Fig. 4A, B), suggesting an increase in the number of autophagic structures. This was accompanied by an increase in the amount of p62/SQSTM1, which accumulates when the autophagic flux is decreased (Fig. 4A, D). These observations have been corroborated by IF studies in N43/5 cells stained against LC3, which show PA treatment stimulates the formation of autophagic puncta (Fig. 4E, F), and increases SQSTM1 protein dots (Fig. 4E, G), compared to control conditions (BSA). Furthermore, we confirmed the effect of PA on autophagic flux by using BafA1, determining that BafA1 does not further enhance the PA-triggered induction of LC3-II protein levels (Fig. 4A-C) or LC3 puncta (Fig. 4E-F), suggesting that the increase in the LC3 levels induced by PA is the consequence of the accumulation of autophagic structures. These results indicate that PA inhibits the autophagic flux in N43/5 cells, a model of hypothalamic POMC neurons (Oh et al., 2016).

In addition, we also evaluated the effect of PA exposure on primary hypothalamic neurons in terms of modulation of autophagy. Consistently with the results obtained in N43/5 cells, 16 hours of PA treatment increases the number of autophagic structures (Fig. 4H, I), as well as the amount of SQSTM1/p62 protein aggregates (Fig. 4H-J). Treatment with BafA1

confirmed that, also, in primary hypothalamic neurons, PA inhibits the autophagic flux (Fig. 4H-J).

6.2. Palmitic acid does not affect autophagy related genes involved in autophagosome formation in N43/5 cells

To corroborate that the effect of PA on the increase of LC3 puncta as well as LC3-II protein levels was due to autophagic flux inhibition and not to *de novo* synthesis of autophagosomes, we evaluated several autophagy related genes (*Atg*) involved in the formation of these structures. As shown in Figure 5A, PA treatment increases the number of LC3 puncta as well as the number of SQSTM1 dots, already 1 h following PA exposure, which is maintained until 6 h of treatment (Fig. 5A-C). Importantly, the levels of *Atg5*, *Atg7*, *Atg16*, *Beclin 1*, *Fip200* and *Gabarap*, which are essential autophagy genes required for autophagosome formation, are not increased by PA exposure, and *Lc3* and *Sqstm1* levels, even if affected, are significantly increased only 6 h and 4 h, respectively, following PA exposure, and thus after the increase in the number of autophagic structures (Fig. 5D-K). These results suggest that the increase in LC3 puncta and the increase in LC3-II proteins levels are not due to newly formed autophagosomes but rather to an accumulation of autophagic structures, as consequence of the decrease in the autophagic flux, confirming PA treatment specifically inhibits the autophagic flux in N43/5 cells.

6.3. Palmitic acid induces lysosomal swelling and reduces autophagosome-lysosome fusion in N43/5 cells exposed to Bafilomycin A1

During the autophagic process cytosolic components are first sequestered in a double-membrane vesicle called autophagosome, which acquires the hydrolases required for cargo degradation upon fusion with lysosomes, forming autolysosomes, in which the substrates are degraded and the simple molecules are released for recycling. Thus, the decrease in the autophagic flux could be caused by impaired fusion of autophagic vacuoles with lysosomes, or because of compromised proteolytic activity of the lysosomal hydrolases (Klionsky et al., 2016). Therefore, to elucidate the mechanism involved in reduced autophagic flux induced by PA, we first evaluated if the process of autophagosome-lysosome fusion was affected, by performing a classic analysis of co-localization between autophagosomes and lysosomes by IF staining of LAMP1, as a lysosomal marker, and LC3 to identify autophagic structures (Klionsky et al., 2016).

As seen in Figure 6A-B, lysosomes of N43/5 cells treated with BSA show the classic a punctate appearance, whereas lysosomes of cells treated with PA are more likely circular and larger, a morphology defined as “lysosome swelling” (Choy et al., 2018), which is generally associated with impaired lysosomal activity (Ballabio and Gieselmann, 2009; Settembre and Ballabio, 2014), and with autophagic flux inhibition (Yamamoto et al., 2017). Cells were also co-stained against LC3, and, as expected, PA treatment increases LC3 dots compared to BSA condition (Fig. 6A), however we do not observe significant differences in the percentage of co-localization between LAMP1 and LC3 after PA treatment (Fig. 6A, C). Despite this, in cells co-incubated with PA and BafA1 the co-localization between both markers is significantly

decreased compared to cells treated only with BafA1, where the co-localization levels of LAMP1 and LC3 are significantly higher than in control cells (Fig. 6A, C). These data indicate that PA induces lysosome enlargement and, in presence of BafA1, it impairs autophagosome-lysosome fusion. Thus, these results suggest that the decrease in autophagic flux induced by PA could be consequence of both lysosomal dysfunction as well as reduced autophagosome-lysosome fusion.

6.4. Palmitic acid does not abolish lysosomal acidity or lysosomal activity in N43/5 cells

In this study, we have observed that PA induces lysosomal swelling after 6 h of treatment in N43/5 cells (Fig. 6). As mentioned, this has been associated with a decrease in lysosomal function, which directly impairs autophagosome-lysosome fusion in some cellular models (Kawai et al., 2007). Thus, we next evaluated if PA treatment affects lysosomal pH, using the pH-sensitive lysosomal dye LysoTracker Red, which accumulates and emits red fluorescence in acidic compartments with $\text{pH} < 6.5$ (Duvvuri et al., 2004), including endosomes and lysosomes (Hu et al., 2015). Then, we measured cathepsin B activity using the Magic Red assay. As shown in Figure 7, PA does not decrease LysoTracker (Fig. 7A-B) or Magic Red fluorescence intensity (Fig. 7E-F), which instead results higher in both cases, compared to control. Moreover, a decreased number of big puncta positive for LysoTracker (Fig. 7A, C-D) and for Magic Red dyes (Fig. 7E, G-H) was seen. In contrast with these observations, BafA1, which targets the vacuolar type H^+ -ATPase preventing lysosomal acidification (Mauvezin and Neufeld, 2015), as expected, increases cellular pH (Fig 7A-B) and impairs cathepsin B activity (Fig. 7E-F), as shown by the reduced fluorescence of LysoTracker and Magic Red dye,

respectively. These data indicate that PA induces the accumulation of enlarged endo-lysosomal vesicles, without affecting lysosomes acidity and their hydrolytic activity.

6.5. Palmitic acid reduces the dynamics of endolysosomal structures in N43/5 cells

Previous studies have shown that an altered endolysosomal dynamics contributes to autophagic defects leading to different neurodegenerative and non-neurodegenerative diseases (Colacurcio et al., 2018; Malik et al., 2019; Xie et al., 2015). Thus, we evaluated by live cell imaging if PA affects the dynamics of endolysosomal structures in N43/5 cells. Our data show that exposure to PA significantly decreases the velocity (Fig. 8A,B) and the traveled distance (Fig. 8C) of large LysoTracker vesicles, indicating PA reduces the trafficking of endolysosomal vesicles. These results suggest that autophagic flux inhibition in N43/5 cells might be caused by impaired fusion of autophagic and endolysosomal vesicles as consequence of a reduced intracellular vesicle trafficking.

6.6. Palmitic acid induces the formation of large autophagic vesicles in N43/5 hypothalamic neuronal cells

Our results show PA reduces the autophagic flux (Fig. 4), that lysosomes do not show reduced hydrolytic activity (Fig. 7), they are bigger and swollen (Fig. 6 and 7) and that their movement is reduced (Fig. 8). Thus, we decided to evaluate whether PA decreases autophagic flux by impairing autophagosome-lysosome fusion. To this aim, we used a dynamic autophagic flux sensor consisting on a tandem fluorescence construct of mCherry coupled to GFP-LC3 (Kimura et al., 2007; Pankiv et al., 2007), which is based on the inactivation of GFP fluorescence

in acidic compartments, such as lysosomes (Castillo et al., 2017). Accordingly, increased number of red puncta indicates enhanced autophagic flux (delivery of cargo into lysosomes), whereas yellow puncta (merge of green and red channels) are indicative of autophagosome formation and accumulation (Castillo et al., 2017). To ensure the correct interpretation of the results, we used as positive control for autophagy induction the drug rapamycin, a mTORC1 inhibitor, and BafA1, to inhibit the autophagic flux (Rubinsztein et al., 2012). As expected, rapamycin treated cells show a higher number of LC3 red dots than controls (Fig. 9A-C), which indicates the autophagic flux is enhanced. Conversely, BafA1 significantly increases the number of LC3 red puncta as well as the number of LC3 yellow puncta, indicating a decrease in GFP-LC3 degradation, confirming BafA1 treatment decreases the autophagic flux (Fig. 9A-C), because of diminished lysosomal acidification (Mauthe et al., 2018). Interestingly, cells treated with PA show a significant higher number of LC3 red dots, compared to control cells, but also a significant increase in LC3 yellow puncta (Fig. 9A, B), resulting in reduced autophagic flux (Fig. 9C). Importantly, the size of LC3 yellow dots is the biggest compared to all conditions (Fig. 9A, D), consistently with our previous observations (Fig. 4). These data suggest that PA induces the accumulation of large autophagic structures lacking degradative capacity possibly as consequence of impaired fusion between autophagic vesicles and lysosomes.

6.7. Palmitic acid induces the accumulation of large cellular degradative compartments in N43/5 hypothalamic neuronal cells

Our data suggest that PA inhibits the autophagic flux in hypothalamic neurons and induces the accumulation of big autophagic structures (Fig. 4, Fig. 9). Next, we performed an

electron microscopy (EM) analysis, which is considered as gold standard to recognize autophagic vesicles (Eskelinen, 2008a, c; Klionsky et al., 2016), to evaluate the morphology of cytosolic structures of N43/5 cells treated with PA, and to confirm whether PA impairs autophagosome-lysosome fusion.

As already mentioned, the distinctive characteristic of autophagy is that cytosolic components are first sequestered in a double-membrane vesicle called autophagosome, which acquires the hydrolases required for cargo degradation after fusion with lysosomes, forming degradative autolysosomes. However, the autophagic cargo can also reach the lysosomal lumen through fusion of autophagosomes with early endosomes or with late endosomes to form amphisomes (Liou et al., 1997). Without performing an immunogold staining, it is difficult to distinguish between lysosomes, autolysosomes or amphisomes, thus, in agreement with a recent study (Mauthe et al., 2018); we decided to group these organelles in a single category called “cellular degradative compartments” (DGCs). EM images show that PA treatment increases the number of large DGCs (Fig. 10A-C). Importantly, the big DGCs we identified are mostly limited by a single membrane and show an intra-luminal heterogeneous content (Fig. 10A). Within the vesicles we can distinguish multilamellar bodies, composed of concentric membrane layers, multivesicular bodies, containing multiple internal vesicles, and portions of the endoplasmic reticulum (Fig. 10A). Importantly, in PA-treated cells, we could not find conventional autophagosome-like structures, characterized by a double membrane vesicle composed by morphologically intact cargo (Eskelinen, 2005), suggesting that an additional process may be occurring rather than just the disruption of autophagosome-lysosome fusion. Since in PA treated cells we observed an accumulation of large vesicles with heterogeneous intraluminal content, indicative of partially degraded cargo, we can speculate that these structures could be large

amphisomes or aberrant autolysosomes (Eskelinen, 2005, 2008c). Taking into account these data and together with our previous results indicating a decrease in endolysosomal dynamics (Fig. 8), we suggest PA induces the accumulation of big DGCs (Fig. 10) as consequence of impaired endo-lysosomal trafficking in N43/5 cells.

6.8. Palmitic acid increases Rab7 activation in N43/5 cells

As we observed large DGCs following PA exposure, and since our data show PA impairs endo-lysosomal trafficking, we evaluated whether the activation state of the small GTPase Rab7, a key protein involved in this process. Rab7 defines the maturation of endosomes and autophagosomes, directing the trafficking of cargos along microtubules, participating in the final step of autophagosome-lysosome fusion (Guerra and Bucci, 2016; Hyttinen et al., 2013), which is essential for the degradation of the autophagosomal content (Gutierrez et al., 2004).

Thus, we evaluated if PA affects Rab7 activity in our cellular model. First, we examined by IF whether PA alters the morphology of Rab7, and, as shown in Figure 11A, we observe that after 6 h of treatment, PA induces the formation of enlarged Rab7 positive structures, which have been associated with a hyper-activated Rab7 (Bucci et al., 2000). Next, using a pull down assay, we evaluated the activation state of Rab7, and in agreement with the previous results, we see that PA increases the protein levels of Rab7-GTP compared to control conditions (Fig. 11B, C), indicating PA promotes Rab7 activation state. To note, Rab7 hyper-activation causes the accumulation of enlarged autolysosomes (Yu et al., 2010), and enlarged endolysosomal vesicles, containing aberrant intraluminal content, as consequence of the disruption of intracellular transport routes involved in the maintenance and maturation of endolysosomal membranes

(Jongsma et al., 2020). These results suggest that PA is able to modulate the activation state of Rab7, impairing the later phases of the autophagic process, including autophagic maturation and/or autophagic fusion with endolysosomal vesicles.

6.9. Palmitic acid affects the levels of proteins linked to the endolysosomal and to the autophagic pathways

Considering that lysosomes serve as terminal degradation hubs for autophagic and endosomal components, we performed a SILAC based proteomic analysis from isolated lysosomes of N43/5 cells treated with PA. The aim of this experiment was to identify proteins related to the endo-lysosomal and with the autophagic trafficking pathways mainly linked to the small GTPase Rab7 regulation and with autolysosome formation. In the Table I are summarized the list of significantly upregulated proteins found in lysosomes of N43/5 cells exposed to PA for 6 h.

We found increased protein levels of TBC1 domain family member 15 (TBC1D15), a Rab7 GAP responsible for promoting GTP hydrolysis inactivating Rab7, resulting in its dissociation from the lysosomal membrane (Zhang et al., 2005). This data suggests its increase in the lysosomes of PA-treated cells could be associated with the previously observed hyper-activation state of Rab7 (Fig. 11). This indicates that Rab7 activation/inactivation cycle state might be dysregulated as consequence of altered TBC1D15 levels in lysosomes of PA-treated cells.

Also, we identify increased levels of the biogenesis of lysosomal organelles complex 1 subunit 1 (BLOC1S1), of the BLOC-1 related complex subunit 5 (BORCS5/myrlysin), and of BLOC-1 related complex subunit 7 (BORCS7/diaskedin). All these subunits are part of the lysosome-associated multiprotein complex named BLOC-1 related complex (BORC) (Pu et al., 2015). BORC associates with the cytoplasmic leaflet of the limiting late endosomal/lysosomal membrane and promote its migration through the cell periphery (Guardia et al., 2016; Pu et al., 2015). In addition, BORC complex, participates in the recruitment of proteins involved in autophagosome-lysosome fusion (Jia et al., 2017). Moreover, the BORC complex regulates PIKfyve-dependent production of the lipid phosphatidylinositol 3,5-bisphosphate (PI(3,5)P₂) modulating lysosomal reformation and lysosomal size (Yordanov et al., 2019). Furthermore, BLOC1S1, is also part of the biogenesis of lysosome-related organelles complex 1 (BLOC1), which is found on tubular endosomes and plays an important role in the biogenesis of lysosome related organelles such as melanosomes (Di Pietro et al., 2006; Langemeyer and Ungermann, 2015). BLOC1 also has been associated with endosomal maturation and cargo transport from early endosomes toward lysosomes (John Peter et al., 2013; Setty et al., 2007; Zhang et al., 2014). This suggests that, in PA treated cells, the increased lysosomal localization of these proteins, that are required for the proper trafficking of autophagosomes/lysosomes and for the regulation of lysosomal size, could be affecting the fusion of autophagosomes with endolysosomal vesicles.

Additionally we found increased levels of the Protein VAC14 homolog (Vac14), also named Associated Regulator of PIKfyve (ArPIKfyve) in isolated lysosomes from N43/5 treated with PA. Vac14 maintains the integrity of the PIKfyve complex via homo and heteromeric interactions with the remaining subunits (Jin et al., 2008; Sbrissa et al., 2007). It has been

observed that malfunction of one of these complex members, particularly Vac14 dysfunction, leads to cellular vacuolization (Sbrissa et al., 2007; Schulze et al., 2014; Schulze et al., 2017). Furthermore, Vac14 is crucial for Rab7-dependent endolysosomal maturation process and Rab9-dependent transport of lysosomal membranes to the trans-Golgi network (Schulze et al., 2014). These data suggest that Vac14 increase in lysosomes of PA-treated cells might lead to endo-lysosomal maturation impairment promoting lysosomal swelling (Fig. 6, 7).

We also found increased levels of Rab22a, a small GTPase that associates with early and late endosomes, but not with lysosomes (Mesa et al., 2001). Interestingly, overexpression of RAB22a in CHO cells causes a prominent morphological enlargement of the early and late endosomes, and cells expressing a constitutively active mutant showed its presence in early and late endosomes as well as lysosomes and autophagosomes (Mesa et al., 2001). Furthermore, it has been confirmed that Rab22a can affect the trafficking from endosomes to the Golgi (Mesa et al., 2005), again suggesting that PA might be affecting intracellular vesicle trafficking.

All these data suggest PA, in N43/5 cells, increase lysosomal localization of key proteins involved in the autophagic and endo-lysosomal intracellular trafficking pathway, impairing autophagic flux and, in consequence, leading to the accumulation of DGCs.

6.10. Palmitic acid reduces insulin sensitivity in N43/5 cells

Once we confirmed that PA inhibits the autophagic flux in our hypothalamic cellular models, we decided to evaluate if this impairment in autophagy has a physiological consequence. Considering that consumption of HFDs increases PA levels in the hypothalamus

(Rodriguez-Navas et al., 2016; Vagena et al., 2019), and that intracerebroventricular injection of PA blunts hypothalamic insulin signaling (Benoit et al., 2009), we first evaluated if N43/5 cells could respond to insulin and the role of autophagy in maintaining this response. Following exposure to insulin, levels of AKT phosphorylation (p-AKT) increased (Fig. 12A-B), showing that N43/5 hypothalamic neuronal cells are, indeed, sensitive to insulin. Critically, PA treatment reduced AKT phosphorylation levels (Fig. 12A-B) and consistently, PA exposure inhibited insulin-induced glucose uptake (Fig. 12C-D), compared to control cell. Altogether, these results indicate PA reduces insulin sensitivity in N43/5 hypothalamic neuronal cells.

6.11. Inhibition of autophagy reduces insulin sensitivity in N43/5 cells

Our data indicate PA inhibits the autophagic flux and reduces insulin sensitivity. In the next series of experiments, we determined if this response is specific to PA or if other compounds that inhibit the autophagic flux also affect the insulin response. First, we exposed N43/5 cells to BafA1 or vehicle (DMSO) for 6 h and added insulin during the last 3 or 15 min. While insulin treatment increased p-Insulin Receptor (IR) and p-AKT levels (3 and 15 mins following insulin treatment, respectively), confirming N43/5 cells are sensitive to insulin, pretreatment with BafA1 prevented the increase in their phosphorylation (Fig. 13A-C). Importantly, the reduction in insulin sensitivity was also confirmed by the decrease in insulin-dependent glucose uptake, which as observed in Figure 13 (D-E), was blunted by BafA1 treatment. In addition, BafA1 exposure increased the levels of LC3-II and SQSTM1 (Fig. 13A), suggesting that inhibition of the autophagic flux reduces the insulin response in N43/5 cells.

Then, we assessed if inhibition of autophagy, and not only the inhibition of the autophagic flux, could affect the response to insulin in our cellular model. To do this, we downregulated the expression of two autophagy essential genes *Beclin1* and *Atg7* (Fig. 13F, J) and evaluated the levels of IR and AKT phosphorylation in response to insulin treatment. Interestingly, downregulation of both autophagy essential genes significantly reduced the levels of p-IR and p-AKT following insulin treatment (Figure 13F-L). Altogether, these results indicate inhibition of autophagy, by downregulation of autophagy essential genes, reduces insulin sensitivity of N43/5 cells.

Importantly, it has been demonstrated that hypothalamic GLUT4 neurons is a key mediator of insulin action (Ren et al., 2015), and that insulin-mediated GLUT4 membrane translocation is required for the transportation of glucose in hypothalamic neurons (Changou et al., 2017; Jurcovicova, 2014; Thierry Alquier et al., 2006). Interestingly, our SILAC based proteomic analysis (Table I) shows that the Rab7 GAP, TBC1D15 is increased in lysosomes following PA treatment. As previously mentioned, TBC1D15 is involved with autophagic and endolysosomal trafficking pathway and regulates glucose uptake by affecting the translocation of GLUT4 through late endosomal pathway in different cell lines (Wu et al., 2019). Additionally, PA treatment increases lysosomal levels of the PIKfyve activator Vac14, which is linked to insulin-activated GLUT4 translocation and glucose transport in 3T3-L1 adipocytes (Ikonov et al., 2007). The increase in these two proteins following PA treatment suggests the insulin-dependent translocation of GLUT 4 to the cells membrane is impaired.

Altogether, these data strongly suggest that, in N43/5 hypothalamic neuronal cells, the inhibition of the autophagic flux caused by PA reduces insulin sensitivity and glucose uptake, as consequence of impairment of endolysosomal trafficking.

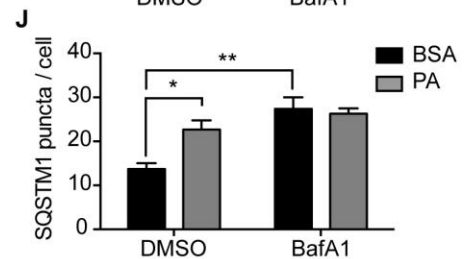
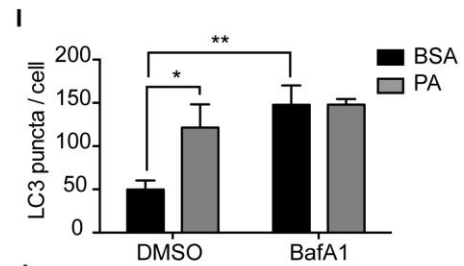
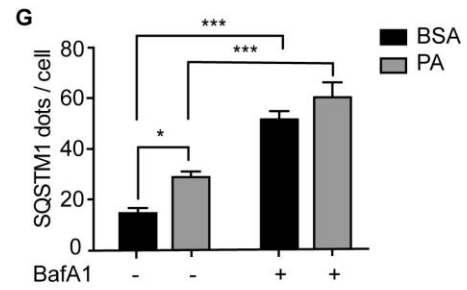
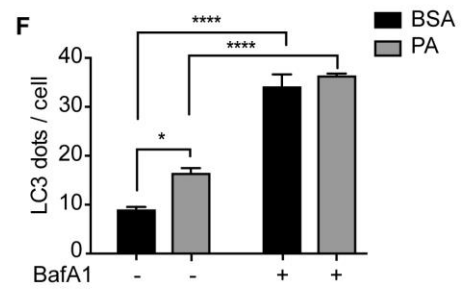
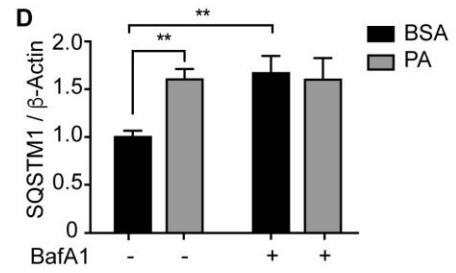
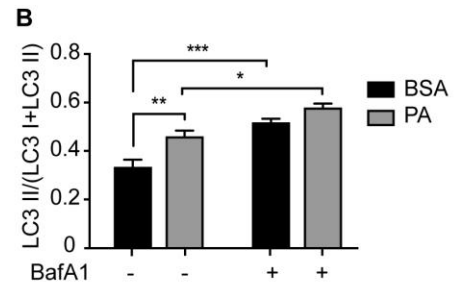
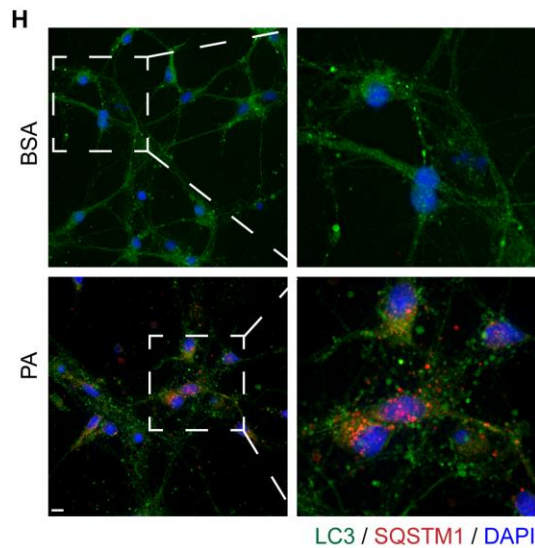
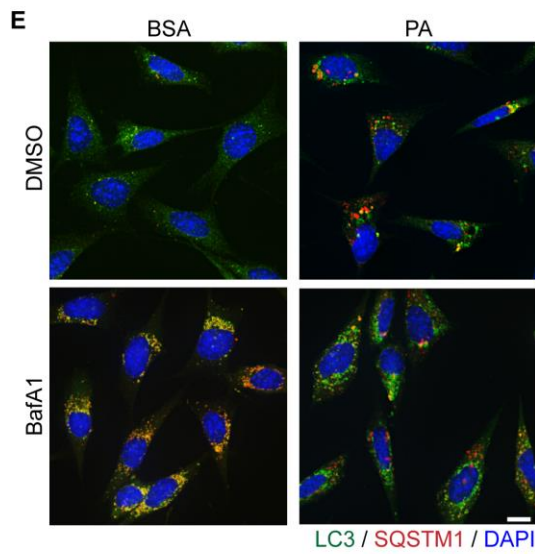
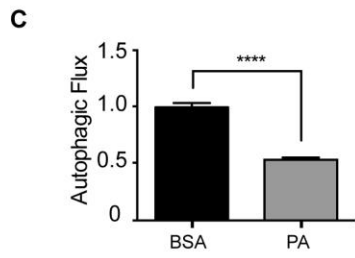
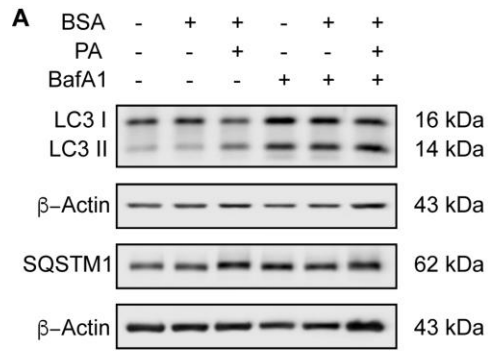


Figure 4: Palmitic acid inhibits the autophagic flux in hypothalamic cells. (A) Representative western blot of LC3 and SQSTM1 levels in N43/5 cell lysates, incubated with vehicle (BSA) or PA (100 μ M) for 6 h, in presence or absence of BafA1 (100 nM) or its vehicle (DMSO), with their respective quantifications (B, D). (C) Autophagic flux calculated as the difference in LC3II levels in presence and absence of BafA1 (100 nM). (E) Representative images of N43/5 cells treated with BSA or PA (100 μ M) for 6 h in presence or absence of BafA1 (100 nM) and stained against LC3 (green) and SQSTM1 (red). Nuclei were stained with DAPI (blue). Quantification of LC3 (F) and SQSTM1 (G) dots per cell. Size bar: 10 μ m. (H) Representative images showing primary hypothalamic neurons stained with LC3 and SQSTM1 exposed to PA (100 μ M) or BSA for 16 h, with its respective quantifications (I, J), which also includes cells co-incubated with BafA1 (100 nM) for the last 4 h of treatments. Inserts show a magnification of structures within the dotted square. Data are presented as mean \pm SEM. *p < 0.05, **p < 0.01, ***p < 0.001, ****p < 0.0001. n= 3.

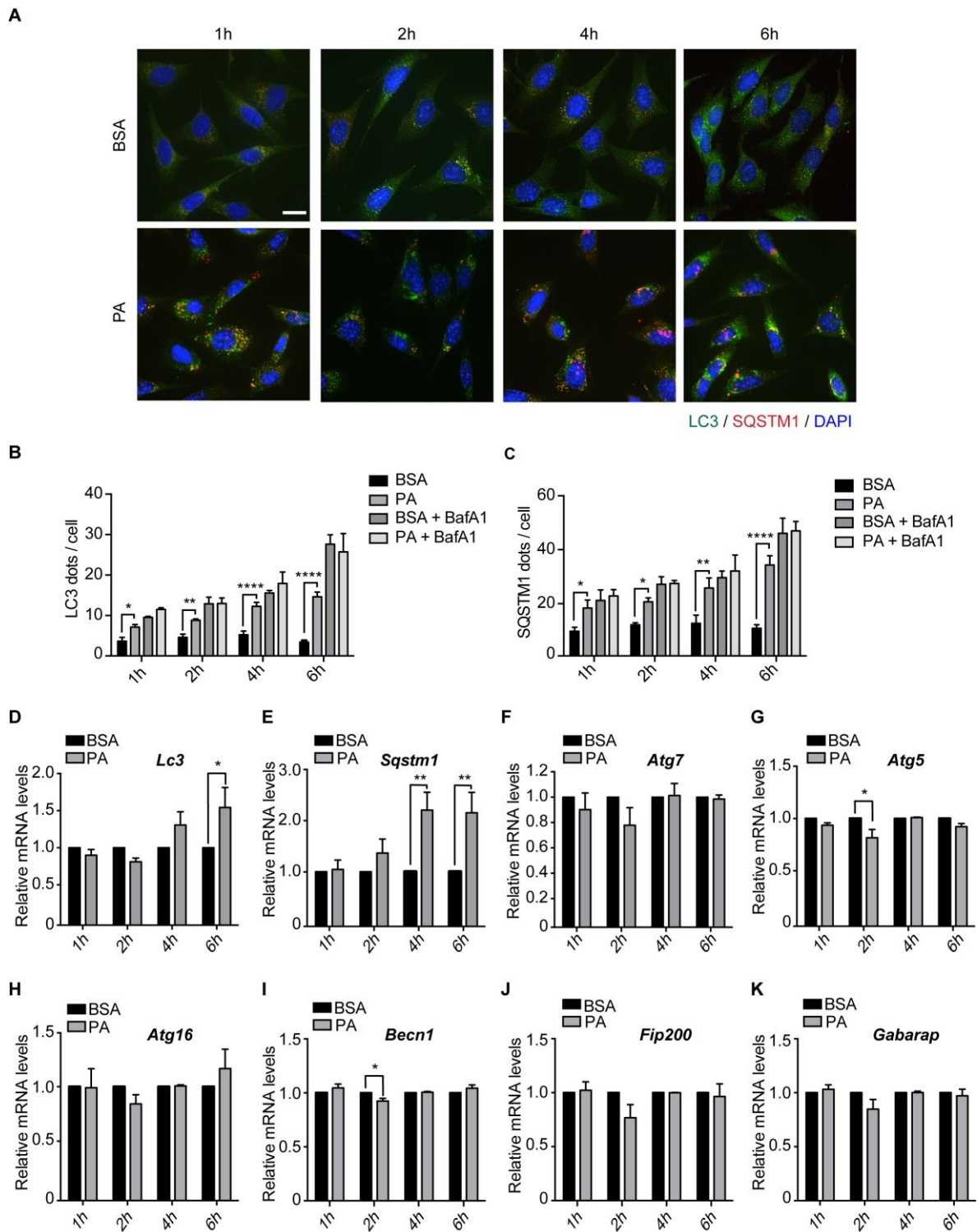


Figure 5: Effect of palmitic acid on autophagy related proteins and *Atg* genes in N43/5 cells. (A) Representative images of N43/5 hypothalamic neuronal cells incubated with BSA or PA for 1 h, 2 h, 4 h or 6 h and stained against LC3 (green) and SQSTM1 (red). Nuclei are stained with DAPI (blue). Bar size 10 μm . Quantification of LC3 (B) and SQSTM1 (C) dots per cell. (D-K) Relative mRNA gene expression of the indicated genes in N43/5 cells treated with BSA or PA for 1 h, 2 h, 4 h and 6 h. Data are presented as mean \pm SEM. * $p \leq 0.05$, ** $p \leq 0.01$, *** $p < 0.0001$. n = 3.

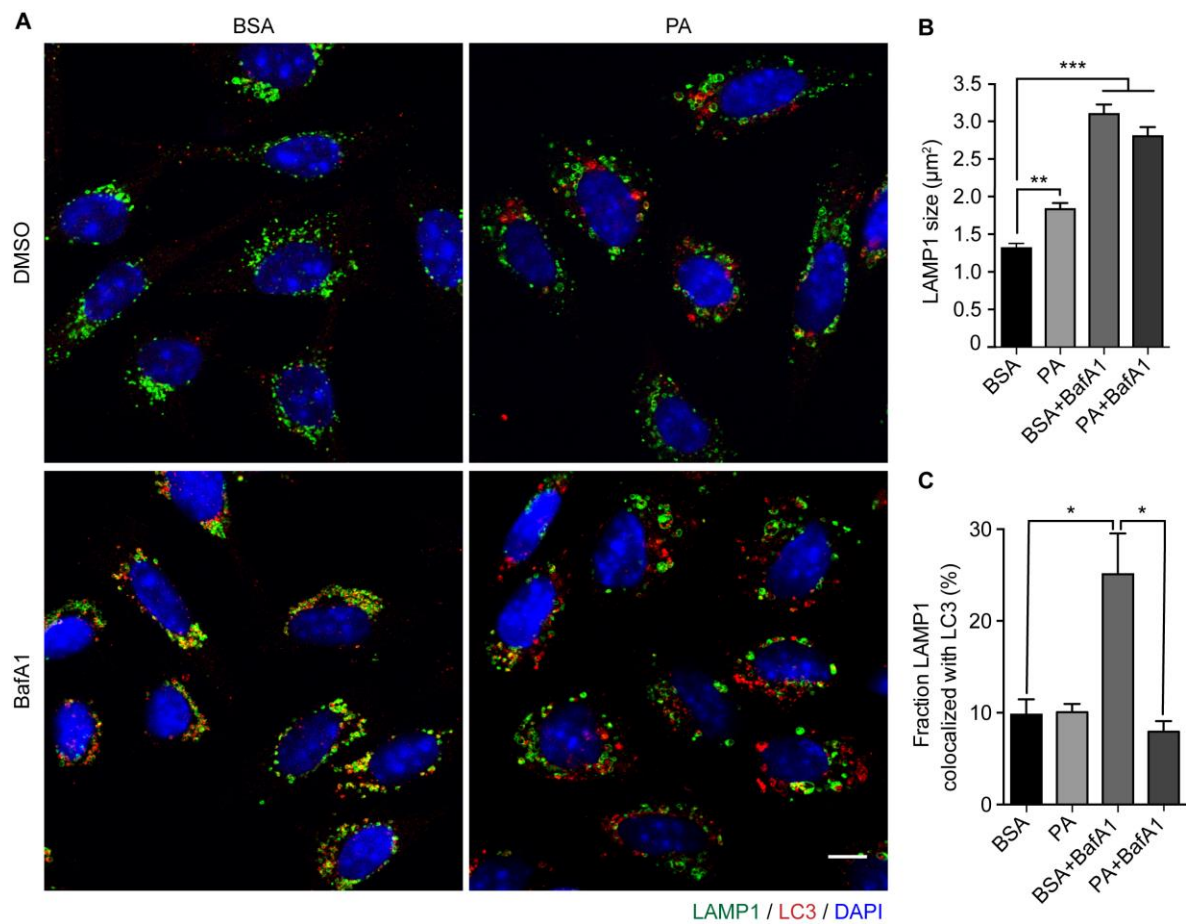


Figure 6. Palmitic acid exposure increases the size of LAMP1 positive vesicles and, in presence of BafA1, decreases LAMP1 and LC3 co-localization in N43/5 cells. (A) Representative images of N43/5 hypothalamic neuronal cells treated with BSA or PA (100 μM) for 6 h in presence or absence of BafA1 (100 nM) or its vehicle (DMSO) and stained against LAMP1 and LC3. **(B)** LAMP1 average dots size. **(C)** % of co-localization between LAMP1 and LC3 according to Manders' Coefficient Analysis. Scale bar: 10 μm . Data are presented as mean \pm SEM, ** $p < 0.01$, *** $p < 0.001$. $n = 3$.

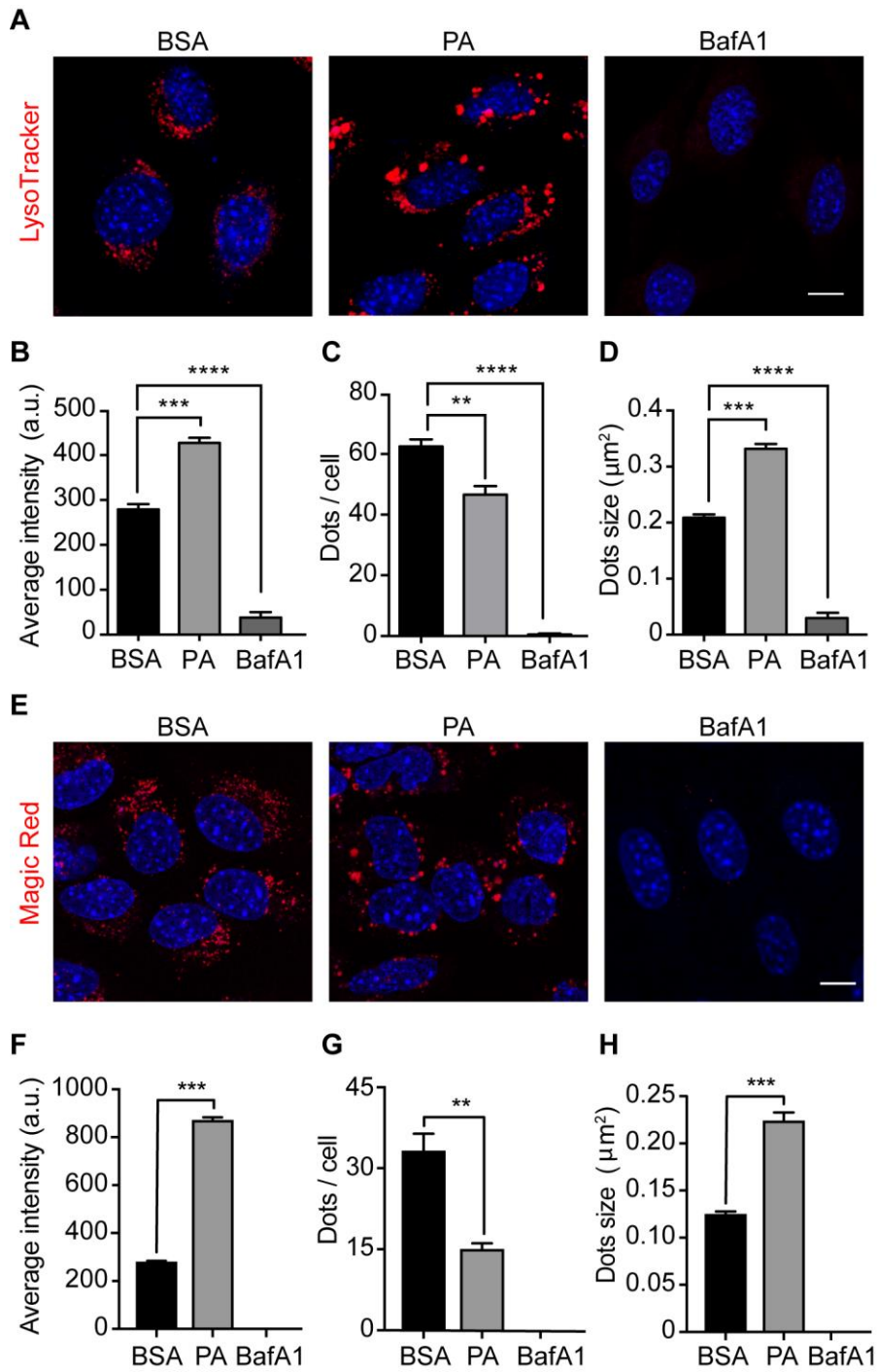


Figure 7: Palmitic acid does not reduce lysosomes acidity or lysosomal cathepsin B activity in N43/5 cells. (A) Representative confocal images of N43/5 hypothalamic neuronal cells treated with BSA, PA (100 μ M), or BafA1 (100 nM) for 6 h and stained with LysoTracker. Nuclei were stained with DAPI (blue). Quantification of LysoTracker average fluorescence intensity in arbitrary units (a.u.), LysoTracker positive dots per cell and dots size are shown in (B), (C), (D), respectively. (E) Representative confocal images of N43/5 cells treated with BSA, PA (100 μ M), or BafA1 (100 nM) for 6 h and stained with Magic Red, with its respective quantification of average fluorescence intensity in arbitrary units (a.u.) (F), number of positive dots per cell (G), and dots size (H). Nuclei were stained with Hoechst (blue). Scale bar: 10 μ m. Data are presented as mean \pm SEM, **p < 0.01, ***p < 0.001, ****p < 0.0001. n = 3.

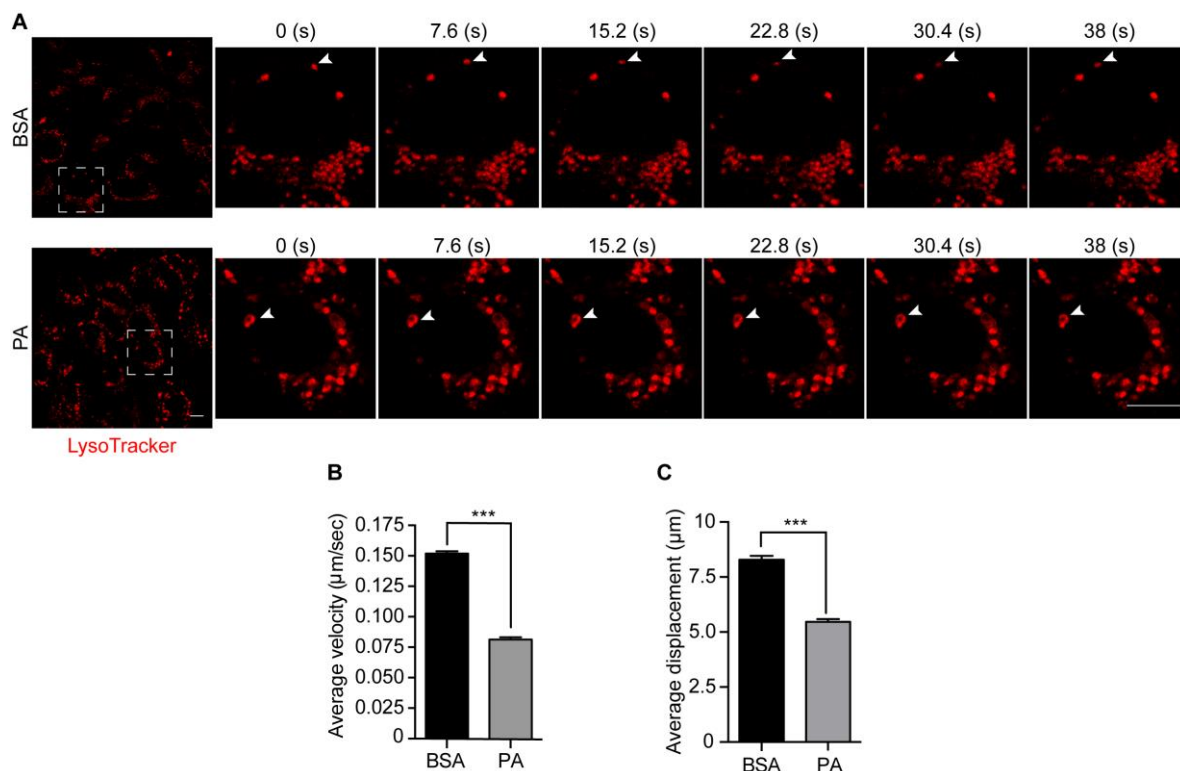


Figure 8. Palmitic acid reduces endolysosomal motility in N43/5 cells. (A) Representative images and zoomed-in time-lapse confocal sequence images of N43/5 hypothalamic neuronal cells treated with BSA or PA (100 μM) for 6 h and stained with LysoTracker. Zoom-ed in inserts represent one cell magnification within the dashed square, showing the dynamic movement of LysoTracker positive vesicles. Arrowhead indicates one LysoTracker positive vesicle movement over time. Average velocity ($\mu\text{m}/\text{s}$) and average total displacement (μm) of positive LysoTracker vesicles are shown in (B) and (C), respectively. Scale bar: 10 μm . Data are presented as mean \pm SEM. *** $p < 0.001$. $n = 3$.

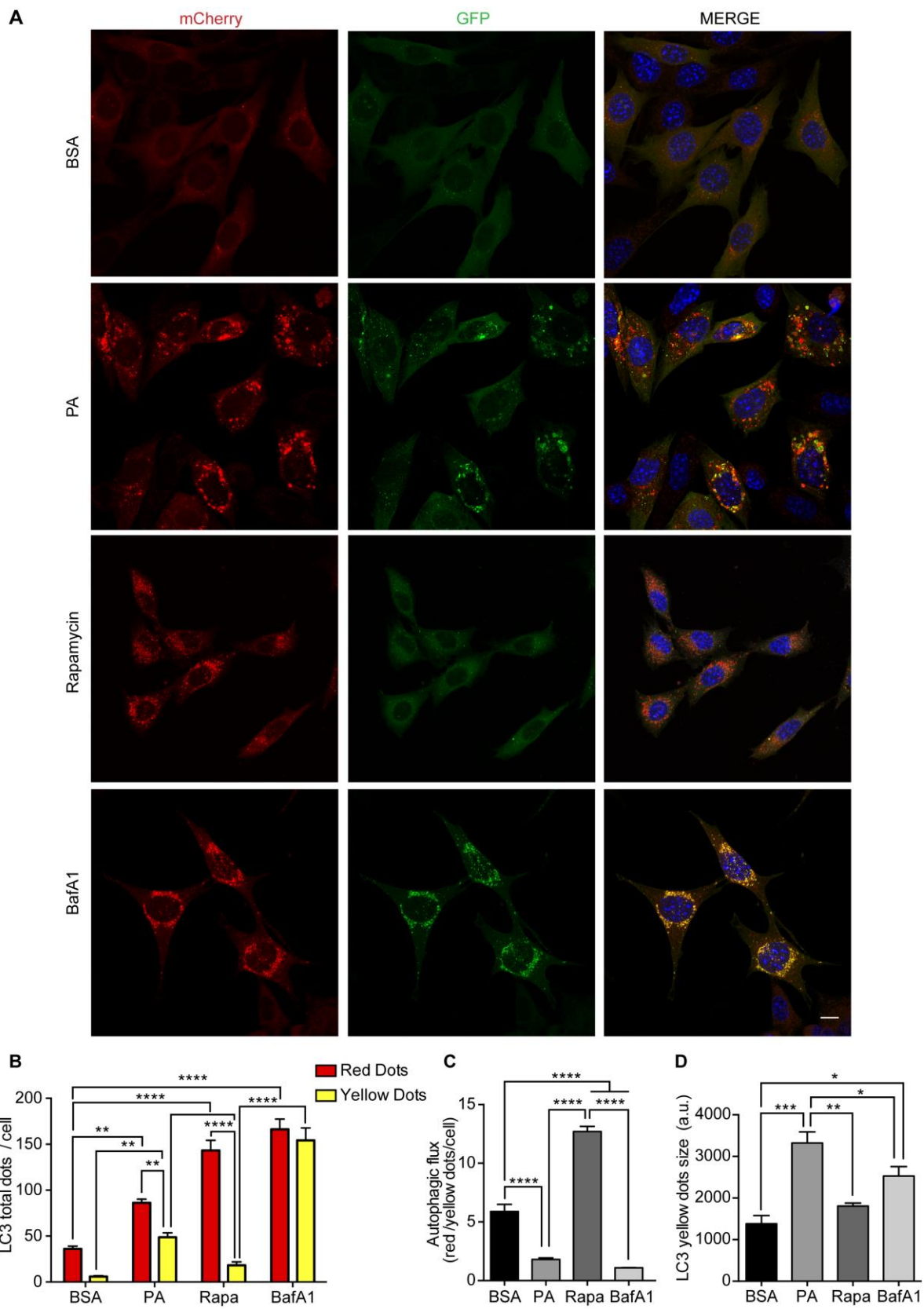


Figure 9. Palmitic acid induces the accumulation of big autophagic vesicles in N43/5 cells.

(A) Representative images of N43/5 hypothalamic neuronal cells expressing the tandem fluorescent-tagged LC3 (mCherry-GFP-LC3), treated with BSA or PA (100 μ M) for 6 h, Rapamycin (Rapa) 1 μ M for 3 h, or BafA1 (100 nM) for 6 h. Scale bar: 10 μ m. Nuclei are stained with DAPI (blue). (B) Quantification of LC3 total dots per cell. Red bars represent the number of mCherry positive dots and yellow bars denote the number of mCherry and GFP dots that co-localized. (C) Autophagic flux was determined by quantifying the ratio between mCherry and yellow-positive puncta per cell. (D) Quantification of LC3 yellow positive vesicles size in arbitrary units (a.u.). Data are presented as mean \pm SEM, * p < 0.05, ** p < 0.01, *** p < 0.001, **** p < 0.0001. n = 3.

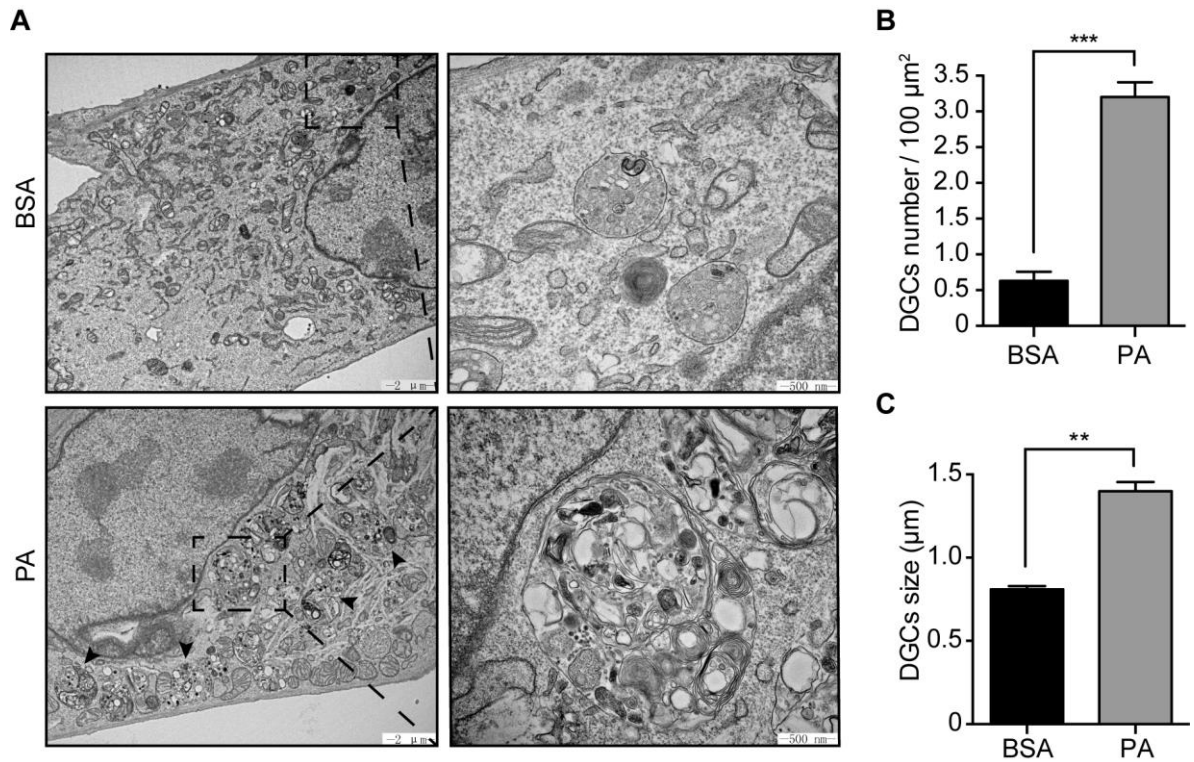


Figure 10. Palmitic acid induces the accumulation of large cellular degradative compartments (DGCs) in N43/5 cells. (A) Representative electronic microscopy images of N43/5 hypothalamic neuronal cells treated with BSA or PA (100 μM) for 6 h. Cellular degradative compartments (DGCs) are indicated by arrowheads. Inserts show a magnification of structures within the dashed square. DGCs number and size are shown in (B) and (C), respectively. Data are presented as mean \pm SEM, ** $p < 0.01$, *** $p < 0.001$. $n = 3$.

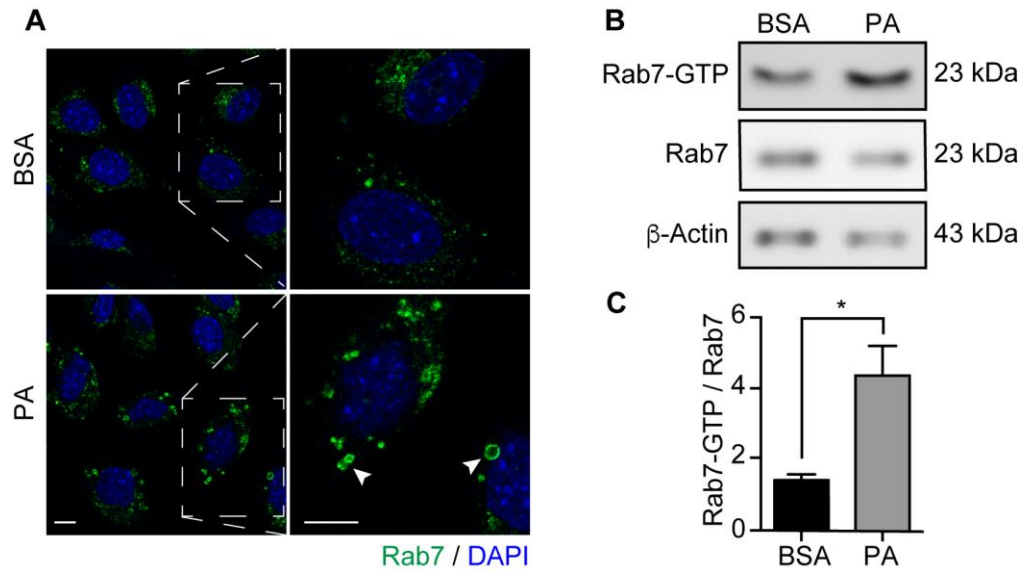


Figure 11: Palmitic acid increases Rab7 activation in N43/5 cells. (A) Representative confocal images of N43/5 hypothalamic neuronal cells treated with BSA or PA (100 μ M) for 6 h and then stained against Rab7. Inserts show a magnification of structures within the dotted square. Arrowheads denotes enlarged Rab7 positive vesicles. Scale bar: 10 μ m. (B) Representative blot showing Rab7 protein bound to GTP and Rab7 total protein levels with its respective quantification (C) in cells following 6 h of the aforementioned treatments. * $p < 0.05$. Data are presented as mean \pm SEM. $n = 3$.

Table I

SILAC based proteomic analysis from isolated lysosomes of N43/5 hypothalamic cells treated with palmitic acid (PA) associated with the endo-lysosomal and the autophagic trafficking pathways. List of significantly upregulated proteins induced by 6 h of PA incubation in N43/5 hypothalamic cells.

Uniprot identifier	Protein name	Gene I.D.	Cellular function	Reference (s)
Q9CXF4	TBC1 domain family member 15	<i>Tbc1d15</i>	Rab7 GAP Mitophagy initiation Autophagosome-lysosome fusion Regulates late endosomal transport Regulates GLUT4 translocation	Zhang et al., 2015 Yamano et al., 2014 Jongsma et al., 2020 Wu et al., 2014
O55102	Biogenesis of lysosome-related organelles complex 1 subunit 1	<i>Bloc1s1</i>	Subunit of BLOC-1 and BORC complexes Implicated in lysosomal trafficking of membrane proteins Involved in endosomal maturation and cargo transport from early endosomes toward lysosomes	Langemeyer et al., 2015 Zhang et al., 2014 Peter et al., 2013 Setty et al., 2007
Q9D920	BLOC-1-related complex subunit 5	<i>Borcs5</i>	Subunits of BORCS complex Regulates Arl8b-SKIP-Kinesin-1 lysosomal transport toward cell periphery	Pu et al., 2015 Guardia et al., 2016
Q9CRC6	BLOC-1-related complex subunit 7	<i>Borcs7</i>	Regulates autophagosome-lysosome fusion through the recruitment of the trans-SNARE complex Regulates lysosomal size and lysosomal reformation through PIKfyve activation	Jia et al., 2017 Jordanov et al., 2017
Q80WQ2	Protein VAC14 homolog Associated Regulator of PIKfyve (ArPIKfyve)	<i>Vac14</i>	Associates with PIKfyve complex Modulates vacuolization in eukaryotic cells Involved in Rab7-dependent endo-lysosomal maturation Involved in Rab9-dependent transport of lysosomal membranes to the trans-Golgi network Linked to insulin-activated GLUT4 translocation and glucose transport	Sbrissa et al., 2007 Jin et al., 2008 Schulze et al. 2017 Schulze et al. 2014 Ikononov et al., 2007
P35285	Ras-related protein Rab-22A	<i>Rab22a</i>	Regulates the morphology of endo-lysosomes and autophagosomes Controls trafficking between endosomes and Golgi apparatus	Mesa et al., 2001 Mesa et al., 2005

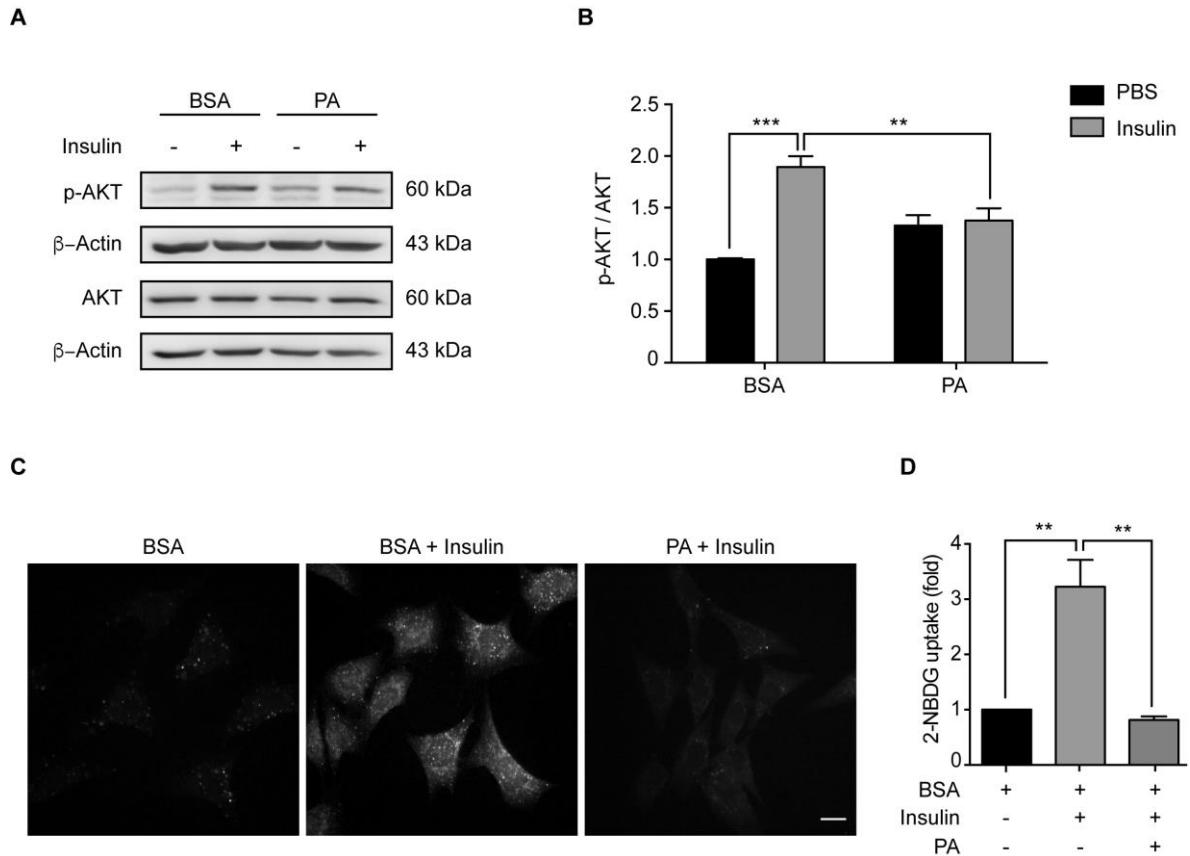


Figure 12: Palmitic acid reduces insulin sensitivity in N43/5 cells. (A) Representative western blot showing relative levels of AKT phosphorylation (Ser473) induced by 15 min of 1 nM insulin or PBS (insulin vehicle) treatment in N43/5 cells pre-incubated with PA (100 μ M) or BSA for 6 h, with its respective quantification (B). (C) Representative images of 2-NBDG uptake in N43/5 cells incubated with vehicle (BSA) or PA (100 μ M) for 6 h and then stimulated with insulin 1 nM for 30 min, with its representative quantification (D). Size bar: 10 μ m. Data are presented as mean \pm SEM, ** $p < 0.01$, *** $p < 0.001$. $n = 3$.

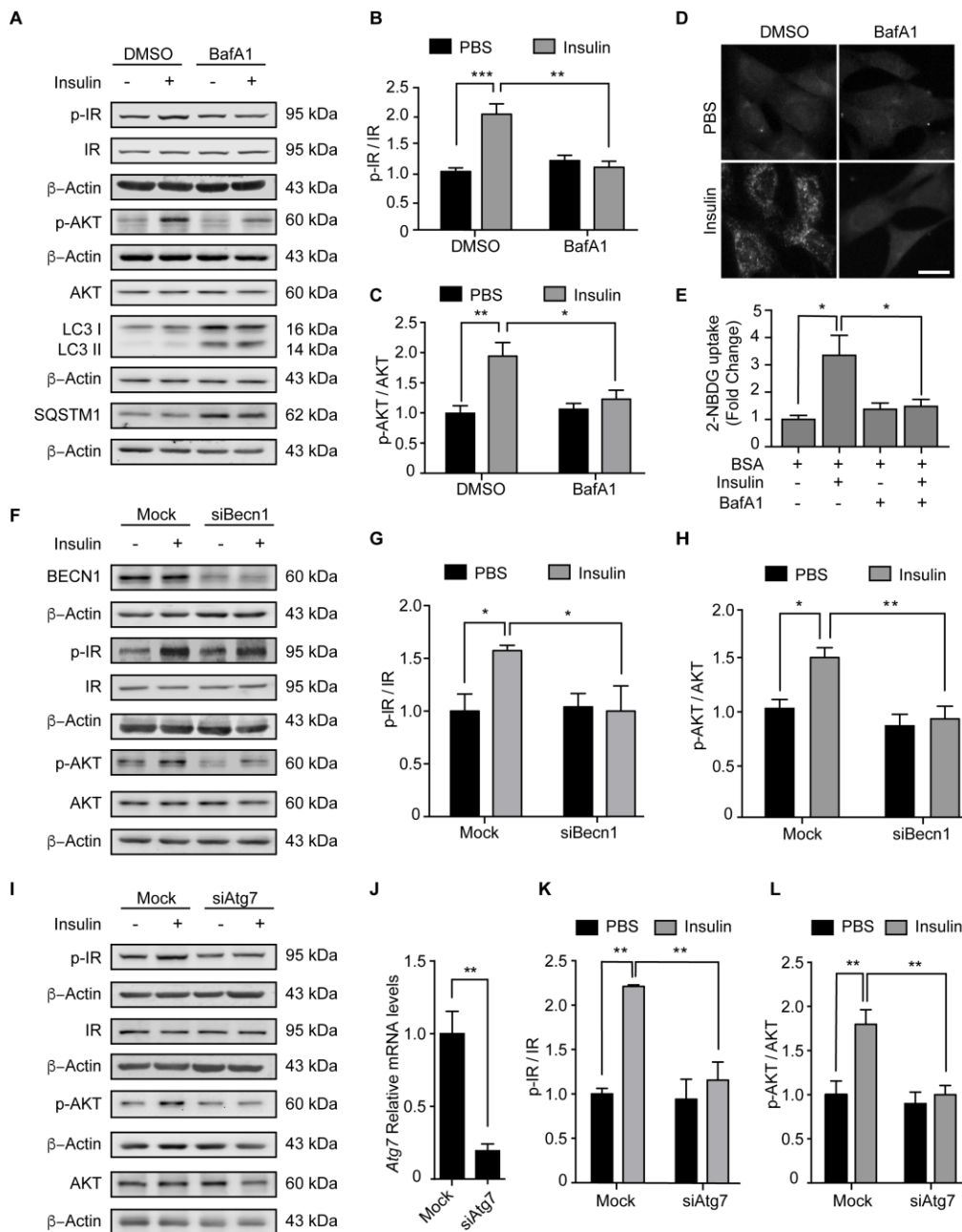


Figure 13: Inhibition of autophagy reduces insulin sensitivity in N43/5 cells. (A) Representative western blots of the indicated proteins of N43/5 cells pre-incubated with BafA1 (100 nM) or its vehicle (DMSO) during 6 h and then stimulated with insulin for 3 min to evaluate IR phosphorylation (Tyr1150/1151) or 15 min to evaluate AKT phosphorylation. (B-C) Quantification of IR (Tyr1150/1151) and AKT (Ser473) phosphorylation in cells exposed to the

treatments as indicated in **(A)**. **(D)** Representative images and quantification **(E)** of 2-NBDG uptake in N43/5 cells pre-incubated with BafA1 (100 nM) or its vehicle (DMSO) during 6 h and then stimulated with insulin for 30 min. Size bar: 10 μ m. Representative blot of the indicated proteins of N43/5 cells transfected with siRNA against BECN1 **(F)** or ATG7 **(I)** followed by insulin or PBS treatment for 3 min to evaluate IR phosphorylation or 15 min to evaluate AKT phosphorylation, with its respective quantifications **(G, H, K, L)**. **(J)** mRNA levels of *Atg7* in N43/5 cells transfected with a siRNA to downregulate ATG7. As control condition, cells were incubated with Lipofectamine RNAiMAX reagent only (Mock). Data are presented as mean \pm SEM, * $p < 0.05$, ** $p < 0.01$, *** $p < 0.001$. n= 3.

7. DISCUSSION

According to the World Health Organization obesity and its associated metabolic complications have become a major public health concern worldwide (WHO, 2018). One of the main factors increasing the prevalence of obesity is the consumption of HFD, which contains high levels of SatFAs, increases body weight and promotes metabolic dysfunction such as insulin resistance (Milanski et al., 2009; Zhang et al., 2009a). Chronic HFD consumption increases SatFAs levels in the brain of male mice (Rodriguez-Navas et al., 2016); specifically the long-chain SatFA PA accumulates in the hypothalamus (Vagena et al., 2019), where it promotes hypothalamic insulin resistance among other co-morbidities associated with obesity (Benoit et al., 2009; Gerozissis, 2008; Posey et al., 2009). Interestingly, autophagy impairment has been observed in mice hypothalamus following chronic HFD exposure (Morselli et al., 2014a). This results in accumulation of misfolded proteins, superfluous and damaged organelles, which could lead to cell death and disease (Sridhar et al., 2012). Indeed, defects in autophagy homeostasis are implicated in metabolic disorders, including obesity, insulin resistance and diabetes mellitus, among others (Zhang et al., 2018). Specifically, in hypothalamic neurons, autophagy disruption has been involved in the progression of metabolic diseases associated with obesity including increased food intake, adiposity and glucose intolerance (Aveleira et al., 2015; Coupe et al., 2012; Kaushik et al., 2011; Meng and Cai, 2011). Importantly, Portovedo et al. show that autophagic dysfunction in the hypothalamus may be due to the direct effect of PA (Portovedo et al., 2015); however, how PA dysregulates autophagy in hypothalamic neurons, as well as its metabolic consequences, has not been elucidated.

This thesis was focused in understanding the cellular and molecular mechanisms involved in autophagy dysfunction induced by increased levels of the SatFA PA in hypothalamic neuronal cells.

Palmitic acid inhibits autophagic flux in hypothalamic neuronal cells inducing the accumulation of enlarged autophagic structures and big endolysosomal vesicles with reduced motility

We demonstrated, in N43/5 hypothalamic neuronal cells and in primary hypothalamic neurons, that PA decreases the autophagic flux (Fig. 4). This was supported by the fact that, even if PA treatment for 4 h and 6 h increases the mRNA expression levels of *Sqstm1/p62* and *Lc3* (Fig. 5), respectively, the accumulation of autophagic structures as well as increased SQSTM1/p62 protein aggregates, were seen after 1 h of PA exposure, suggesting autophagic flux inhibition has been affected. In addition, SQSTM1/p62 has a role in the oxidative stress response pathway (Nezis and Stenmark, 2012), and considering that PA also activates several intracellular stress pathways (Fatima et al., 2019), this could explain our observations.

Autophagic flux inhibition induced by PA, could be caused by both impaired fusion of autophagic vacuoles with the lytic compartments, or because of a compromised proteolytic activity of lysosomal hydrolases (Koga et al., 2010). Our results show no difference in the percentage of colocalization of LAMP1 and LC3, indicative of autophagosome-lysosome fusion, between control (BSA) and PA treated cells (Fig. 6). However, this parameter is significantly reduced in cells co-exposed to PA and BafA1, when compared to BafA1 treatment alone, suggesting PA might inhibit the autophagosome-lysosome fusion in N43/5 cells.

Importantly, we also observed a significant increase in the size of LAMP1 positive structures in PA treated cells, phenotype that has been associated with decreased autophago-lysosomal fusion (Mauthe et al., 2018). Previous studies *in vivo* and *in vitro*, using the autophagosome marker GFP-LC3, indicate that autophagosomes are rare in healthy neurons under nutrient-rich conditions (Mizushima et al., 2004; Nikolettou et al., 2015). However, inhibition of lysosomal degradation under nutrient-rich conditions causes the rapid accumulation of autophagosomes in a model of cortical neurons, suggesting that autophagy constitutively occurs in neurons, and that the progression rate from vesicle formation to degradation is extremely quick (Boland et al., 2008; Lee et al., 2011; Nikolettou et al., 2015). It is possible that in neurons, which have a high energy demand, and which are post-mitotic cells, the quality control and homeostasis maintenance are vital (Tsunemi et al., 2012), thus, it is suggested that the autophagic machinery is so efficient that autophagosomes are not accumulated in healthy neurons at detectable levels (Nikolettou et al., 2015). In this context, considering the low levels of LC3 dots observed in control conditions in our hypothalamic cellular model, it is possible that the co-localization analysis between LC3 and LAMP1 is meaningless at basal levels. Thus, the accumulation of autophagic structures due to lysosomal inhibition could reveal PA real effects on autophagosome-lysosome fusion, suggesting PA decreases this process. Indeed, this hypothesis is supported by the result showing that treatment with BafA1, which inhibits the degradation of the autophagic cargo, shows a high percentage of LC3 and LAMP1 co-localization levels compared to control and to PA-BafA1 co-treatment, suggesting that BafA1 does not affect autophagosome-lysosome fusion, while PA does.

In agreement with these observations, by using a tandem fluorescence construct of mCherry coupled to GFP-LC3 (Fig. 9), we also found that PA decreases autophagic flux in N43/5 cells and induces the accumulation of big size autophagic structures lacking degradative capacity probably as consequence of impaired fusion between autophagic vesicles and lysosomes. In addition to these results, we found that PA did not compromise the acidity or the hydrolytic activity of lysosomes (Fig. 7); thereby strongly suggesting that PA-induced autophagic flux inhibition is caused by decreased autophagosome-lysosome fusion. Importantly, we observed an increased fluorescence intensity of both LysoTracker and Magic red positive vesicles in PA treated cells, compared to control (Fig. 7A, B, E, F). In this context, Schulze et al. also observed the formation of large intracellular vacuoles with increased LysoTracker staining in podocytes when the PIKfyve complex was defective (Schulze et al., 2017). The PIKfyve complex consists of three main components Vac14, the phosphatase Fig4 and the lipid kinase PIKfyve (Schulze et al., 2017). PIKfyve is involved in the production of the lipid PI(3,5)P₂, which levels are carefully tuned to maintain the turnover of vacuolar membranes to less mature endocytic compartments, hence, regulating organelle's size (Odorizzi et al., 1998). PIKfyve complex deficiency or dysregulation of one of its components leads to the development of large intracellular vacuoles (Schulze et al., 2014). These cellular manifestations are linked to several forms of neurological disorders, emphasizing that endolysosomal or autophagic trafficking or maturation defects are the cause for severe diseases (Chow et al., 2007). Thus, it is possible that PA is affecting the levels of one or more proteins involved in the formation of the PIKfyve complex.

In accordance with our previous results, we determined by live microscopy that endolysosomal vesicles (LysoTracker positive dots; Fig. 8) of PA-treated cells showed

decreased motility, suggesting that PA also causes impairment in intracellular trafficking. The reduction in intracellular trafficking is accompanied by an increased activation state of the small GTPase Rab7 (Fig. 11) in PA-treated cells. Rab7 on late endosomes/lysosomes recruits tethering factors, as PLEKHM1, and HOPS, to promote the assembly of trans-SNARE complexes for fusion of autophagosomes and lysosomes. Rab7, as well, controls trafficking of cargos along microtubules, thus, regulating the final step of autophagosome fusion with lysosomes and/or endosomes (Guerra and Bucci, 2016; Hyttinen et al., 2013). Additionally, it has been shown that Rab7 hyper-activation inhibits autophagic lysosomal reformation, leading to the accumulation of enlarged autolysosomes (Yu et al., 2010) and swelling of endo-lysosomal vesicles, containing aberrant intraluminal content. Rab7 hyper-activation also dysregulates intracellular transport routes involved in the maintenance and maturation of endo-lysosomal membranes (Jongsma et al., 2020). Future research should evaluate if PA, in addition to Rab7, affects other proteins involved in autophagosome-lysosome fusion. Despite this, our data suggest that PA inhibits the autophagic flux inducing the accumulation of big DGCs by affecting intracellular vesicular trafficking mediated by increased Rab7 activity, in N43/5 cells.

Palmitic acid modulates the recruitment to lysosomes of proteins involved in the autophagic and endolysosomal trafficking pathways in N43/5 cells

We identified by a SILAC proteomic from isolated lysosomes treated with PA, a set of proteins involved with the control of endo-lysosomal trafficking and with the autophagic process, including autophagic maturation or autophagic fusion with endo-lysosomal vesicles (Table I). Among those, we identified TBC1D15, which is increased in lysosomes exposed to

PA. Several Rab7 GEFs and GAPs are involved in the dynamic cycling between active and functional Rab7 (Rab7-GTP) and inactive, cytosolic Rab7 (Rab7-GDP), respectively. TBC1D15 is a Rab7 GAP responsible for promoting GTP hydrolysis rendering Rab7 inactive, resulting in its dissociation from the lysosomal membrane (Zhang et al., 2005). TBC1D15 has been also implicated in mitophagy induction (Yamano et al., 2014). Additionally, TBC1D15 silenced cells presented enlarged autophagosomes that extend bi-directionally along microtubule tracts. Moreover, autophagic structures, in TBC1D15 silenced cells showed impaired fusion with lysosomes accompanied with disturbed distribution in the cell (Yamano et al., 2014), which suggests that the increased recruitment of TBC1D15 to lysosomes might cause the impairment in autophagy we see following PA treatment.

In addition, we also found increased levels of Vac14 in PA-treated lysosomes. Interestingly, Schulze and collaborators found that Vac14 specifically binds to the Rab7 GAP, TBC1D15 (Schulze et al., 2014), which could explain the increased recruitment of both proteins in lysosomes following treatment with PA. However, we observed increased levels of Rab7 bound to GTP (Fig. 11) suggesting that, even if Vac14 is able to sequester TBC1D15 in some lysosomes, it might reduce the cytosolic pool of TBC1D15 required for the inactivation of Rab7 on the membrane of other vesicles, including late endosomes, amphisomes, and/or autophagosomes. This hypothesis is supported by the fact that the SILAC Proteomic analysis was performed using samples from lysosomes isolated through the method of gradient ultracentrifugation. Considering PA induces changes in lysosome morphology, characterized by enlarged structures (Fig. 6 and 7), it is possible that our samples do not include larger size aberrant endolysosome vesicles. Thus, EM analysis of the lysosomal fraction following PA

treatment needs to be performed to determine the vesicles contained in the fraction following PA exposure.

Furthermore, Schulze et al. showed that Vac14 is able to bind the PIKfyve complex, acting as structural mediator, and maintaining its integrity via homo and heteromeric interactions with the remaining subunits (Jin et al., 2008). As already mentioned, PIKfyve kinase catalyzes the phosphorylation of phosphatidylinositol 3-phosphate (PI3P) into PI(3,5)P₂ (Sbrissa et al., 2007). Importantly, the overexpression of Vac14 impairs the process of endolysosomal maturation, which results in strong vacuolization of the cells (Schulze et al., 2014). Vacuolization can be explained as a morphological consequence of disturbed membrane fusion of incoming vesicles with target membranes, reduced formation of intraluminal vesicles, or a defect in the budding of vesicles (Wada, 2013). Malfunction of any of the PIKfyve complex members leads to cellular vacuolization, which in mice is linked to lethal phenotypes due to damaging of neuronal cells emphasizing that neurons are highly susceptible to endolysosomal or autophagosomal impairment (Chow et al., 2007; Ferguson et al., 2009; Zhang et al., 2007). Vac14-dependent vacuoles and PIKfyve inhibitor-dependent vacuoles resulted in elevated levels of late endosomal, lysosomal, and autophagy-associated proteins. However, only late endosomal marker proteins were bound to the membranes of these enlarged vacuoles (Schulze et al., 2014), which might give us some clues about the nature of the big DGCs observed in N43/5 cells treated with PA (Fig. 10). Thus, we might speculate that increased levels of Vac14 found in lysosomes exposed to PA could dysregulate PIKfyve kinase activity contributing to the formation of autophagic and endolysosomal/DGCs vesicles observed in our results.

Additionally, Vac14 is also able to interact with ATP6V1H, a subunit of the v-ATPase responsible for the maintenance of pH homeostasis, and both, lack or overexpression of Vac14 promotes the formation of enlarged intracellular vesicles positive for endo-lysosomal markers (Schulze et al., 2014). This vacuolization phenotype, which is associated with maturation defects in the endolysosomal system (Schulze et al., 2017), was completely rescued by starvation or using BafA1 (Schulze et al., 2017). In agreement with this, Mundy et al. found that starvation was accompanied by an increased basification of endolysosomal compartments (Mundy et al., 2012). These data suggest that increased acidification of endolysosomal compartments could induce enlarged intracellular vesicles. These data might help explaining the increase in LysoTracker fluorescence intensity observed in cells treated with PA (Fig. 7). We might speculate that PA, in N43/5 cells, rather than abolishing lysosomes acidity or lysosomal cathepsin B activity, increases their acidity, leading to the formation of big endosomes/lysosomes, as consequence of increased Vac14 lysosomal recruitment.

On other side, we observed increased proteins levels of BORC complex subunits (BORCS5/myrlysin; BORCS7/diaskedin; BLOC1S1) in lysosomes following PA exposure. BORC associates with the cytoplasmic leaflet of the limiting late endosomal/lysosomal membrane, at least partially through an N-terminal myristoyl group on Myrlysin (Pu et al., 2015). The main function of BORC is the recruitment of the small Arf-like GTPase Arl8b from the cytoplasm into the lysosomal membrane. Arl8b interacts with an effector SKIP, which links to the microtubule motor protein Kinesin-1, resulting in lysosomal migration towards the cell periphery (Guardia et al., 2016; Pu et al., 2015). Thus, BORC acts as a promoter of Arl8b-SKIP-Kinesin-1 lysosomal transport, mirroring the role of the Rab7-RILP-Dynein-Dynactin complex (which moves lysosomes to the perinuclear cell area), involved in lysosomal transport towards

the microtubule-organizing center (Pu et al., 2015). It has been observed that knockout (KO) or knockdown (KD) of BORC subunits causes the collapse of the lysosome population, which migrates to the perinuclear area of the cell (Guardia et al., 2016; Pu et al., 2015). In addition, Jia et al. reported in HeLa cells that KO of any of the genes encoding BORC subunits increased LC3-II and SQSTM1 levels, a sign of altered autophagy. Furthermore, BORC KO impairs both the encounter and fusion of autophagosomes with lysosomes, as a result of an inability of lysosomes to move toward the peripheral cytoplasm, where many autophagosomes are formed (Jia et al., 2017). Moreover, BORC KO also reduces the Arl8-dependent recruitment of HOPS tethering complex to lysosomes and assembly of the STX17-VAMP8-SNAP29 trans-SNARE complex involved in autophagosome-lysosome fusion. Through these dual roles, BORC integrates the kinesin-dependent movement of lysosomes toward autophagosomes with HOPS-dependent autophagosome-lysosome fusion (Jia et al., 2017). Importantly, overexpression of the BORCS7 also induces lysosomal accumulation in neurons as consequence of impaired intracellular trafficking (Farias et al., 2017). Considering our results, future experiments should be performed to determine if increased levels of the BORC subunits in the lysosome could impair its function.

Furthermore, Yordanov et al. observed that the BORC complex regulates late endosomal/lysosomal size in a PIKfyve-dependent manner (Yordanov et al., 2019). They found that specific deletion of the BORC subunits Myrlysin (BORCS5) and Diaskedin (BORCS7) compromises the assembly of the complex on the organelle membrane and triggers a decrease in lysosomal size (Yordanov et al., 2019). Importantly, the specific deletion of BORCS7 induced the formation of small size endosomes, suggesting an inhibitory role for the BORC complex toward PIKfyve activity. Taking into account that we observed increased levels of BORCS5

and BORCS7 in lysosomes exposed to PA, we might speculate that upregulation of these proteins is inducing the formation of large lysosome, as consequence of dysregulated PIKfyve activity. Future studies should elucidate if PA is able to regulate BORC.

Finally, we also found in lysosomes exposed to PA, increased levels of Rab22a, which associates with early and late endosome, but not with lysosomes (Mesa et al., 2001). Interestingly, overexpression of Rab22a in CHO cells causes the enlargement of early and late endosomes. Furthermore, Rab22a can affect the trafficking from endosomes to the Golgi apparatus probably by promoting fusion among endosomes and impairing the proper segregation of membrane domains required for targeting to the trans-Golgi network (TGN) (Mesa et al., 2005). Additional studies show that the overexpression of Rab22a caused, in HeLa cells, a complete vacuolization of the Golgi apparatus (Kauppi et al., 2002), suggesting again that Rab22a may have a function in the communication between Golgi and early endosome. These data suggest, that increased levels of Rab22a found in lysosomes exposed to PA could cause impairment in intracellular trafficking, which involves the TGN.

Altogether our data suggest that PA modulates the recruitment to lysosomes of proteins involved in autophagic and endolysosomal trafficking pathways associated with Rab7 hyper-activation and, possibly, with BORC and/or PIKfyve dysregulation.

Palmitic acid and the inhibition of autophagy reduces insulin sensitivity in N43/5 cells

Here, we demonstrate that exposure to the SatFA PA inhibits the autophagic flux (Fig. 4, 5) and reduces insulin sensitivity (Fig. 12) in N43/5 hypothalamic neurons. Furthermore, we

show that inhibition of autophagy and the autophagic flux reduces insulin sensitivity in the same cellular model (Fig. 13). To note, previous studies indicate autophagy impairment in hypothalamic POMC neurons contributes to obesity-associated metabolic dysfunctions, including insulin resistance (Kaushik et al., 2012). The existence of a crosstalk between autophagy and insulin sensitivity has been previously suggested and identified in peripheral metabolic tissues (Ebato et al., 2008; Jung et al., 2008; Yamamoto et al., 2018). Interestingly, it was recently demonstrated that autophagy degrades insulin-containing vesicles in β -cells of autophagy-hyperactive mice, whereas in insulin-sensitive cells, autophagy enhances insulin response (Yamamoto et al., 2018). Indeed, induction of autophagy, by different means, in skeletal muscle, hepatocytes, podocytes and adipocytes (Ahlstrom et al., 2017; Xin et al., 2016; Zhou and Ye, 2018), stimulates insulin sensitivity; suggesting increased autophagy might be a general mechanism to boost insulin response. Despite this, there are no reports that determine if this crosstalk also occurs in the CNS, specifically, in the hypothalamus where insulin sensitive neurons key in the regulation of food intake and peripheral glucose homeostasis reside. In the present study, we evaluated if inhibition of autophagy or autophagic flux inhibition in a hypothalamic neuronal cell line affects insulin response. Our data indicate that this might be the case, as downregulation of different autophagy essential genes (*Atg7* and *Beclin1*), as well as inhibition of the autophagic flux using BafA1, reduced the ability of the neuron to respond to insulin, as indicated by p-IR and p-AKT level and the reduction in glucose uptake following BafA1 exposure (Fig. 13). How this might be occurring has not been elucidated; however, a possibility is that, by inhibiting autophagy we prevent the degradation of negative regulators of the insulin signaling pathway, such as the protein phosphatase and tensin homolog (PTEN), which can be degraded by the autophagic/lysosomal pathway (Wang et al., 2017). In addition,

based on these results, it is tempting to speculate that the maintenance of the autophagic balance in hypothalamic neurons might be key in the regulation of peripheral glucose homeostasis, as well as food intake. Future studies in neuron-specific transgenic mouse models need to be performed to confirm this hypothesis *in vivo*.

As mentioned above, we observed that N43/5 cells exposed to PA (Fig. 12), as well as BafA1 (Fig. 13), showed decreased glucose uptake in response to insulin. Importantly, it has been shown that the hypothalamic Glucose Transporter 4 (GLUT4) in neurons is a key mediator of insulin action (Ren et al., 2015). In basal conditions, most of GLUT4 is stored in intracellular compartments that include endosomes, TGN and tubular-vesicular structures consisting of endosomal sorting intermediates and GLUT4 storage vesicles (Leto and Saltiel, 2012). After insulin stimulation, GLUT4 is distributed to the plasma membrane, and failure of this translocation in response to insulin results in insulin resistance and type 2 diabetes mellitus (Leto and Saltiel, 2012; Saltiel and Kahn, 2001). Importantly, insulin-mediated GLUT4 membrane translocation is necessary for the transportation of glucose in hypothalamic neurons (Changou et al., 2017; Jurcovicova, 2014; Thierry Alquier et al., 2006). Interestingly, it has been shown that TBC1D15 is also able to regulate glucose uptake by affecting the translocation of GLUT4 through the late endosomal pathway in different cell lines (Wu et al., 2019). Furthermore, Wu and collaborators found in TBC1D15 KO cells higher levels of Rab7 in LAMP-1 decorated late endosomes/lysosomes and an increase in the co-localization between GLUT4 and Rab7 (Wu et al., 2019). In addition, also Vac14 has been associated to insulin-activated GLUT4 translocation and glucose transport in 3T3-L1 adipocytes (Ikonomov et al., 2007). Thus, considering that Vac14 interacts with TBC1D15, it is tempting to speculate PA increases their recruitment to lysosomes, thereby reducing the cytosolic pool of TBC1D15 and/or Vac14 required for an

efficient translocation of GLUT4 to the membrane. Therefore, the lysosomal increase of these two proteins following PA treatment might indicate that the insulin-dependent translocation of GLUT4 to the cell membrane is impaired.

Altogether, these data suggest that, in hypothalamic neuronal cells, autophagic flux inhibition induced by PA reduces insulin sensitivity and glucose uptake due to a dysregulation in endolysosomal trafficking.

8. CONCLUSIONS

In this thesis we confirmed that exposure to the SatFA PA inhibits the autophagic flux in hypothalamic neurons. Furthermore, we demonstrated in the hypothalamic neuronal cell line N43/5 that the accumulation of enlarged autophagic and endolysosomal structures, generated by autophagy impairment, is not the result of the reduction in lysosomal activity, but by an alteration in endolysosomal dynamics that impairs autophagosome-lysosome fusion. Additionally, we founded that PA regulates Rab7 GTPase activity, as well as the recruitment to lysosomes of proteins related with autophagic and endolysosomal trafficking pathways associated with Rab7 activation and, possibly, with BORC and/or PIKfyve dysregulation. Finally, our data show that, in N43/5 cells, PA and the inhibition of the autophagic flux reduced insulin sensitivity and glucose uptake, probably by a mechanism that involves endolysosomal trafficking dysregulation.

Altogether, these results suggest that an increase in endolysosomal dynamics should be considered as a strategy to recover the impairment in autophagy caused by PA overload in hypothalamic neurons.

9. REFERENCES

- Abbott, N.J., Patabendige, A.A., Dolman, D.E., Yusof, S.R., and Begley, D.J. (2010). Structure and function of the blood-brain barrier. *Neurobiol Dis* 37, 13-25.
- Abumrad, N.A., Ajmal, M., Pothakos, K., and Robinson, J.K. (2005). CD36 expression and brain function: does CD36 deficiency impact learning ability? *Prostaglandins Other Lipid Mediat* 77, 77-83.
- Ahlstrom, P., Rai, E., Chakma, S., Cho, H.H., Rengasamy, P., and Sweeney, G. (2017). Adiponectin improves insulin sensitivity via activation of autophagic flux. *J Mol Endocrinol* 59, 339-350.
- Andrews, Z.B., Liu, Z.W., Wallingford, N., Erion, D.M., Borok, E., Friedman, J.M., Tschop, M.H., Shanabrough, M., Cline, G., Shulman, G.I., et al. (2008). UCP2 mediates ghrelin's action on NPY/AgRP neurons by lowering free radicals. *Nature* 454, 846-851.
- Avalos, Y., Hernández-Cáceres, M., Toledo, L., and Morselli, E. (2017). Loss of autophagy in hypothalamic neurons may be involved in the pathogenesis of obesity. *Autophagy* 12, 295–312.
- Aveleira, C.A., Botelho, M., Carmo-Silva, S., Pascoal, J.F., Ferreira-Marques, M., Nobrega, C., Cortes, L., Valero, J., Sousa-Ferreira, L., Alvaro, A.R., et al. (2015). Neuropeptide Y stimulates autophagy in hypothalamic neurons. *Proc Natl Acad Sci U S A* 112, E1642-1651.
- Ballabio, A., and Gieselmann, V. (2009). Lysosomal disorders: from storage to cellular damage. *Biochim Biophys Acta* 1793, 684-696.
- Banks, W.A. (2004). The source of cerebral insulin. *Eur J Pharmacol* 490, 5-12.
- Banks, W.A. (2019). The blood-brain barrier as an endocrine tissue. *Nat Rev Endocrinol* 15, 444-455.
- Banks, W.A., Jaspán, J.B., and Kastin, A.J. (1997). Effect of diabetes mellitus on the permeability of the blood-brain barrier to insulin. *Peptides* 18, 1577-1584.

Bazinet, R.P., and Laye, S. (2014). Polyunsaturated fatty acids and their metabolites in brain function and disease. *Nat Rev Neurosci* *15*, 771-785.

Bellenger, J., Bellenger, S., Escoula, Q., Bidu, C., and Narce, M. (2019). N-3 polyunsaturated fatty acids: An innovative strategy against obesity and related metabolic disorders, intestinal alteration and gut microbiota dysbiosis. *Biochimie* *159*, 66-71.

Belsham, D.D., Cai, F., Cui, H., Smukler, S.R., Salapatek, A.M., and Shkreta, L. (2004). Generation of a phenotypic array of hypothalamic neuronal cell models to study complex neuroendocrine disorders. *Endocrinology* *145*, 393-400.

Ben-Zvi, A., Lacoste, B., Kur, E., Andreone, B.J., Mayshar, Y., Yan, H., and Gu, C. (2014). Mfsd2a is critical for the formation and function of the blood-brain barrier. *Nature* *509*, 507-511.

Bennett, L., Yang, M., Enikolopov, G., and Iacovitti, L. (2009). Circumventricular organs: a novel site of neural stem cells in the adult brain. *Mol Cell Neurosci* *41*, 337-347.

Benoit, S.C., Air, E.L., Coolen, L.M., Strauss, R., Jackman, A., Clegg, D.J., Seeley, R.J., and Woods, S.C. (2002). The catabolic action of insulin in the brain is mediated by melanocortins. *J Neurosci* *22*, 9048-9052.

Benoit, S.C., Clegg, D.J., Seeley, R.J., and Woods, S.C. (2004). Insulin and leptin as adiposity signals. *Recent Prog Horm Res* *59*, 267-285.

Benoit, S.C., Kemp, C.J., Elias, C.F., Abplanalp, W., Herman, J.P., Migrenne, S., Lefevre, A.L., Cruciani-Guglielmacci, C., Magnan, C., Yu, F., et al. (2009). Palmitic acid mediates hypothalamic insulin resistance by altering PKC-theta subcellular localization in rodents. *J Clin Invest* *119*, 2577-2589.

Benomar, Y., and Taouis, M. (2019). Molecular Mechanisms Underlying Obesity-Induced Hypothalamic Inflammation and Insulin Resistance: Pivotal Role of Resistin/TLR4 Pathways. *Front Endocrinol (Lausanne)* *10*, 140.

Bernal-Sore, I., Navarro-Marquez, M., Osorio-Fuentealba, C., Diaz-Castro, F., Del Campo, A., Donoso-Barraza, C., Porras, O., Lavandero, S., and Troncoso, R. (2018). Mifepristone enhances insulin-stimulated Akt phosphorylation and glucose uptake in skeletal muscle cells. *Mol Cell Endocrinol* *461*, 277-283.

Blouet, C., and Schwartz, G.J. (2010). Hypothalamic nutrient sensing in the control of energy homeostasis. *Behav Brain Res* 209, 1-12.

Boland, B., Kumar, A., Lee, S., Platt, F.M., Wegiel, J., Yu, W.H., and Nixon, R.A. (2008). Autophagy induction and autophagosome clearance in neurons: relationship to autophagic pathology in Alzheimer's disease. *J Neurosci* 28, 6926-6937.

Bright, N.A., Davis, L.J., and Luzio, J.P. (2016). Endolysosomes Are the Principal Intracellular Sites of Acid Hydrolase Activity. *Curr Biol* 26, 2233-2245.

Brightman, M.W., and Reese, T.S. (1969). Junctions between intimately apposed cell membranes in the vertebrate brain. *J Cell Biol* 40, 648-677.

Bruce, K.D., Zsombok, A., and Eckel, R.H. (2017). Lipid Processing in the Brain: A Key Regulator of Systemic Metabolism. *Front Endocrinol (Lausanne)* 8, 60.

Bucci, C., Thomsen, P., Nicoziani, P., McCarthy, J., and van Deurs, B. (2000). Rab7: a key to lysosome biogenesis. *Mol Biol Cell* 11, 467-480.

Bustamante, H.A., Cereceda, K., Gonzalez, A.E., Valenzuela, G.E., Cheuquemilla, Y., Hernandez, S., Arias-Munoz, E., Cerda-Troncoso, C., Bandau, S., Soza, A., et al. (2020). The Proteasomal Deubiquitinating Enzyme PSMD14 Regulates Macroautophagy by Controlling Golgi-to-ER Retrograde Transport. *Cells* 9.

Cabrera, M., Nordmann, M., Perz, A., Schmedt, D., Gerondopoulos, A., Barr, F., Piehler, J., Engelbrecht-Vandre, S., and Ungermann, C. (2014). The Mon1-Ccz1 GEF activates the Rab7 GTPase Ypt7 via a longin-fold-Rab interface and association with PI3P-positive membranes. *J Cell Sci* 127, 1043-1051.

Carmo-Silva, S., and Cavadas, C. (2017). Hypothalamic Dysfunction in Obesity and Metabolic Disorders. *Adv Neurobiol* 19, 73-116.

Castillo, K., Valenzuela, V., Onate, M., and Hetz, C. (2017). A Molecular Reporter for Monitoring Autophagic Flux in Nervous System In Vivo. *Methods Enzymol* 588, 109-131.

Cebollero, E., van der Vaart, A., Zhao, M., Rieter, E., Klionsky, D.J., Helms, J.B., and Reggiori, F. (2012). Phosphatidylinositol-3-phosphate clearance plays a key role in autophagosome completion. *Curr Biol* 22, 1545-1553.

Changou, C.A., Ajoy, R., and Chou, S.Y. (2017). Live Images of GLUT4 Protein Trafficking in Mouse Primary Hypothalamic Neurons Using Deconvolution Microscopy. *J Vis Exp*.

Chen, C.T., and Bazinet, R.P. (2015). beta-oxidation and rapid metabolism, but not uptake regulate brain eicosapentaenoic acid levels. *Prostaglandins Leukot Essent Fatty Acids* 92, 33-40.

Chen, W., Balland, E., and Cowley, M.A. (2017). Hypothalamic Insulin Resistance in Obesity: Effects on Glucose Homeostasis. *Neuroendocrinology* 104, 364-381.

Cheng, X.T., Zhou, B., Lin, M.Y., Cai, Q., and Sheng, Z.H. (2015). Axonal autophagosomes recruit dynein for retrograde transport through fusion with late endosomes. *J Cell Biol* 209, 377-386.

Chow, C.Y., Zhang, Y., Dowling, J.J., Jin, N., Adamska, M., Shiga, K., Szigeti, K., Shy, M.E., Li, J., Zhang, X., et al. (2007). Mutation of FIG4 causes neurodegeneration in the pale tremor mouse and patients with CMT4J. *Nature* 448, 68-72.

Choy, C.H., Saffi, G., Gray, M.A., Wallace, C., Dayam, R.M., Ou, Z.A., Lenk, G., Puertollano, R., Watkins, S.C., and Botelho, R.J. (2018). Lysosome enlargement during inhibition of the lipid kinase PIKfyve proceeds through lysosome coalescence. *J Cell Sci* 131.

Codogno, P., and Meijer, A.J. (2010). Autophagy: a potential link between obesity and insulin resistance. *Cell Metab* 11, 449-451.

Colacurcio, D.J., Pensalfini, A., Jiang, Y., and Nixon, R.A. (2018). Dysfunction of autophagy and endosomal-lysosomal pathways: Roles in pathogenesis of Down syndrome and Alzheimer's Disease. *Free Radic Biol Med* 114, 40-51.

Cone, R.D. (2005). Anatomy and regulation of the central melanocortin system. *Nat Neurosci* 8, 571-578.

Cone, R.D., Cowley, M.A., Butler, A.A., Fan, W., Marks, D.L., and Low, M.J. (2001). The arcuate nucleus as a conduit for diverse signals relevant to energy homeostasis. *Int J Obes Relat Metab Disord* 25 Suppl 5, S63-67.

Coupe, B., Ishii, Y., Dietrich, M.O., Komatsu, M., Horvath, T.L., and Bouret, S.G. (2012). Loss of autophagy in pro-opiomelanocortin neurons perturbs axon growth and causes metabolic dysregulation. *Cell Metab* 15, 247-255.

Creasy, B.M., Hartmann, C.B., White, F.K., and McCoy, K.L. (2007). New assay using fluorogenic substrates and immunofluorescence staining to measure cysteine cathepsin activity in live cell subpopulations. *Cytometry A* 71, 114-123.

Czech, M.P., Klarlund, J.K., Yagaloff, K.A., Bradford, A.P., and Lewis, R.E. (1988). Insulin receptor signaling. Activation of multiple serine kinases. *J Biol Chem* 263, 11017-11020.

Daneman, R., and Prat, A. (2015). The blood-brain barrier. *Cold Spring Harb Perspect Biol* 7, a020412.

de Mello, N.P., Orellana, A.M., Mazucanti, C.H., de Morais Lima, G., Scavone, C., and Kawamoto, E.M. (2019). Insulin and Autophagy in Neurodegeneration. *Front Neurosci* 13, 491.

De Meyts, P. (1976). Cooperative properties of hormone receptors in cell membranes. *J Supramol Struct* 4, 241-258.

De Souza, C.T., Araujo, E.P., Bordin, S., Ashimine, R., Zollner, R.L., Boschero, A.C., Saad, M.J., and Velloso, L.A. (2005). Consumption of a fat-rich diet activates a proinflammatory response and induces insulin resistance in the hypothalamus. *Endocrinology* 146, 4192-4199.

Dehouck, B., Prevot, V., and Langlet, F. (2014). [Plasticity of the blood-hypothalamus barrier: a role in energy homeostasis]. *Med Sci (Paris)* 30, 627-630.

Di Pietro, S.M., Falcon-Perez, J.M., Tenza, D., Setty, S.R., Marks, M.S., Raposo, G., and Dell'Angelica, E.C. (2006). BLOC-1 interacts with BLOC-2 and the AP-3 complex to facilitate protein trafficking on endosomes. *Mol Biol Cell* 17, 4027-4038.

Diao, J., Liu, R., Rong, Y., Zhao, M., Zhang, J., Lai, Y., Zhou, Q., Wilz, L.M., Li, J., Vivona, S., et al. (2015). ATG14 promotes membrane tethering and fusion of autophagosomes to endolysosomes. *Nature* 520, 563-566.

Diaz, J., Mendoza, P., Ortiz, R., Diaz, N., Leyton, L., Stupack, D., Quest, A.F., and Torres, V.A. (2014). Rab5 is required in metastatic cancer cells for Caveolin-1-enhanced Rac1 activation, migration and invasion. *J Cell Sci* 127, 2401-2406.

Dietrich, M.O., and Horvath, T.L. (2013). Hypothalamic control of energy balance: insights into the role of synaptic plasticity. *Trends Neurosci* 36, 65-73.

Dragano, N.R., Monfort-Pires, M., and Velloso, L.A. (2019). Mechanisms Mediating the Actions of Fatty Acids in the Hypothalamus. *Neuroscience*.

Duca, F.A., and Lam, T.K. (2014). Gut microbiota, nutrient sensing and energy balance. *Diabetes Obes Metab* 16 *Suppl 1*, 68-76.

Duvvuri, M., Gong, Y., Chatterji, D., and Krise, J.P. (2004). Weak base permeability characteristics influence the intracellular sequestration site in the multidrug-resistant human leukemic cell line HL-60. *J Biol Chem* 279, 32367-32372.

Ebato, C., Uchida, T., Arakawa, M., Komatsu, M., Ueno, T., Komiya, K., Azuma, K., Hirose, T., Tanaka, K., Kominami, E., et al. (2008). Autophagy is important in islet homeostasis and compensatory increase of beta cell mass in response to high-fat diet. *Cell Metab* 8, 325-332.

Engelhardt, S., Patkar, S., and Ogunshola, O.O. (2014). Cell-specific blood-brain barrier regulation in health and disease: a focus on hypoxia. *Br J Pharmacol* 171, 1210-1230.

ENS (2018). Encuesta Nacional de Salud. Primeros y Segundos Resultados ENS 2016-2017. (MINSAL).

Eskelinen, E.L. (2005). Maturation of autophagic vacuoles in Mammalian cells. *Autophagy* 1, 1-10.

Eskelinen, E.L. (2008a). Fine structure of the autophagosome. *Methods Mol Biol* 445, 11-28.

Eskelinen, E.L. (2008b). New insights into the mechanisms of macroautophagy in mammalian cells. *Int Rev Cell Mol Biol* 266, 207-247.

Eskelinen, E.L. (2008c). To be or not to be? Examples of incorrect identification of autophagic compartments in conventional transmission electron microscopy of mammalian cells. *Autophagy* 4, 257-260.

Eskelinen, E.L., and Saftig, P. (2009). Autophagy: a lysosomal degradation pathway with a central role in health and disease. *Biochim Biophys Acta* 1793, 664-673.

Farias, G.G., Guardia, C.M., De Pace, R., Britt, D.J., and Bonifacino, J.S. (2017). BORC/kinesin-1 ensemble drives polarized transport of lysosomes into the axon. *Proc Natl Acad Sci U S A* *114*, E2955-E2964.

Farooqi, I.S., Keogh, J.M., Yeo, G.S., Lank, E.J., Cheetham, T., and O'Rahilly, S. (2003). Clinical spectrum of obesity and mutations in the melanocortin 4 receptor gene. *N Engl J Med* *348*, 1085-1095.

Fatima, S., Hu, X., Gong, R.H., Huang, C., Chen, M., Wong, H.L.X., Bian, Z., and Kwan, H.Y. (2019). Palmitic acid is an intracellular signaling molecule involved in disease development. *Cell Mol Life Sci* *76*, 2547-2557.

Feng, Y., He, D., Yao, Z., and Klionsky, D.J. (2014). The machinery of macroautophagy. *Cell Res* *24*, 24-41.

Fenstermacher, J., Gross, P., Sposito, N., Acuff, V., Pettersen, S., and Gruber, K. (1988). Structural and functional variations in capillary systems within the brain. *Ann N Y Acad Sci* *529*, 21-30.

Ferguson, C.J., Lenk, G.M., and Meisler, M.H. (2009). Defective autophagy in neurons and astrocytes from mice deficient in PI(3,5)P2. *Hum Mol Genet* *18*, 4868-4878.

Fitscher, B.A., Riedel, H.D., Young, K.C., and Stremmel, W. (1998). Tissue distribution and cDNA cloning of a human fatty acid transport protein (hsFATP4). *Biochim Biophys Acta* *1443*, 381-385.

Flier, J.S. (2004). Obesity wars: molecular progress confronts an expanding epidemic. *Cell* *116*, 337-350.

Gali Ramamoorthy, T., Begum, G., Harno, E., and White, A. (2015). Developmental programming of hypothalamic neuronal circuits: impact on energy balance control. *Front Neurosci* *9*, 126.

Galluzzi, L., Baehrecke, E.H., Ballabio, A., Boya, P., Bravo-San Pedro, J.M., Cecconi, F., Choi, A.M., Chu, C.T., Codogno, P., Colombo, M.I., et al. (2017). Molecular definitions of autophagy and related processes. *EMBO J* *36*, 1811-1836.

Geronimo-Olvera, C., and Massieu, L. (2019). Autophagy as a Homeostatic Mechanism in Response to Stress Conditions in the Central Nervous System. *Mol Neurobiol* 56, 6594-6608.

Gerozissis, K. (2008). Brain insulin, energy and glucose homeostasis; genes, environment and metabolic pathologies. *Eur J Pharmacol* 585, 38-49.

Gremmels, H., Bevers, L.M., Fledderus, J.O., Braam, B., van Zonneveld, A.J., Verhaar, M.C., and Joles, J.A. (2015). Oleic acid increases mitochondrial reactive oxygen species production and decreases endothelial nitric oxide synthase activity in cultured endothelial cells. *Eur J Pharmacol* 751, 67-72.

Gual, P., Le Marchand-Brustel, Y., and Tanti, J.F. (2005). Positive and negative regulation of insulin signaling through IRS-1 phosphorylation. *Biochimie* 87, 99-109.

Guardia, C.M., Farias, G.G., Jia, R., Pu, J., and Bonifacino, J.S. (2016). BORC Functions Upstream of Kinesins 1 and 3 to Coordinate Regional Movement of Lysosomes along Different Microtubule Tracks. *Cell Rep* 17, 1950-1961.

Guerra, F., and Bucci, C. (2016). Multiple Roles of the Small GTPase Rab7. *Cells* 5.

Gustafson, D.R., Karlsson, C., Skoog, I., Rosengren, L., Lissner, L., and Blennow, K. (2007). Mid-life adiposity factors relate to blood-brain barrier integrity in late life. *J Intern Med* 262, 643-650.

Gutierrez, M.G., Munafo, D.B., Beron, W., and Colombo, M.I. (2004). Rab7 is required for the normal progression of the autophagic pathway in mammalian cells. *J Cell Sci* 117, 2687-2697.

Hamilton, J.A. (1999). Transport of fatty acids across membranes by the diffusion mechanism. *Prostaglandins Leukot Essent Fatty Acids* 60, 291-297.

Hamilton, J.A., Guo, W., and Kamp, F. (2002). Mechanism of cellular uptake of long-chain fatty acids: Do we need cellular proteins? *Mol Cell Biochem* 239, 17-23.

Hamilton, J.A., Hillard, C.J., Spector, A.A., and Watkins, P.A. (2007). Brain uptake and utilization of fatty acids, lipids and lipoproteins: application to neurological disorders. *J Mol Neurosci* 33, 2-11.

Hanada, T., Noda, N.N., Satomi, Y., Ichimura, Y., Fujioka, Y., Takao, T., Inagaki, F., and Ohsumi, Y. (2007). The Atg12-Atg5 conjugate has a novel E3-like activity for protein lipidation in autophagy. *J Biol Chem* 282, 37298-37302.

Hara, T., Nakamura, K., Matsui, M., Yamamoto, A., Nakahara, Y., Suzuki-Migishima, R., Yokoyama, M., Mishima, K., Saito, I., Okano, H., et al. (2006). Suppression of basal autophagy in neural cells causes neurodegenerative disease in mice. *Nature* 441, 885-889.

Hawkins, B.T., and Davis, T.P. (2005). The blood-brain barrier/neurovascular unit in health and disease. *Pharmacol Rev* 57, 173-185.

Hegedus, K., Takats, S., Boda, A., Jipa, A., Nagy, P., Varga, K., Kovacs, A.L., and Juhasz, G. (2016). The Ccz1-Mon1-Rab7 module and Rab5 control distinct steps of autophagy. *Mol Biol Cell* 27, 3132-3142.

Heni, M., Wagner, R., Kullmann, S., Veit, R., Mat Husin, H., Linder, K., Benkendorff, C., Peter, A., Stefan, N., Haring, H.U., et al. (2014). Central insulin administration improves whole-body insulin sensitivity via hypothalamus and parasympathetic outputs in men. *Diabetes* 63, 4083-4088.

Hernandez-Caceres, M., Oses, C., Peña, D., Criollo, A., and Morselli, E. (2016). Mutant p53 Located in the Cytoplasm Inhibits Autophagy. *Autophagy: Cancer, Other Pathologies, Inflammation, Immunity, Infection, and Aging*, 189-203.

Hu, Y.B., Dammer, E.B., Ren, R.J., and Wang, G. (2015). The endosomal-lysosomal system: from acidification and cargo sorting to neurodegeneration. *Transl Neurodegener* 4, 18.

Hussain, G., Schmitt, F., Loeffler, J.P., and Gonzalez de Aguilar, J.L. (2013). Fattening the brain: a brief of recent research. *Front Cell Neurosci* 7, 144.

Hyttinen, J.M., Niittykoski, M., Salminen, A., and Kaarniranta, K. (2013). Maturation of autophagosomes and endosomes: a key role for Rab7. *Biochim Biophys Acta* 1833, 503-510.

Ikedo, H., West, D.B., Pustek, J.J., Figlewicz, D.P., Greenwood, M.R., Porte, D., Jr., and Woods, S.C. (1986). Intraventricular insulin reduces food intake and body weight of lean but not obese Zucker rats. *Appetite* 7, 381-386.

Ikonomov, O.C., Sbrissa, D., Dondapati, R., and Shisheva, A. (2007). ArPIKfyve-PIKfyve interaction and role in insulin-regulated GLUT4 translocation and glucose transport in 3T3-L1 adipocytes. *Exp Cell Res* 313, 2404-2416.

Itakura, E., Kishi-Itakura, C., and Mizushima, N. (2012). The hairpin-type tail-anchored SNARE syntaxin 17 targets to autophagosomes for fusion with endosomes/lysosomes. *Cell* 151, 1256-1269.

Itakura, E., and Mizushima, N. (2010). Characterization of autophagosome formation site by a hierarchical analysis of mammalian Atg proteins. *Autophagy* 6, 764-776.

Jia, R., Guardia, C.M., Pu, J., Chen, Y., and Bonifacino, J.S. (2017). BORC coordinates encounter and fusion of lysosomes with autophagosomes. *Autophagy* 13, 1648-1663.

Jin, N., Chow, C.Y., Liu, L., Zolov, S.N., Bronson, R., Davisson, M., Petersen, J.L., Zhang, Y., Park, S., Duex, J.E., et al. (2008). VAC14 nucleates a protein complex essential for the acute interconversion of PI3P and PI(3,5)P(2) in yeast and mouse. *EMBO J* 27, 3221-3234.

Johansen, T., and Lamark, T. (2011). Selective autophagy mediated by autophagic adapter proteins. *Autophagy* 7, 279-296.

John Peter, A.T., Lachmann, J., Rana, M., Bunge, M., Cabrera, M., and Ungermann, C. (2013). The BLOC-1 complex promotes endosomal maturation by recruiting the Rab5 GTPase-activating protein Msb3. *J Cell Biol* 201, 97-111.

Jongsma, M.L., Bakker, J., Cabukusta, B., Liv, N., van Elsland, D., Fermie, J., Akkermans, J.L., Kuijl, C., van der Zanden, S.Y., Janssen, L., et al. (2020). SKIP-HOPS recruits TBC1D15 for a Rab7-to-Arl8b identity switch to control late endosome transport. *EMBO J*, e102301.

Jordens, I., Fernandez-Borja, M., Marsman, M., Dusseljee, S., Janssen, L., Calafat, J., Janssen, H., Wubbolts, R., and Neefjes, J. (2001). The Rab7 effector protein RILP controls lysosomal transport by inducing the recruitment of dynein-dynactin motors. *Curr Biol* 11, 1680-1685.

Jung, H.S., Chung, K.W., Won Kim, J., Kim, J., Komatsu, M., Tanaka, K., Nguyen, Y.H., Kang, T.M., Yoon, K.H., Kim, J.W., et al. (2008). Loss of autophagy diminishes pancreatic beta cell mass and function with resultant hyperglycemia. *Cell Metab* 8, 318-324.

Jurcovicova, J. (2014). Glucose transport in brain - effect of inflammation. *Endocr Regul* 48, 35-48.

Kahn, C.R., and White, M.F. (1988). The insulin receptor and the molecular mechanism of insulin action. *J Clin Invest* 82, 1151-1156.

Kamp, F., Guo, W., Souto, R., Pilch, P.F., Corkey, B.E., and Hamilton, J.A. (2003). Rapid flip-flop of oleic acid across the plasma membrane of adipocytes. *J Biol Chem* 278, 7988-7995.

Kanoski, S.E., Zhang, Y., Zheng, W., and Davidson, T.L. (2010). The effects of a high-energy diet on hippocampal function and blood-brain barrier integrity in the rat. *J Alzheimers Dis* 21, 207-219.

Karmi, A., Iozzo, P., Viljanen, A., Hirvonen, J., Fielding, B.A., Virtanen, K., Oikonen, V., Kemppainen, J., Viljanen, T., Guiducci, L., et al. (2010). Increased brain fatty acid uptake in metabolic syndrome. *Diabetes* 59, 2171-2177.

Kauppi, M., Simonsen, A., Bremnes, B., Vieira, A., Callaghan, J., Stenmark, H., and Olkkonen, V.M. (2002). The small GTPase Rab22 interacts with EEA1 and controls endosomal membrane trafficking. *J Cell Sci* 115, 899-911.

Kaur, J., and Debnath, J. (2015). Autophagy at the crossroads of catabolism and anabolism. *Nat Rev Mol Cell Biol* 16, 461-472.

Kaushik, S., Arias, E., Kwon, H., Lopez, N.M., Athonvarangkul, D., Sahu, S., Schwartz, G.J., Pessin, J.E., and Singh, R. (2012). Loss of autophagy in hypothalamic POMC neurons impairs lipolysis. *EMBO Rep* 13, 258-265.

Kaushik, S., Rodriguez-Navarro, J.A., Arias, E., Kiffin, R., Sahu, S., Schwartz, G.J., Cuervo, A.M., and Singh, R. (2011). Autophagy in hypothalamic AgRP neurons regulates food intake and energy balance. *Cell Metab* 14, 173-183.

Kawai, A., Uchiyama, H., Takano, S., Nakamura, N., and Ohkuma, S. (2007). Autophagosome-lysosome fusion depends on the pH in acidic compartments in CHO cells. *Autophagy* 3, 154-157.

Kim, J., Kundu, M., Viollet, B., and Guan, K.L. (2011). AMPK and mTOR regulate autophagy through direct phosphorylation of Ulk1. *Nat Cell Biol* 13, 132-141.

Kim, K.H., and Lee, M.S. (2014). Autophagy--a key player in cellular and body metabolism. *Nat Rev Endocrinol* 10, 322-337.

Kimura, S., Noda, T., and Yoshimori, T. (2007). Dissection of the autophagosome maturation process by a novel reporter protein, tandem fluorescent-tagged LC3. *Autophagy* 3, 452-460.

Klionsky, D.J., Abdelmohsen, K., Abe, A., Abedin, M.J., Abeliovich, H., Acevedo Arozena, A., Adachi, H., Adams, C.M., Adams, P.D., Adeli, K., et al. (2016). Guidelines for the use and interpretation of assays for monitoring autophagy (3rd edition). *Autophagy* 12, 1-222.

Klionsky, D.J., Cregg, J.M., Dunn, W.A., Jr., Emr, S.D., Sakai, Y., Sandoval, I.V., Sibirny, A., Subramani, S., Thumm, M., Veenhuis, M., et al. (2003). A unified nomenclature for yeast autophagy-related genes. *Developmental cell* 5, 539-545.

Koch, L., Wunderlich, F.T., Seibler, J., Konner, A.C., Hampel, B., Irlenbusch, S., Brabant, G., Kahn, C.R., Schwenk, F., and Bruning, J.C. (2008). Central insulin action regulates peripheral glucose and fat metabolism in mice. *J Clin Invest* 118, 2132-2147.

Koga, H., Kaushik, S., and Cuervo, A.M. (2010). Altered lipid content inhibits autophagic vesicular fusion. *FASEB J* 24, 3052-3065.

Komatsu, M., Waguri, S., Chiba, T., Murata, S., Iwata, J., Tanida, I., Ueno, T., Koike, M., Uchiyama, Y., Kominami, E., et al. (2006). Loss of autophagy in the central nervous system causes neurodegeneration in mice. *Nature* 441, 880-884.

Konner, A.C., Janoschek, R., Plum, L., Jordan, S.D., Rother, E., Ma, X., Xu, C., Enriori, P., Hampel, B., Barsh, G.S., et al. (2007). Insulin action in AgRP-expressing neurons is required for suppression of hepatic glucose production. *Cell Metab* 5, 438-449.

Kopelman, P.G. (2000). Obesity as a medical problem. *Nature* 404, 635-643.

Korolchuk, V.I., and Rubinsztein, D.C. (2011). Regulation of autophagy by lysosomal positioning. *Autophagy* 7, 927-928.

Krashes, M.J., Koda, S., Ye, C., Rogan, S.C., Adams, A.C., Cusher, D.S., Maratos-Flier, E., Roth, B.L., and Lowell, B.B. (2011). Rapid, reversible activation of AgRP neurons drives feeding behavior in mice. *J Clin Invest* 121, 1424-1428.

Lam, T.K., Schwartz, G.J., and Rossetti, L. (2005). Hypothalamic sensing of fatty acids. *Nat Neurosci* 8, 579-584.

Lamber, E.P., Siedenburg, A.C., and Barr, F.A. (2019). Rab regulation by GEFs and GAPs during membrane traffic. *Curr Opin Cell Biol* 59, 34-39.

Langemeyer, L., and Ungermann, C. (2015). BORC and BLOC-1: Shared subunits in trafficking complexes. *Developmental cell* 33, 121-122.

Lawrence, J.C., Jr., Fadden, P., Haystead, T.A., and Lin, T.A. (1997). PHAS proteins as mediators of the actions of insulin, growth factors and cAMP on protein synthesis and cell proliferation. *Adv Enzyme Regul* 37, 239-267.

Le Foll, C. (2019). Hypothalamic Fatty Acids and Ketone Bodies Sensing and Role of FAT/CD36 in the Regulation of Food Intake. *Front Physiol* 10, 1036.

Le Foll, C., Irani, B.G., Magnan, C., Dunn-Meynell, A.A., and Levin, B.E. (2009). Characteristics and mechanisms of hypothalamic neuronal fatty acid sensing. *Am J Physiol Regul Integr Comp Physiol* 297, R655-664.

Lee, S., Sato, Y., and Nixon, R.A. (2011). Primary lysosomal dysfunction causes cargo-specific deficits of axonal transport leading to Alzheimer-like neuritic dystrophy. *Autophagy* 7, 1562-1563.

Leloup, C., Arluison, M., Kassis, N., Lepetit, N., Cartier, N., Ferre, P., and Penicaud, L. (1996). Discrete brain areas express the insulin-responsive glucose transporter GLUT4. *Brain Res Mol Brain Res* 38, 45-53.

Lenard, N.R., and Berthoud, H.R. (2008). Central and peripheral regulation of food intake and physical activity: pathways and genes. *Obesity (Silver Spring)* 16 Suppl 3, S11-22.

Leto, D., and Saltiel, A.R. (2012). Regulation of glucose transport by insulin: traffic control of GLUT4. *Nat Rev Mol Cell Biol* 13, 383-396.

Levin, B.E. (2006). Metabolic sensing neurons and the control of energy homeostasis. *Physiol Behav* 89, 486-489.

- Levin, V.A. (1980). Relationship of octanol/water partition coefficient and molecular weight to rat brain capillary permeability. *J Med Chem* 23, 682-684.
- Liou, W., Geuze, H.J., Geelen, M.J., and Slot, J.W. (1997). The autophagic and endocytic pathways converge at the nascent autophagic vacuoles. *J Cell Biol* 136, 61-70.
- Lopez, M., Lelliott, C.J., and Vidal-Puig, A. (2007). Hypothalamic fatty acid metabolism: a housekeeping pathway that regulates food intake. *Bioessays* 29, 248-261.
- Luquet, S., Perez, F.A., Hnasko, T.S., and Palmiter, R.D. (2005). NPY/AgRP neurons are essential for feeding in adult mice but can be ablated in neonates. *Science* 310, 683-685.
- Malhotra, R., Warne, J.P., Salas, E., Xu, A.W., and Debnath, J. (2015). Loss of Atg12, but not Atg5, in pro-opiomelanocortin neurons exacerbates diet-induced obesity. *Autophagy* 11, 145-154.
- Malik, B.R., Maddison, D.C., Smith, G.A., and Peters, O.M. (2019). Autophagic and endolysosomal dysfunction in neurodegenerative disease. *Mol Brain* 12, 100.
- Mandelblat-Cerf, Y., Ramesh, R.N., Burgess, C.R., Patella, P., Yang, Z., Lowell, B.B., and Andermann, M.L. (2015). Arcuate hypothalamic AgRP and putative POMC neurons show opposite changes in spiking across multiple timescales. *Elife* 4.
- Masiero, E., Agatea, L., Mammucari, C., Blaauw, B., Loro, E., Komatsu, M., Metzger, D., Reggiani, C., Schiaffino, S., and Sandri, M. (2009). Autophagy is required to maintain muscle mass. *Cell Metab* 10, 507-515.
- Mauthe, M., Orhon, I., Rocchi, C., Zhou, X., Luhr, M., Hijlkema, K.J., Coppes, R.P., Engedal, N., Mari, M., and Reggiori, F. (2018). Chloroquine inhibits autophagic flux by decreasing autophagosome-lysosome fusion. *Autophagy* 14, 1435-1455.
- Mauvezin, C., and Neufeld, T.P. (2015). Bafilomycin A1 disrupts autophagic flux by inhibiting both V-ATPase-dependent acidification and Ca-P60A/SERCA-dependent autophagosome-lysosome fusion. *Autophagy* 11, 1437-1438.
- McCartney, A.J., Zhang, Y., and Weisman, L.S. (2014). Phosphatidylinositol 3,5-bisphosphate: low abundance, high significance. *Bioessays* 36, 52-64.

Mehrpour, M., Esclatine, A., Beau, I., and Codogno, P. (2010). Autophagy in health and disease. 1. Regulation and significance of autophagy: an overview. *Am J Physiol Cell Physiol* 298, C776-785.

Meng, Q., and Cai, D. (2011). Defective hypothalamic autophagy directs the central pathogenesis of obesity via the IkappaB kinase beta (IKKbeta)/NF-kappaB pathway. *J Biol Chem* 286, 32324-32332.

Mesa, R., Magadan, J., Barbieri, A., Lopez, C., Stahl, P.D., and Mayorga, L.S. (2005). Overexpression of Rab22a hampers the transport between endosomes and the Golgi apparatus. *Exp Cell Res* 304, 339-353.

Mesa, R., Salomon, C., Roggero, M., Stahl, P.D., and Mayorga, L.S. (2001). Rab22a affects the morphology and function of the endocytic pathway. *J Cell Sci* 114, 4041-4049.

Migrenne, S., Le Foll, C., Levin, B.E., and Magnan, C. (2011). Brain lipid sensing and nervous control of energy balance. *Diabetes & metabolism* 37, 83-88.

Mijaljica, D., Prescott, M., and Devenish, R.J. (2011). Microautophagy in mammalian cells: revisiting a 40-year-old conundrum. *Autophagy* 7, 673-682.

Milanski, M., Degasperi, G., Coope, A., Morari, J., Denis, R., Cintra, D.E., Tsukumo, D.M., Anhe, G., Amaral, M.E., Takahashi, H.K., et al. (2009). Saturated fatty acids produce an inflammatory response predominantly through the activation of TLR4 signaling in hypothalamus: implications for the pathogenesis of obesity. *J Neurosci* 29, 359-370.

Miller, J.C., Gnaedinger, J.M., and Rapoport, S.I. (1987). Utilization of plasma fatty acid in rat brain: distribution of [14C]palmitate between oxidative and synthetic pathways. *J Neurochem* 49, 1507-1514.

Mitchell, R.W., and Hatch, G.M. (2011). Fatty acid transport into the brain: of fatty acid fables and lipid tails. *Prostaglandins Leukot Essent Fatty Acids* 85, 293-302.

Mitchell, R.W., On, N.H., Del Bigio, M.R., Miller, D.W., and Hatch, G.M. (2011). Fatty acid transport protein expression in human brain and potential role in fatty acid transport across human brain microvessel endothelial cells. *J Neurochem* 117, 735-746.

Mizushima, N., and Komatsu, M. (2011). Autophagy: renovation of cells and tissues. *Cell* 147, 728-741.

Mizushima, N., Yamamoto, A., Matsui, M., Yoshimori, T., and Ohsumi, Y. (2004). In vivo analysis of autophagy in response to nutrient starvation using transgenic mice expressing a fluorescent autophagosome marker. *Mol Biol Cell* 15, 1101-1111.

Monastyrska, I., Rieter, E., Klionsky, D.J., and Reggiori, F. (2009). Multiple roles of the cytoskeleton in autophagy. *Biol Rev Camb Philos Soc* 84, 431-448.

Morgan, K., Obici, S., and Rossetti, L. (2004). Hypothalamic responses to long-chain fatty acids are nutritionally regulated. *J Biol Chem* 279, 31139-31148.

Morselli, E., Criollo, A., Rodriguez-Navas, C., and Clegg, D.J. (2014a). Chronic High Fat Diet Consumption Impairs Metabolic Health of Male Mice. *Inflamm Cell Signal* 1, e561.

Morselli, E., Frank, A.P., Palmer, B.F., Rodriguez-Navas, C., Criollo, A., and Clegg, D.J. (2016). A sexually dimorphic hypothalamic response to chronic high-fat diet consumption. *Int J Obes (Lond)* 40, 206-209.

Morselli, E., Fuente-Martin, E., Finan, B., Kim, M., Frank, A., Garcia-Caceres, C., Navas, C.R., Gordillo, R., Neinast, M., Kalainayakan, S.P., et al. (2014b). Hypothalamic PGC-1alpha protects against high-fat diet exposure by regulating ERalpha. *Cell Rep* 9, 633-645.

Mountjoy, K.G. (2010). Functions for pro-opiomelanocortin-derived peptides in obesity and diabetes. *Biochem J* 428, 305-324.

Mu, H., and Hoy, C.E. (2004). The digestion of dietary triacylglycerols. *Prog Lipid Res* 43, 105-133.

Mundy, D.I., Li, W.P., Luby-Phelps, K., and Anderson, R.G. (2012). Caveolin targeting to late endosome/lysosomal membranes is induced by perturbations of lysosomal pH and cholesterol content. *Mol Biol Cell* 23, 864-880.

Nakamura, S., and Yoshimori, T. (2017). New insights into autophagosome-lysosome fusion. *J Cell Sci* 130, 1209-1216.

Nezis, I.P., and Stenmark, H. (2012). p62 at the interface of autophagy, oxidative stress signaling, and cancer. *Antioxid Redox Signal* 17, 786-793.

Nikoletopoulou, V., Papandreou, M.E., and Tavernarakis, N. (2015). Autophagy in the physiology and pathology of the central nervous system. *Cell Death Differ* 22, 398-407.

Niswender, K.D., Morrison, C.D., Clegg, D.J., Olson, R., Baskin, D.G., Myers, M.G., Jr., Seeley, R.J., and Schwartz, M.W. (2003). Insulin activation of phosphatidylinositol 3-kinase in the hypothalamic arcuate nucleus: a key mediator of insulin-induced anorexia. *Diabetes* 52, 227-231.

Obici, S., Feng, Z., Karkanias, G., Baskin, D.G., and Rossetti, L. (2002a). Decreasing hypothalamic insulin receptors causes hyperphagia and insulin resistance in rats. *Nat Neurosci* 5, 566-572.

Obici, S., and Rossetti, L. (2003). Minireview: nutrient sensing and the regulation of insulin action and energy balance. *Endocrinology* 144, 5172-5178.

Obici, S., Zhang, B.B., Karkanias, G., and Rossetti, L. (2002b). Hypothalamic insulin signaling is required for inhibition of glucose production. *Nat Med* 8, 1376-1382.

Ochiai, Y., Uchida, Y., Ohtsuki, S., Tachikawa, M., Aizawa, S., and Terasaki, T. (2017). The blood-brain barrier fatty acid transport protein 1 (FATP1/SLC27A1) supplies docosahexaenoic acid to the brain, and insulin facilitates transport. *J Neurochem* 141, 400-412.

Odorizzi, G., Babst, M., and Emr, S.D. (1998). Fab1p PtdIns(3)P 5-kinase function essential for protein sorting in the multivesicular body. *Cell* 95, 847-858.

Oh, H., Boghossian, S., York, D.A., and Park-York, M. (2013). The effect of high fat diet and saturated fatty acids on insulin signaling in the amygdala and hypothalamus of rats. *Brain Res* 1537, 191-200.

Oh, T.S., Cho, H., Cho, J.H., Yu, S.W., and Kim, E.K. (2016). Hypothalamic AMPK-induced autophagy increases food intake by regulating NPY and POMC expression. *Autophagy* 12, 2009-2025.

Ohsumi, Y., and Mizushima, N. (2004). Two ubiquitin-like conjugation systems essential for autophagy. *Semin Cell Dev Biol* 15, 231-236.

Oomura, Y., Nakamura, T., Sugimori, M., and Yamada, Y. (1975). Effect of free fatty acid on the rat lateral hypothalamic neurons. *Physiol Behav* *14*, 483-486.

Opie, L.H., and Walfish, P.G. (1963). Plasma free fatty acid concentrations in obesity. *N Engl J Med* *268*, 757-760.

Ouyang, S., Hsuchou, H., Kastin, A.J., Wang, Y., Yu, C., and Pan, W. (2014). Diet-induced obesity suppresses expression of many proteins at the blood-brain barrier. *J Cereb Blood Flow Metab* *34*, 43-51.

Pankiv, S., Alemu, E.A., Brech, A., Bruun, J.A., Lamark, T., Overvatn, A., Bjorkoy, G., and Johansen, T. (2010). FYCO1 is a Rab7 effector that binds to LC3 and PI3P to mediate microtubule plus end-directed vesicle transport. *J Cell Biol* *188*, 253-269.

Pankiv, S., Clausen, T.H., Lamark, T., Brech, A., Bruun, J.A., Outzen, H., Overvatn, A., Bjorkoy, G., and Johansen, T. (2007). p62/SQSTM1 binds directly to Atg8/LC3 to facilitate degradation of ubiquitinated protein aggregates by autophagy. *J Biol Chem* *282*, 24131-24145.

Parzych, K.R., and Klionsky, D.J. (2014). An overview of autophagy: morphology, mechanism, and regulation. *Antioxid Redox Signal* *20*, 460-473.

Pelerin, H., Jouin, M., Lallemand, M.S., Alessandri, J.M., Cunnane, S.C., Langelier, B., and Guesnet, P. (2014). Gene expression of fatty acid transport and binding proteins in the blood-brain barrier and the cerebral cortex of the rat: differences across development and with different DHA brain status. *Prostaglandins Leukot Essent Fatty Acids* *91*, 213-220.

Perrin, C., Knauf, C., and Burcelin, R. (2004). Intracerebroventricular infusion of glucose, insulin, and the adenosine monophosphate-activated kinase activator, 5-aminoimidazole-4-carboxamide-1-beta-D-ribofuranoside, controls muscle glycogen synthesis. *Endocrinology* *145*, 4025-4033.

Pohl, J., Ring, A., Eehalt, R., Herrmann, T., and Stremmel, W. (2004). New concepts of cellular fatty acid uptake: role of fatty acid transport proteins and of caveolae. *Proc Nutr Soc* *63*, 259-262.

Portovedo, M., Ignacio-Souza, L.M., Bombassaro, B., Coope, A., Reginato, A., Razolli, D.S., Torsoni, M.A., Torsoni, A.S., Leal, R.F., Velloso, L.A., et al. (2015). Saturated fatty acids modulate autophagy's proteins in the hypothalamus. *PLoS One* *10*, e0119850.

Posey, K.A., Clegg, D.J., Printz, R.L., Byun, J., Morton, G.J., Vivekanandan-Giri, A., Pennathur, S., Baskin, D.G., Heinecke, J.W., Woods, S.C., et al. (2009). Hypothalamic proinflammatory lipid accumulation, inflammation, and insulin resistance in rats fed a high-fat diet. *Am J Physiol Endocrinol Metab* 296, E1003-1012.

Pryor, P.R. (2012). Analyzing lysosomes in live cells. *Methods Enzymol* 505, 145-157.

Pu, J., Schindler, C., Jia, R., Jarnik, M., Backlund, P., and Bonifacino, J.S. (2015). BORC, a multisubunit complex that regulates lysosome positioning. *Developmental cell* 33, 176-188.

Quan, W., Kim, H.K., Moon, E.Y., Kim, S.S., Choi, C.S., Komatsu, M., Jeong, Y.T., Lee, M.K., Kim, K.W., Kim, M.S., et al. (2012). Role of hypothalamic proopiomelanocortin neuron autophagy in the control of appetite and leptin response. *Endocrinology* 153, 1817-1826.

Ramirez, M., Amate, L., and Gil, A. (2001). Absorption and distribution of dietary fatty acids from different sources. *Early Hum Dev* 65 Suppl, S95-S101.

Ravikumar, B., Sarkar, S., Davies, J.E., Futter, M., Garcia-Arencibia, M., Green-Thompson, Z.W., Jimenez-Sanchez, M., Korolchuk, V.I., Lichtenberg, M., Luo, S., et al. (2010). Regulation of mammalian autophagy in physiology and pathophysiology. *Physiol Rev* 90, 1383-1435.

Reggiori, F., Tucker, K.A., Stromhaug, P.E., and Klionsky, D.J. (2004). The Atg1-Atg13 complex regulates Atg9 and Atg23 retrieval transport from the pre-autophagosomal structure. *Developmental cell* 6, 79-90.

Reggiori, F., and Ungermann, C. (2017). Autophagosome Maturation and Fusion. *J Mol Biol* 429, 486-496.

Ren, H., Lu, T.Y., McGraw, T.E., and Accili, D. (2015). Anorexia and impaired glucose metabolism in mice with hypothalamic ablation of Glut4 neurons. *Diabetes* 64, 405-417.

Rhea, E.M., and Banks, W.A. (2019). Role of the Blood-Brain Barrier in Central Nervous System Insulin Resistance. *Front Neurosci* 13, 521.

Rhea, E.M., Salameh, T.S., Logsdon, A.F., Hanson, A.J., Erickson, M.A., and Banks, W.A. (2017). Blood-Brain Barriers in Obesity. *AAPS J* 19, 921-930.

Rodriguez-Navas, C., Morselli, E., and Clegg, D.J. (2016). Sexually dimorphic brain fatty acid composition in low and high fat diet-fed mice. *Mol Metab* 5, 680-689.

Rong, Y., McPhee, C.K., Deng, S., Huang, L., Chen, L., Liu, M., Tracy, K., Baehrecke, E.H., Yu, L., and Lenardo, M.J. (2011). Spinster is required for autophagic lysosome reformation and mTOR reactivation following starvation. *Proc Natl Acad Sci U S A* 108, 7826-7831.

Rubinsztein, D.C. (2012). Autophagy--alias self-eating--appetite and ageing. *EMBO Rep* 13, 173-174.

Rubinsztein, D.C., Codogno, P., and Levine, B. (2012). Autophagy modulation as a potential therapeutic target for diverse diseases. *Nat Rev Drug Discov* 11, 709-730.

Sainsbury, A., and Zhang, L. (2010). Role of the arcuate nucleus of the hypothalamus in regulation of body weight during energy deficit. *Mol Cell Endocrinol* 316, 109-119.

Saltiel, A.R., and Kahn, C.R. (2001). Insulin signalling and the regulation of glucose and lipid metabolism. *Nature* 414, 799-806.

Sbrissa, D., Ikononov, O.C., Fu, Z., Ijuin, T., Gruenberg, J., Takenawa, T., and Shisheva, A. (2007). Core protein machinery for mammalian phosphatidylinositol 3,5-bisphosphate synthesis and turnover that regulates the progression of endosomal transport. Novel Sac phosphatase joins the ArPIKfyve-PIKfyve complex. *J Biol Chem* 282, 23878-23891.

Schulze, U., Vollenbroker, B., Braun, D.A., Van Le, T., Granado, D., Kremerskothen, J., Franzel, B., Klosowski, R., Barth, J., Fufezan, C., et al. (2014). The Vac14-interaction network is linked to regulators of the endolysosomal and autophagic pathway. *Mol Cell Proteomics* 13, 1397-1411.

Schulze, U., Vollenbroker, B., Kuhl, A., Granado, D., Bayraktar, S., Rescher, U., Pavenstadt, H., and Weide, T. (2017). Cellular vacuolization caused by overexpression of the PIKfyve-binding deficient Vac14(L156R) is rescued by starvation and inhibition of vacuolar-ATPase. *Biochim Biophys Acta Mol Cell Res* 1864, 749-759.

Schwartz, M.W., Sipols, A.J., Marks, J.L., Sanacora, G., White, J.D., Scheurink, A., Kahn, S.E., Baskin, D.G., Woods, S.C., Figlewicz, D.P., et al. (1992). Inhibition of hypothalamic neuropeptide Y gene expression by insulin. *Endocrinology* 130, 3608-3616.

Schwieger, J., Esser, K.H., Lenarz, T., and Scheper, V. (2016). Establishment of a long-term spiral ganglion neuron culture with reduced glial cell number: Effects of AraC on cell composition and neurons. *J Neurosci Methods* 268, 106-116.

Settembre, C., and Ballabio, A. (2014). Lysosomal adaptation: how the lysosome responds to external cues. *Cold Spring Harb Perspect Biol* 6.

Setty, S.R., Tenza, D., Truschel, S.T., Chou, E., Sviderskaya, E.V., Theos, A.C., Lamoreux, M.L., Di Pietro, S.M., Starcevic, M., Bennett, D.C., et al. (2007). BLOC-1 is required for cargo-specific sorting from vacuolar early endosomes toward lysosome-related organelles. *Mol Biol Cell* 18, 768-780.

Shin, A.C., Filatova, N., Lindtner, C., Chi, T., Degann, S., Oberlin, D., and Buettner, C. (2017). Insulin Receptor Signaling in POMC, but Not AgRP, Neurons Controls Adipose Tissue Insulin Action. *Diabetes* 66, 1560-1571.

Singh, R., Xiang, Y., Wang, Y., Baikati, K., Cuervo, A.M., Luu, Y.K., Tang, Y., Pessin, J.E., Schwartz, G.J., and Czaja, M.J. (2009). Autophagy regulates adipose mass and differentiation in mice. *J Clin Invest* 119, 3329-3339.

Singh, R.B., Gupta, S., Dherange, P., De Meester, F., Wilczynska, A., Alam, S.E., Pella, D., and Wilson, D.W. (2012). Metabolic syndrome: a brain disease. *Can J Physiol Pharmacol* 90, 1171-1183.

Slot, J.W., Geuze, H.J., Gigengack, S., James, D.E., and Lienhard, G.E. (1991). Translocation of the glucose transporter GLUT4 in cardiac myocytes of the rat. *Proc Natl Acad Sci U S A* 88, 7815-7819.

Smith, K.B., and Smith, M.S. (2016). Obesity Statistics. *Prim Care* 43, 121-135, ix.

Sohn, J.W. (2015). Network of hypothalamic neurons that control appetite. *BMB Rep* 48, 229-233.

Spector, R. (1988). Fatty acid transport through the blood-brain barrier. *J Neurochem* 50, 639-643.

Sridhar, S., Botbol, Y., Macian, F., and Cuervo, A.M. (2012). Autophagy and disease: always two sides to a problem. *J Pathol* 226, 255-273.

Stenmark, H. (2009). Rab GTPases as coordinators of vesicle traffic. *Nat Rev Mol Cell Biol* 10, 513-525.

Storrie, B., and Madden, E.A. (1990). Isolation of subcellular organelles. *Methods Enzymol* 182, 203-225.

Takahashi, Y., He, H., Tang, Z., Hattori, T., Liu, Y., Young, M.M., Serfass, J.M., Chen, L., Gebru, M., Chen, C., et al. (2018). An autophagy assay reveals the ESCRT-III component CHMP2A as a regulator of phagophore closure. *Nat Commun* 9, 2855.

Tanida, I., Ueno, T., and Kominami, E. (2004). Human light chain 3/MAP1LC3B is cleaved at its carboxyl-terminal Met121 to expose Gly120 for lipidation and targeting to autophagosomal membranes. *J Biol Chem* 279, 47704-47710.

Thaler, J.P., Yi, C.X., Schur, E.A., Guyenet, S.J., Hwang, B.H., Dietrich, M.O., Zhao, X., Sarruf, D.A., Izgur, V., Maravilla, K.R., et al. (2012). Obesity is associated with hypothalamic injury in rodents and humans. *J Clin Invest* 122, 153-162.

Thierry Alquier, Corinne Leloup, Anne Lorsignol, and Pénicaud, L. (2006). Translocable Glucose Transporters in the Brain
Where Are We in 2006? *Diabetes* 55, S131-S138.

Thomson, A.B., Keelan, M., Garg, M.L., and Clandinin, M.T. (1989). Intestinal aspects of lipid absorption: in review. *Can J Physiol Pharmacol* 67, 179-191.

Torres, V.A., Mielgo, A., Barila, D., Anderson, D.H., and Stupack, D. (2008). Caspase 8 promotes peripheral localization and activation of Rab5. *J Biol Chem* 283, 36280-36289.

Tsunemi, T., Ashe, T.D., Morrison, B.E., Soriano, K.R., Au, J., Roque, R.A., Lazarowski, E.R., Damian, V.A., Masliah, E., and La Spada, A.R. (2012). PGC-1alpha rescues Huntington's disease proteotoxicity by preventing oxidative stress and promoting TFEB function. *Sci Transl Med* 4, 142ra197.

Urayama, A., and Banks, W.A. (2008). Starvation and triglycerides reverse the obesity-induced impairment of insulin transport at the blood-brain barrier. *Endocrinology* 149, 3592-3597.

- Vagena, E., Ryu, J.K., Baeza-Raja, B., Walsh, N.M., Syme, C., Day, J.P., Houslay, M.D., and Baillie, G.S. (2019). A high-fat diet promotes depression-like behavior in mice by suppressing hypothalamic PKA signaling. *Transl Psychiatry* 9, 141.
- Valdearcos, M., Xu, A.W., and Koliwad, S.K. (2015). Hypothalamic inflammation in the control of metabolic function. *Annu Rev Physiol* 77, 131-160.
- Vessby, B. (2003). Dietary fat, fatty acid composition in plasma and the metabolic syndrome. *Curr Opin Lipidol* 14, 15-19.
- Wada, Y. (2013). Vacuoles in mammals: a subcellular structure indispensable for early embryogenesis. *Bioarchitecture* 3, 13-19.
- Wang, M., Wu, H., Li, S., Xu, Z., Li, X., Yang, Y., Li, B., Li, Y., Guo, J., and Chen, H. (2017). SYNJ2BP promotes the degradation of PTEN through the lysosome-pathway and enhances breast tumor metastasis via PI3K/AKT/SNAI1 signaling. *Oncotarget* 8, 89692-89706.
- Wang, R., Cruciani-Guglielmacci, C., Migrenne, S., Magnan, C., Cotero, V.E., and Routh, V.H. (2006). Effects of oleic acid on distinct populations of neurons in the hypothalamic arcuate nucleus are dependent on extracellular glucose levels. *J Neurophysiol* 95, 1491-1498.
- WHO (2018). Obesity and overweight. (World Health Organization).
- Wijdeven, R.H., Janssen, H., Nahidiazar, L., Janssen, L., Jalink, K., Berlin, I., and Neefjes, J. (2016). Cholesterol and ORP1L-mediated ER contact sites control autophagosome transport and fusion with the endocytic pathway. *Nat Commun* 7, 11808.
- Williams, K.W., Margatho, L.O., Lee, C.E., Choi, M., Lee, S., Scott, M.M., Elias, C.F., and Elmquist, J.K. (2010). Segregation of acute leptin and insulin effects in distinct populations of arcuate proopiomelanocortin neurons. *J Neurosci* 30, 2472-2479.
- Williams, L.M. (2012). Hypothalamic dysfunction in obesity. *Proc Nutr Soc* 71, 521-533.
- Wu, H., Chen, S., Ammar, A.B., Xu, J., Wu, Q., Pan, K., Zhang, J., and Hong, Y. (2015). Crosstalk Between Macroautophagy and Chaperone-Mediated Autophagy: Implications for the Treatment of Neurological Diseases. *Mol Neurobiol* 52, 1284-1296.

Wu, J., Cheng, D., Liu, L., Lv, Z., and Liu, K. (2019). TBC1D15 affects glucose uptake by regulating GLUT4 translocation. *Gene* 683, 210-215.

Wu, Y., Cheng, S., Zhao, H., Zou, W., Yoshina, S., Mitani, S., Zhang, H., and Wang, X. (2014). PI3P phosphatase activity is required for autophagosome maturation and autolysosome formation. *EMBO Rep* 15, 973-981.

Xie, Y., Zhou, B., Lin, M.Y., Wang, S., Foust, K.D., and Sheng, Z.H. (2015). Endolysosomal Deficits Augment Mitochondria Pathology in Spinal Motor Neurons of Asymptomatic fALS Mice. *Neuron* 87, 355-370.

Xin, W., Li, Z., Xu, Y., Yu, Y., Zhou, Q., Chen, L., and Wan, Q. (2016). Autophagy protects human podocytes from high glucose-induced injury by preventing insulin resistance. *Metabolism* 65, 1307-1315.

Yamamoto, H., Kakuta, S., Watanabe, T.M., Kitamura, A., Sekito, T., Kondo-Kakuta, C., Ichikawa, R., Kinjo, M., and Ohsumi, Y. (2012). Atg9 vesicles are an important membrane source during early steps of autophagosome formation. *J Cell Biol* 198, 219-233.

Yamamoto, S., Kuramoto, K., Wang, N., Situ, X., Priyadarshini, M., Zhang, W., Cordoba-Chacon, J., Layden, B.T., and He, C. (2018). Autophagy Differentially Regulates Insulin Production and Insulin Sensitivity. *Cell Rep* 23, 3286-3299.

Yamamoto, T., Takabatake, Y., Takahashi, A., Kimura, T., Namba, T., Matsuda, J., Minami, S., Kaimori, J.Y., Matsui, I., Matsusaka, T., et al. (2017). High-Fat Diet-Induced Lysosomal Dysfunction and Impaired Autophagic Flux Contribute to Lipotoxicity in the Kidney. *Journal of the American Society of Nephrology : JASN* 28, 1534-1551.

Yamano, K., Fogel, A.I., Wang, C., van der Blik, A.M., and Youle, R.J. (2014). Mitochondrial Rab GAPs govern autophagosome biogenesis during mitophagy. *Elife* 3, e01612.

Yang, L., Li, P., Fu, S., Calay, E.S., and Hotamisligil, G.S. (2010). Defective hepatic autophagy in obesity promotes ER stress and causes insulin resistance. *Cell Metab* 11, 467-478.

Yang, Y., Atasoy, D., Su, H.H., and Sternson, S.M. (2011). Hunger states switch a flip-flop memory circuit via a synaptic AMPK-dependent positive feedback loop. *Cell* 146, 992-1003.

Yang, Y., and Klionsky, D.J. (2020). Autophagy and disease: unanswered questions. *Cell Death Differ* 27, 858-871.

Yang, Z., and Klionsky, D.J. (2010). Mammalian autophagy: core molecular machinery and signaling regulation. *Curr Opin Cell Biol* 22, 124-131.

Yaswen, L., Diehl, N., Brennan, M.B., and Hochgeschwender, U. (1999). Obesity in the mouse model of pro-opiomelanocortin deficiency responds to peripheral melanocortin. *Nat Med* 5, 1066-1070.

Yordanov, T.E., Hipolito, V.E.B., Liebscher, G., Vogel, G.F., Stasyk, T., Herrmann, C., Geley, S., Teis, D., Botelho, R.J., Hess, M.W., et al. (2019). Biogenesis of lysosome-related organelles complex-1 (BORC) regulates late endosomal/lysosomal size through PIKfyve-dependent phosphatidylinositol-3,5-bisphosphate. *Traffic* 20, 674-696.

Yoshii, S.R., and Mizushima, N. (2017). Monitoring and Measuring Autophagy. *Int J Mol Sci* 18.

Yu, L., Chen, Y., and Tooze, S.A. (2018). Autophagy pathway: Cellular and molecular mechanisms. *Autophagy* 14, 207-215.

Yu, L., McPhee, C.K., Zheng, L., Mardones, G.A., Rong, Y., Peng, J., Mi, N., Zhao, Y., Liu, Z., Wan, F., et al. (2010). Termination of autophagy and reformation of lysosomes regulated by mTOR. *Nature* 465, 942-946.

Yu, S., and Melia, T.J. (2017). The coordination of membrane fission and fusion at the end of autophagosome maturation. *Curr Opin Cell Biol* 47, 92-98.

Yu, S., Tooyama, I., Ding, W.G., Kitasato, H., and Kimura, H. (1995). Immunohistochemical localization of glucose transporters (GLUT1 and GLUT3) in the rat hypothalamus. *Obes Res* 3 *Suppl* 5, 753S-776S.

Zhan, C., Zhou, J., Feng, Q., Zhang, J.E., Lin, S., Bao, J., Wu, P., and Luo, M. (2013). Acute and long-term suppression of feeding behavior by POMC neurons in the brainstem and hypothalamus, respectively. *J Neurosci* 33, 3624-3632.

Zhang, A., He, X., Zhang, L., Yang, L., Woodman, P., and Li, W. (2014). Biogenesis of lysosome-related organelles complex-1 subunit 1 (BLOS1) interacts with sorting nexin 2 and

the endosomal sorting complex required for transport-I (ESCRT-I) component TSG101 to mediate the sorting of epidermal growth factor receptor into endosomal compartments. *J Biol Chem* 289, 29180-29194.

Zhang, L., Bruce-Keller, A.J., Dasuri, K., Nguyen, A.T., Liu, Y., and Keller, J.N. (2009a). Diet-induced metabolic disturbances as modulators of brain homeostasis. *Biochim Biophys Acta* 1792, 417-422.

Zhang, X.M., Walsh, B., Mitchell, C.A., and Rowe, T. (2005). TBC domain family, member 15 is a novel mammalian Rab GTPase-activating protein with substrate preference for Rab7. *Biochem Biophys Res Commun* 335, 154-161.

Zhang, Y., Goldman, S., Baerga, R., Zhao, Y., Komatsu, M., and Jin, S. (2009b). Adipose-specific deletion of autophagy-related gene 7 (*atg7*) in mice reveals a role in adipogenesis. *Proc Natl Acad Sci U S A* 106, 19860-19865.

Zhang, Y., Sowers, J.R., and Ren, J. (2018). Targeting autophagy in obesity: from pathophysiology to management. *Nat Rev Endocrinol* 14, 356-376.

Zhang, Y., Zolov, S.N., Chow, C.Y., Slutsky, S.G., Richardson, S.C., Piper, R.C., Yang, B., Nau, J.J., Westrick, R.J., Morrison, S.J., et al. (2007). Loss of Vac14, a regulator of the signaling lipid phosphatidylinositol 3,5-bisphosphate, results in neurodegeneration in mice. *Proc Natl Acad Sci U S A* 104, 17518-17523.

Zhao, Y.G., and Zhang, H. (2019). Autophagosome maturation: An epic journey from the ER to lysosomes. *J Cell Biol* 218, 757-770.

Zhen, Y., and Stenmark, H. (2015). Cellular functions of Rab GTPases at a glance. *J Cell Sci* 128, 3171-3176.

Zhou, W., and Ye, S. (2018). Rapamycin improves insulin resistance and hepatic steatosis in type 2 diabetes rats through activation of autophagy. *Cell Biol Int* 42, 1282-1291.

Zimmerman, A.W., van Moerkerk, H.T., and Veerkamp, J.H. (2001). Ligand specificity and conformational stability of human fatty acid-binding proteins. *Int J Biochem Cell Biol* 33, 865-876.